SISSA - SCUOLA
INTERNAZIONALE
SUPERIORE
DI STUDI AVANZATI
TRIESTE
Strada Costiera 11

ISAS - INTERNATIONAL SCHOOL FOR ADVANCED STUDIES

ATTESTATO DI RICERCA
"DOCTOR PHILOSOPHIAE"

ADIABATIC ACCRETION ONTO A BLACK HOLE

CANDIDATE

Lu Jufu

SUPERVISOR

Prof. M. Abramowicz

Academic Year 1984/85

TRIESTE

Adiabatic accretion onto a black hole

Lu Jufu 卢炬甫

Thesis submitted for the degree of Doctor of Philosophy

December 1985

文章千古事

得失寸心知

杜甫

A piece of literature is meant for the millennium.

But its ups and downs are known already in the author's heart.

Du Fu (AD 712-770)

Acknowledgements

I would like to express my heartfelt thanks to my supervisor, Dr. Marek A. Abramowicz, for his introducing into this interesting field and his helpful instruction.

I am very grateful to Dr. Mario Livio. The work contained in Chapter 4 was done in collaboration with him.

I appreciate Prof. N. Dallaporta and Prof. D. W. Sciama for their encouragement during the course of my study.

I also thank Dr. Xiang Shouping for drawing graphs and Mr. Omer M. Blaes for improving my English.

Contents

Abstract

Accretion onto a black hole must be transonic. For a stationary, adiabatic flow the specific energy E, specific angular momentum L and mass accretion rate $\dot{M}$ are constant in space. The condition for regularity of the transonic solution, $F(L,E,\dot{M}) = 0$, reduces the number of independent parameters to two. For a fixed pair of $E(>0)$ and L satisfying $E_c > E > E_{Barr}(L)$, where E_c is a critical value and E_{Barr} is the potential barrier connected with the centrifugal force, the regularity condition equation gives two different formal accretion rates corresponding to different locations of the sonic point in the flow. However, the physically acceptable global solution is unique: it is always realized for the smaller of the two accretion rates.

For a non-rotating or slowly rotating black hole the accretion occurs in two regimes: Bondi-type in which both the rotational and relativistic effects are negligible in the transonic part, and disclike in which they are dominant. Transition between the two, which is based on a discontinuous jump in location of the sonic point, is caused by a continuous change in the flow parameter (angular momentum, say). The Bondi-type accretion defines a high state and the disklike a low state, in the sense that the former always requires a higher accretion

rate. When the black hole rotates very rapidly, however, the two-regime-character of accretion no longer occurs, only the Bondi-type is possible.

For a flow characterized by the initial data L, E and $\dot{M}$ which do not obey the regularity condition, the stationary, regular, transonic accretion is impossible. The flow would oscillate between the Bondi-type and disclike solutions, exhibiting a quasi-periodic or chaotic behaviour. This could be used to explain the luminosity variability of active galactic nuclei and Cyg X-1, thus providing strong observational support for the existence of black holes.

1. Introduction

A black hole accretes matter from its surroundings. The radial drift velocity of the accreted matter tends to zero at infinity and approaches the velocity of light at the event horizon (Thorne et al. 1981). Thus, somewhere in between, there must exist a boundary defining the transition from subsonic to supersonic flow. This boundary is called the sonic point, or sound horizon, since it separates the region which can send sound signals out to a distant observer (who is immersed in the subsonic flow) from the region which cannot (Moncrief 1980). The existence of the sound horizon is an important global property of the accretion flow onto a black hole.

1.1 Historical review

a) Spherical accretion

The first page in the history of the field was written by Bondi (1952) who investigated steady, adiabatic and spherically symmetrical accretion onto a star. For a polytropic gas with $n > 3/2$, he showed that among all the theoretically possible solutions to the basic equations describing the accretion flow, there is one in particular which is transonic:
the radial drift velocity of the accreted gas is highly subsonic near

infinity, increases smoothly and monotonically with decreasing distance to the central object,and reaches the local velocity of sound at a certain radius (the sonic point) after which the gas moves supersonically. The transonic solution corresponds to the greatest possible mass accretion rate and is physically most likely to be realized. All other solutions with smaller accretion rates are either always subsonic, or always supersonic. For the case where the polytropic index $n < 3/2$, there is no transonic flow at all.

Bondi's results can be written more explicitly as follows (see, e.g. Zel'dovich and Novikov 1971). The location of the sonic point is given by

$$r_s = \frac{n - 3/2}{4} \left(\frac{a_\infty}{c}\right)^{-2} r_g \quad , \qquad (1.1.1)$$

where a_∞ is the sound speed at infinity, c is the light speed, and $r_g \equiv 2GM/c^2$ is the gravitational radius of the central object, with G being the gravitational constant and M the mass of the central object. The radial velocity of the accreted gas at the sonic point is

$$v_s = a_s = \frac{1}{2} (r_g/r_s)^{1/2} c \quad . \qquad (1.1.2)$$

The mass accretion rate is a unique function of a_∞ and M,

$$\dot{m} = \pi (GM)^2 \left[\frac{n}{k(1+n)}\right]^n \left[\frac{a_\infty^2}{n-3/2}\right]^{n-3/2} , \qquad (1.1.3)$$

where k is the constant in the polytropic equation of state, $P = k\rho^{1+1/n}$ with P and ρ being the pressure and density, respectively. Although in realistic situations Bondi's model is far too simple (see, e.g. Alcock and Illarionov 1980, Bisnovatyi-Kogan and Blinnikov 1980), its basic ideas, like transonic solutions, sonic points, etc. contribute to a general understanding of spherical accretion.

The relativistic generalization of Bondi's purely Newtonian model was first discussed by Michel(1972). He derived the general relativistic equations for steady spherical flow of a perfect fluid in the Schwarzschild metric. Solving the equations in the case of a polytropic gas with n = 3/2 and n = 3, respectively, he also came to the conclusion that there exists a unique analytical solution which passes through a critical point (sonic point). Begelman (1978) further argued that for a gas with $n > 3/2$, the only critical point is the one found by Bondi (1952), which lies well outside the black hole event horizon. He also found that for the case $1/2 < n < 3/2$, there is a relativistic (also unique) critical point which lies near the horizon, and thus was missed in Bondi's Newtonian study. For $n < 1/2$ all the critical points would be within the horizon, and

are therefore unphysical.

The uniqueness of the critical point stated above was queried by Ray (1980). He showed by a more careful study that there are two critical points for a flow of a $n > 3/2$ gas. However, as clarified by a very simple argument in this thesis (§3.2), only one of Ray's two critical points is physical. Thus the critical point in spherical accretion whenever it exists is unique.

Spherical black hole accretion has been studied also by many other authors under a wide range of flow regimes. Blumenthal and Mathews (1976), Carter et al. (1976), and Brinkmann (1980) have considered also adiabatic flows, but using more sophesticated equations of state, rather than a simple polytropic one. Optically thin accretion with radiative cooling has been treated by Shvartzman (1971), Shapiro (1973 a,b), Bisnovatyi-Kogan and Ruzmaikin (1974), and Isper and Price (1977). Optically thick flows have been investigated by Mészàros (1975 a,b), Schmidt-Burgk (1978), Maraschi et al. (1979), Yahel and Brinkmann (1981), Yahel (1982), Maraschi et al. (1982), Flammang (1982), Isper and Price (1982, 1983), and Vitello (1984). The most complete equations applicable to quite general astrophysical context were derived by Thorne et al. (1981).

b) Accretion of rotating matter

In many astrophysically realistic situations (e.g. in binary

systems) the accreted gas possesses significant angular momentum. In this case, accretion is no longer spherical, rather, a disk around the central object forms.

The study of the dynamics of rotating gas masses started long ago as an early stage in the consideration of the formation and evolution of the solar nebula with particular regard to Laplace's nebular hypothesis. The general properties of the evolution of rotating gas disks were well understood by the 1920s (Jeffreys 1924). In the 1940s, Peek (1942) and von Weizsäcker (1943) pointed out the importance of the effect of turbulent viscosity on the evolution of the solar nebula. von Weizsäcker (1948) derived the equations of motion of disk gas. The general solutions for time-dependent, viscous disks were given by Lüst (1952) and Lynden-Bell (1960).

In the 1960s interest switched from the secular dynamics of rotating gas masses to the radiation they might emit, owing to the discoveries of X-ray stars and quasars. Salpeter (1964) and Zel'dovich (1964) were the first to suggest that quasi-stellar objects could be massive black holes accreting the interstellar medium. Hayakawa and Matsuoko (1964) proposed firstly that X-rays might be produced by accretion of gas between two normal stars in close binary systems. Zel'dovich and Guseynov (1966), and Novikov and Zel'dovich (1966) pointed out that gas accretion onto compact components in binary systems should produce X-rays, and thus could be the explanation of the newly

discovered X-ray sources. Shklovsky (1967) applied this idea to Sco X-1 which is supposed to contain a neutron star. Cameron and Mock (1967) suggested that gas accretion onto white dwarfs could also produce X-rays. The history of these early ideas was reviewed by Burbidge (1972).

The essential role of the angular momentum of the gas in binary accretion was first emphasized by Prendergast (Prendergast and Burbidge 1968). He built a model for disk-type accretion onto white dwarfs in binary systems. On a larger scale, Lynden-Bell (1969) argued that galaxies may have supermassive black holes at their centers and analyzed disk-type accretion onto such holes.

In the early 1970s the theory was established in a more complete form by several authors. Shvartsman (1971) studied disks around isolated stars. Lynden-Bell and Rees (1971) extended the work on supermassive holes hidden in the centres of galaxies. Pringle and Rees (1972) applied the theory to Cyg X-1 which supposelly contains a black hole. Shakura (1972 a,b), and Shakura and Sunyaev (1973) derived formulations which are now followed by most authors in the field. Lynden-Bell and Pringle (1974) also gave an elegant description of the problem. Lightman (1974 a,b) constructed a time-dependent model of accretion disks. The general relativistic model was made by Cunningham (1973), Novikov and Thorne (1973), Page and Thorne (1974) and Thorne (1974).

The models constructed in these classical papers are all of a

geometrically thin , Keplerian variety. The elements of the accreted fluid follow circular geodesics to a very good approximation, with the addition of a very small inward radial drift velocity because the angular momentum is gradually removed and transported outwards by viscous stresses. The energy of the shearing orbital motion of the gas is dissipated by viscosity as heat, and thence radiated away. Since the only energy source is the gravitational potential (release of the internal energy of the accreted material was considered by Fang 1981, Zhu 1981, and Zhang and Jiang 1983, however), the total amount of energy radiated by a unit mass of gas during its passage inward through the disk must equal approximately the gravitational binding energy of the unit mass when it eventually reaches the inner edge of the disk. Thus, a proper description of the inner edge of the accretion disk is very important, as it determines the total disk luminosity and, as will be seen later, influences the structure of the whole disk.

The conditions at the inner edge depend of course on the nature of the central object. For a main-sequence star, white dwarf or neutron star the inner edge of the disk is close to the star's surface (when the central object is a strongly magnetized neutron star or white dwarf, the disk extends inward only as far as the Alférn radius, see Lamb and Pethick 1974). In the case of a black hole, it was assumed in all the classical papers that the disk extends down to the marginally stable circular orbit of a test particle (r_{ms}), given by Bardeen et al.

(1973) (for a Schwarzschild black hole this orbit has a radius of 3 r_g). Inside this edge, the gas falls freely towards the hole and the gas density is low in comparison with that in the region outside the edge. Because of this sharp density discontinuity, the edge is regarded as a free surface -- viscous stresses do not act across it.

Due to this rather artificial boundary condition, however, some physical quantities become infinite at the edge (Stoeger 1976). For example, the surface density becomes infinite in the radiation-pressure dominant case, while in the gas-pressure dominant case the radial velocity becomes infinite. This singular behaviour can be removed by considering carefully gravitational and viscous effects, as done by Stoeger (1980) and Kato et al. (1982). It was argued that there must be a very narrow region near r_{ms} where the viscosity is very important -- due to its influence in this layer, the material in the disk flows from the circular geodesics, across r_{ms}, to the geodesics of spiral infall, and into the black hole.

There is yet another way to solve the problem. A theory of thick accretion disks developed since the late 1970s (Abramowicz et al. 1978, Kozlowski et al. 1978, Paczyński and Witta 1980, Jaroszynski et al. 1980, Abramowicz et al. 1980, Abramowicz and Lasota 1980, Paczyński and Abramowicz 1982, Wiita 1982) helped to understand the conditions at the inner edge. Though it was assumed in the classical models that the disk is thin, there is no reason why this should always be so. Disks may become geometrically thick if the internal

pressure builds up so that the thermal energy is competitive with the gravitational energy. This can happen either because the disk radiates at a super-Eddington luminosity, thus radiation pressure is competitive with gravity, or because the material is unable to radiate the energy dissipated by viscous friction, which then remains as internal energy. It was shown by Abramowicz et al. (1978) and Kozlowski et al. (1978) that the inner edge of the thick disk is the "cusp" where an equipotential surface crosses itself. The cusp resembles very much a similar one located on the Roche lobe in a close binary system (the inner Lagrange point). Noting this analogy Paczyński (1978) proposed that the accretion onto the black hole is driven through the vicinity of the cusp, due to a little overflowing of the critical equipotential surface(this surface crosses itself and forms the cusp) by the surface of the disk, i.e. by a little violation of the hydrostatic equilibrium caused by the pressure gradient forces (Figure 1), just as material leaves a star that fills its Roche lobe in a binary system. In this scenario viscosity is not necessary to support the accretion through the inner edge.

The cusp is located between the marginally bound and marginally stable particle orbits. For a Schwarzschild black hole one has

$$2r_g = r_{mb} < r_{in} < r_{ms} = 3r_g \ . \qquad (1.1.4)$$

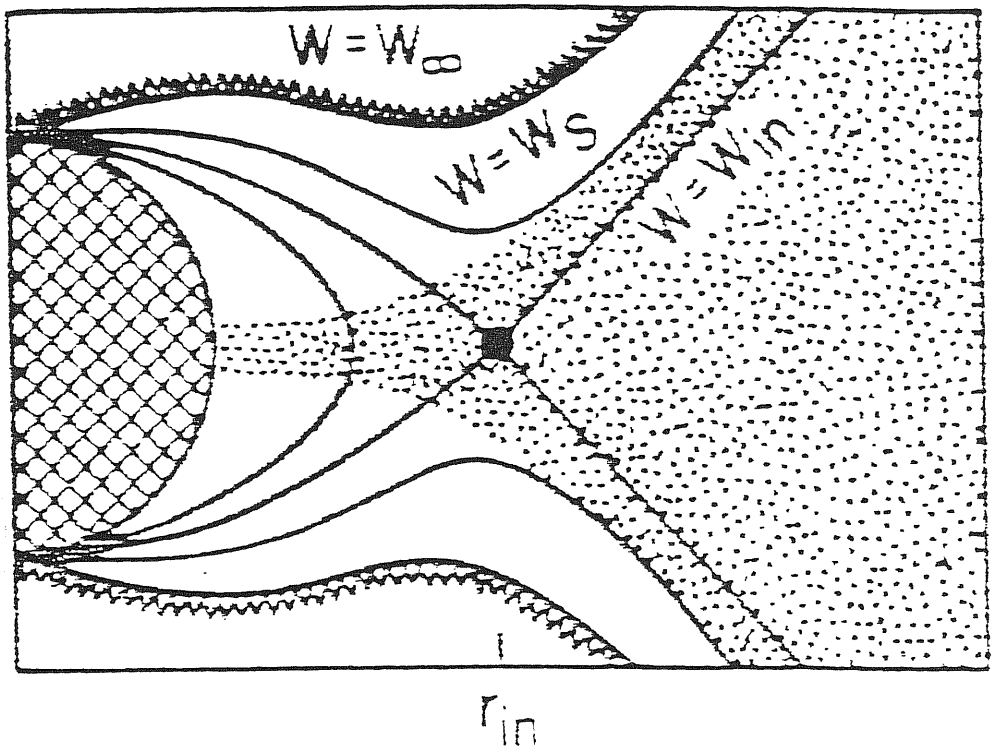

Fig. 1 Paczyński's mechanism for accretion through the inner edge of an accretion disk, where W is the effective potential (gravitational plus centrifugal). (Adopted from Abramowicz et al. 1980)

The radial drift velocity of the accreted gas is subsonic for radii $r > r_{in}$, while for $r < r_{in}$ a stream forms and the gas is freely falling towards the hole with a supersonic velocity. The sonic point is expected to be located close to r_{in}.

Several attempts have been made to analyse more carefully the transonic nature of the accretion flow at the inner disk boundary. The earliest published paper concerning this subject was that by Henriksen and Heaton (1975). Those authors studied the hydrodynamical accretion and effluxion of isentropic or isothermal material with uniform specific angular momentum, and clarified the nature of the critical points (the sonic points). However, because a Newtonian gravitational potential was used, they found only the outer sonic point (Bondi-type), and missed the inner one (disklike) which is due to general relativistic effects (see §2.4 of this thesis). Also using Newtonian dynamics, Maraschi et al. (1976) showed that when radiation pressure is important, the Keplerian approximation for the rotation of the gas, what was adopted in the classical models, becomes inadequate in the inner region of the accretion disk. The first relativistic model of transonic accretion was made by Liang and Thompson (1980). They assumed a quasi-radial flow confined to a solid angle ω, and argued that the critical transonic solution whenever it exists is unique, similar to the case of spherical Bondi accretion. Abramowicz and Zurek (1981) also used this simple flow model and simulated the relevant general relativistic effects by using a pseudo-Newtonian gravitational potential. They considered for the first time the case of positive total (specific) energy of the gas, and found what they called bistability. There exist two separate regimes: disklike accretion for large specific angular momenta, and quasi spherical

accretion for small angular momenta. For the former, the sonic point is always inside, and very close to, the cusp. With a decrease of angular momentum, the sonic point jumps discontinuously to $r_s \gg r_g$. Thus, the important role of angular momentum in transonic accretion was first emphasized. Later on, Loska (1982) described the detailed structure of the cusp region of an adiabatic accretion flow. He neglected viscosity, assumed that the radial velocity is a function of radius only, and that hydrostatic equilibrium holds in the vertical direction. Paczyński and Bisnovatyi-Kogan (1981), Muchotrzeb and Paczyński (1982), and Muchotrzeb (1983a) built a thin disk model with an emphasis on the structure of disk's inner region. They took into account the radial pressure gradients and the inertial term in the equation of radial motion, and the viscosity, radial heat diffusion and heat carried with the accretion flow in the energy conservation equation. This model removed the infinities present in the classical thin disk models at the inner disk boundary $r_{in} = 3r_g$, while it had its inner boundary somewhat closer to the black hole, and the radial flow transonic at that place. Contrary to the results of Stoeger (1980), the "no torque" condition at the inner boundary, which was assumed in the classical models, was shown to be very good. Another interesting result in the model was that there is an upper limit (of the order of 0.02) for the value of α (the Shakura-Sunyaev viscosity parameter), above which stationary transonic solution does not exist. The effect of viscosity on the flow around the disk's inner edge was also discussed by Matsumoto et al. (1984). They found that if the viscosity is large ($\alpha \gtrsim 0.05$), all transonic solutions which

are Keplerian in the outer region pass through a nodal type critical point outside the radius of the marginally stable circular orbit. After passing through the nodal point, there is a set of continuous solutions which are connected smoothly with the outer solution. One cannot determine which solution should be chosen, unless one follows the flow structure up to the black hole horizon. Thus the physical meaning of a nodal critical point is not yet clear, and needs to be studied further.

There has been a considerable body of literature with many remarkable achievements in the exploration of transonic accretion onto a black hole. However, none of the previous works is complete enough. All of them dealt with only the case of negative energy except Abramowicz and Zurek (1981), and all of them were in the framework of the pseudo-Newtonian model of black holes except Liang and Thompson (1980). Furthermore, they assumed exclusively that the flow is quasi-radial -- the validity of this assumption was never examined, and they considered only the stationary case -- time dependent problem has not been touched.

1.2 Framework of the thesis

In this thesis adiabatic, transonic accretion onto a black hole is studied more completely. The entire physically acceptable range of values of the energy and angular momentum of the accreted gas is considered, Both spherical accretion and that of rotating matter are included.

Although the pseudo-Newtonian model of black holes is used in a main chapter (Chapter 2) in order to simplify the calculations, the correct relativistic equations describing the accretion are also solved, both in the Schwarzschild and the Kerr spacetimes (Chapter 3). The influence of the meridional velocity of the gas on the transonic solution is examined for the first time (Urpin 1983 calculated also the vertical component of the gas velocity, but for a different purpose). The problem of the time-dependent flow is attacked by using a simple model which shows the possible existence of periodic or quasi-periodic behaviour in non-stationary transonic accretion flows (Chapter 4). Astrophysical implications of the results are evaluated in Chapter 5. Perhaps the only restriction made here is that viscosity is assumed to be unimportant in the transonic part of the flow. But, as argued in the next section, this assumption appears reasonable.

1.3 Basic assumptions

The following assumptions are made throughout the thesis.

a) The transonic part of the flow is geometrically thin

Paczyński and Bisnovatyi-Kogan (1981) argued that even though the disk may be geometrically thick for $r > r_{in}$, it forms a thin cusp at the transition radius, and flows in a thin supersonic stream for $r < r_{in}$. Recently, Abramowicz (1985) showed that for a

flow composed of a mixture of ideal gas and black body radiation, the relative geometrical thickness of the transonic part

$$H_o = \frac{(\text{vertical thickness})_{in}}{(\text{radius})_{in}} \qquad (1.3.1)$$

depends strongly on

$$\beta = \frac{(\text{gas pressure})}{(\text{total pressure})} \ , \qquad (1.3.2)$$

and only very weakly on all other parameters, namely, the mass of the central object and the accretion rate. It is given by

$$H_o \approx 10^{-2} X/\sqrt{\beta} \ , \qquad (1.3.3)$$

with $X \approx 1$ for black holes with mass $M \sim 10 M_\odot$, and $X \approx 0.1$ for those with $M \sim 10^8 M_\odot$. It is seen that increasing radiation pressure makes the flow thicker, but only when $\beta < 10^{-4}$ for galactic black holes and $\beta < 10^{-6}$ for the extragalactic ones can the thickness of the flow not be small.

b) Dissipation is not important in the transonic part

Disk accretion is driven by angular momentum transfer due to some viscosity. The physical nature of this viscosity is not yet understood.

Nevertheless, some general arguments can be made. It is likely that viscous processes can transfer angular momentum only with a subsonic speed; this is the reason why in the classical "alpha disk" model the viscosity parameter α should not exceed unity. Thus, in the transonic part of the flow, dissipation should not be important, and the angular momentum as well as the energy of the fluid element are likely to be conserved.

Kozlowski et al. (1978) first realized that the transonic motion of the fluid cannot be strongly influenced by dissipation, as the travel time for a fluid element in the transonic part of the flow is shorter than the time scale for dissipative processes to occur at that place. Define the travel time, t_{trav}, as the time in which a fluid element located at the radius r travels a distance r,

$$t_{trav} = r/v_r \ , \qquad (1.3.4)$$

where v_r is the radial drift velocity of the element. The dissipation time, t_{diss} , is defined as the heat content per unit volume divided by the local energy dissipation rate per unit volume,

$$t_{diss} \approx \varrho a^2/Q^+ \ , \qquad (1.3.5)$$

where ϱ is the density, a is the sound speed, and Q^+ is the local dissipation rate :

$$Q^+ = 2\eta\sigma^2 \ , \qquad (1.3.6)$$

with η being the dynamic viscosity and σ^2 the magnitude of the shear tensor. These last two quantities were expressed in the classical models (Shakura and Sunyaev 1973, Novikov and Thorne 1973) as

$$\eta = \rho \alpha H a \ , \qquad (1.3.7)$$

and

$$\sigma = \frac{9}{8} \Omega^2 \ , \qquad (1.3.8)$$

where α is the Shakura-Sunyaev viscosity parameter, H is the half-thickness of the flow, and Ω is the angular velocity of the fluid element. From (1.3.4)-(1.3.8) and replacing v_r by a for the transonic flow, the condition

$$t_{trav} << t_{diss} \qquad (1.3.9)$$

is equivalent to

$$\alpha << H_o \ . \qquad (1.3.10)$$

This is always fulfilled when $\alpha \lesssim 0.05$, as Muchotrzeb (1983a) showed that for $\alpha \approx 0.05$ one has $\alpha \lesssim 0.4H/r_g$, but typically $\alpha < 0.1H/r_g$. If one adopts a more realistic value $\alpha \lesssim 10^{-3}$ as Shakura and Sunyaev

(1973) estimated, then the dissipation is totally negligible. This conclusion can also be supported by the result of Muchotrzeb (1973a) which shows the variation of the angular momentum with radius for the transonic part of the flow (Figure 2). The angular momentum

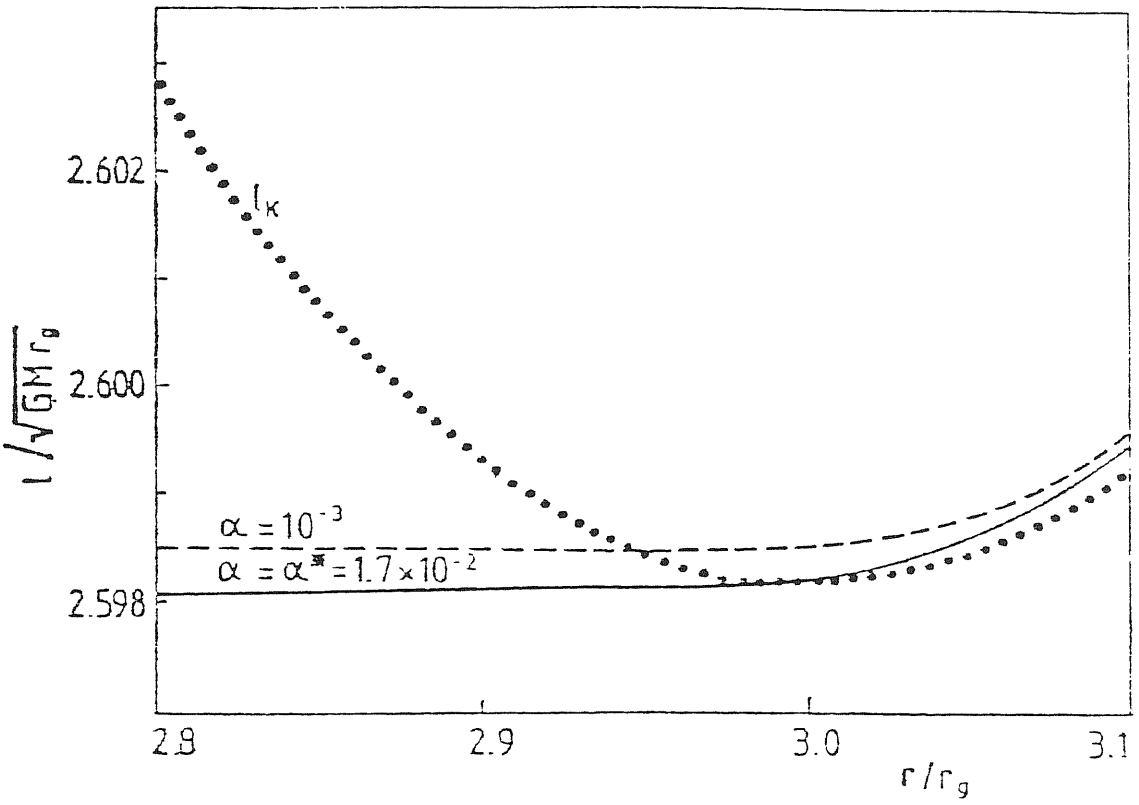

Fig. 2 Variation of specific angular momentum with radius, for two different values of viscosity parameter α. Note that α^* is the upper limit on α. l_k is the Keplerian distribution of angular momentum. (Adopted from Muchotrzeb 1983a)

is almost constant: $|d\ln l/d\ln r| \lesssim 10^{-2}$. Note that the centrifugal force F_c changes in the same region with the characteristic scale $|d\ln F_c/d\ln r| \approx 3$.

Although he had a different opinion on the structure of the inner disk edge, Stoeger (1980) came to the same conclusion that very little energy or angular momentum is radiated or transported outward from inside the inner edge.

It is not clear, however, whether the above conclusion is changed by the recent work of Papaloizou and Pringle (1984). They demonstrated the existence of a dynamical instability in non-accreting, purely circular tori subject to non-axisymmetric perturbations. This instability may saturate at a finite amplitude causing turbulence and therefore providing viscosity. The question whether this instability is important for accretion systems, particularly for thick accretion disks was discussed by Abramowicz (1985) and Abramowicz et al. (1985).

Other assumptions are standard and need no explanation: self-gravity of the accreted matter is negligible; accretion flows are symmetric with respect to the axis and the equatorial plane; accreted matter obeys a polytropic equation of state.

2. Stationary flow: pseudo-Newtonian theory

In this chapter stationary accretion is studied within the framework of the pseudo-Newtonian theory. A Newtonian model of black holes first introduced by Paczyński and Witta (1980) is used to simulate the relevant general relativistic effects. Although the model was employed by several authors to study accretion onto black holes, it is necessary to describe its properties and compare them with the corresponding properties of the correct relativistic model of black holes.

2.1 Newtonian model of a black hole

The Newtonian effective potential for radial motion of a test particle with non-zero specific angular momentum l in a spherically symmetric gravitational field (written on the equatorial plane),

$$W = -GM/r + l^2/2r^2 \quad , \qquad (2.1.1)$$

depends on the angular momentum of the particle. It always has the characteristic shape shown in Figure 3a. Asymptotically ($r \to \infty$) it goes to zero. Then, at some $r_+ = r_+(l)$ it has a minimum which corresponds to a stable circular orbit, and at $r = 0$ it blows up forming an infinite potential barrier. Because of this barrier

---

Fig. 3 Effective potential and Keplerian angular momentum distribution

Newtonian

Black hole

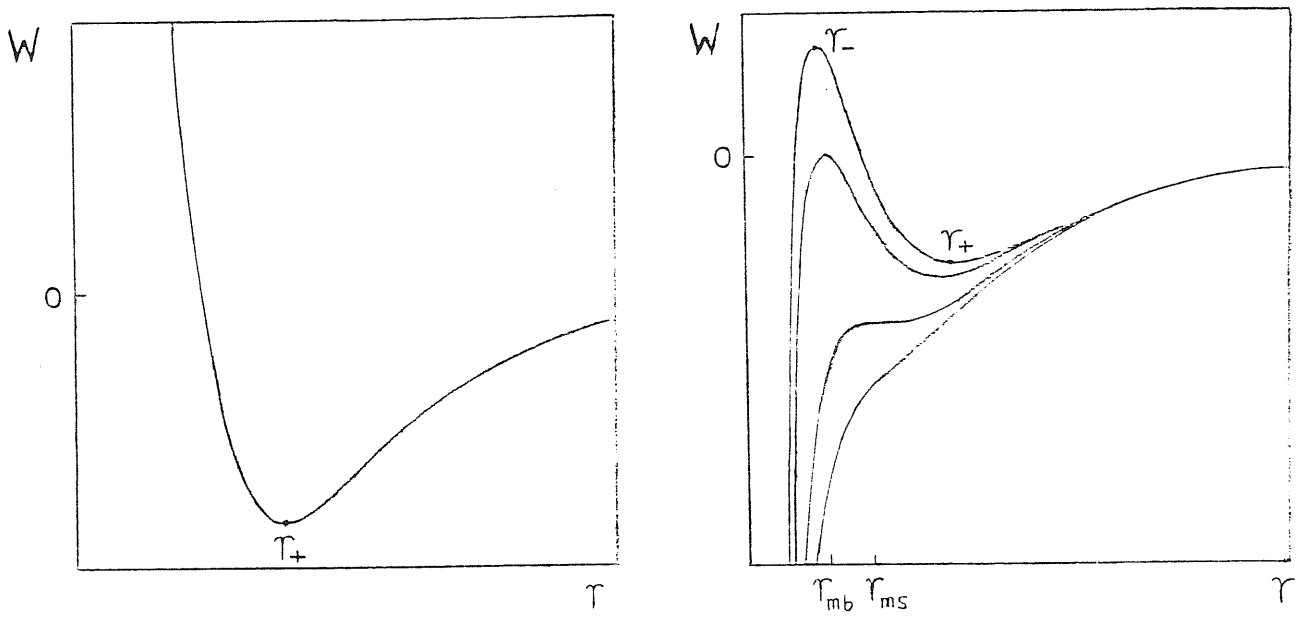

(a)

(b)

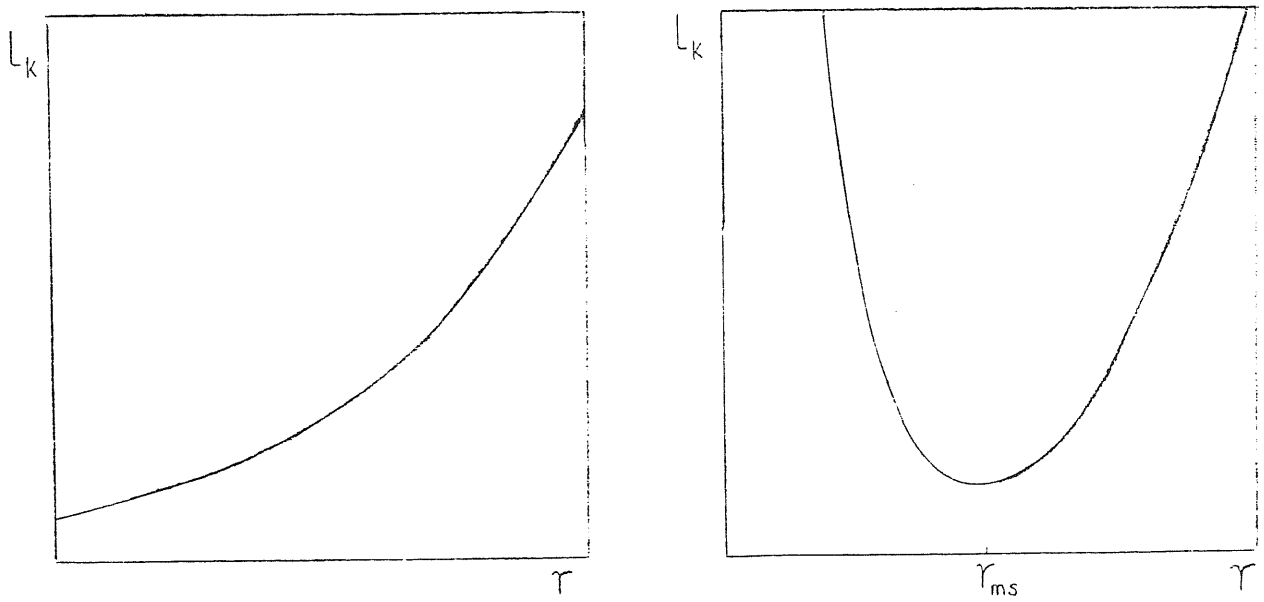

(c)

(d)

Figure 3

a particle with non-zero angular momentum cannot be accreted by the gravity center. The radius of the stable circular orbit on the equatorial plane for a given angular momentum is

$$r_+ = l^2/GM \ . \qquad (2.1.2)$$

The inverse of (2.1.2) gives the Keplerian distribution of angular momentum

$$l = \sqrt{GMr} \ , \qquad (2.1.3)$$

which is shown in Figure 3c.

The effective potential in the gravitational field of a black hole is quite different (see, e.g. Misner, Thorne and Wheeler 1973, Chapter 25). Its asymptotic behaviour when $r \rightarrow \infty$ is the same as in the Newtonian case. But, instead of always having a minimum as in the Newtonian case, its shape depends on the value of the angular momentum of the particle. For angular momenta langer than that corresponding to the marginally stable circular orbit, l_{ms} , the effective potential not only has a minimum at $r_+ = r_+(l)$ corresponding to the stable circular orbit, but also a finite maximum at $r_- = r_-(l)$ corresponding to the unstable circular orbit, and then drops to minus infinity. The fact that the potential barrier is finite for any value of the angular momentum means that any particle can be accreted by the central black hole provided the particle has high

enough energy. As the angular momentum decreases, r_- increases while r_+ decreases. When $l = l_{ms}$, $r_- = r_+ = r_{ms}$ (for a Schwarzschild black hole $r_{ms} = 3r_g$). Thus l_{ms} is the critical value of the angular momentum for the stable circular orbit to exist. This is the reason why the orbit with radius r_{ms} is called the marginally stable circular orbit. For angular momenta less than l_{ms} , neither minima, nor maxima exist; the effective potential decreases monotonically to minus infinity so that circular orbits are not possible. Any particle with $l < l_{ms}$ can be accreted by the black hole, independently of the particle's energy. In addition, there is one potential curve corresponding to a particular value of the angular momentum, $l = l_{mb}$, whose maximum is equal to the asymptotic value of the effective potential at infinity. The unstable circular orbit corresponding to this maximum is called the marginally bound orbit because, obviously, it defines the transition from bound to unbound orbits of the particle (for a Schwarzschild black hole $r_{mb} = 2r_g$). All these properties of the effective potential are shown in Figure 3b. Also in contrast with the Newtonian case, the Keplerian angular momentum distribution is not monotonic, but has a minimum at $r = r_{ms}$ (Figure 3d).

Paczyński (1977) noticed that one can construct a purely Newtonian model to describe accurately all these properties by assuming an artificial Newtonian gravitational potential

$$\Phi = -\frac{GM}{r - r_g}, \qquad (2.1.4)$$

and the effective potential now becomes

$$W = -\frac{GM}{r - r_g} + \frac{l^2}{2r^2}. \qquad (2.1.5)$$

In this model the evaluation of the "Keplerian" (i.e. corresponding to the circular geodesic orbits) quantities follows from the usual Newtonian definitions:

$$(\text{linear velocity}) \equiv v_k \equiv \left(r\frac{d\Phi}{dr}\right)^{1/2}, \qquad (2.1.6)$$

$$(\text{angular velocity}) \equiv \Omega_k \equiv v_k/r, \qquad (2.1.7)$$

$$(\text{mechanical energy}) \equiv e_k \equiv v_k^2/2 + \Phi, \qquad (2.1.8)$$

$$(\text{angular momentum}) \equiv l_k \equiv v_k r \equiv \Omega_k r^2 = r\left(r\frac{d\Phi}{dr}\right)^{1/2}. \qquad (2.1.9)$$

All these quantities are defined on the equatorial plane, $\theta = \pi/2$. The explicite formulae read (Paczyński and Witta 1980)

$$e_k = \left(-\frac{1}{2}\frac{GM}{r}\right)\left\{\frac{(1 - 2r_g/r)}{(1 - r_g/r)^2}\right\}, \qquad (2.1.10)$$

$$\frac{de_k}{dr} = \left(\frac{1}{2}\frac{GM}{r^2}\right)\left[\frac{1 - 3r_g/r}{(1 - r_g/r)^3}\right], \tag{2.1.11}$$

$$l_k = (GMr)^{1/2}\left[\frac{1}{1 - r_g/r}\right], \tag{2.1.12}$$

$$\frac{dl_k}{dr} = \frac{1}{2}\left(\frac{GM}{r}\right)^{1/2}\left[\frac{1 - 3r_g/r}{(1 - r_g/r)^2}\right], \tag{2.1.13}$$

$$\Omega_k = \left(\frac{GM}{r^3}\right)^{1/2}\left[\frac{1}{1 - r_g/r}\right], \tag{2.1.14}$$

$$\frac{d\Omega_k}{dr} = -\frac{3}{2}\left(\frac{GM}{r^5}\right)^{1/2}\left[\frac{1 - 3r_g/r}{(1 - r_g/r)^2}\right], \tag{2.1.15}$$

$$v_k = \left(\frac{GM}{r}\right)^{1/2}\left[\frac{1}{1 - r_g/r}\right], \tag{2.1.16}$$

$$\frac{dv_k}{dr} = -\frac{1}{2}\left(\frac{GM}{r^3}\right)^{1/2}\left[\frac{1 + r_g/r}{(1 - r_g/r)^2}\right]. \tag{2.1.17}$$

In the square brackets the corrections to the otherwise purely Newtonian quantities for the case of a central point-mass are given.

Equation (2.1.10) shows that e_k vanishes at $r = 2r_g$, thus it is identified with $r_{mb} = 2r_g$, as for the Schwarzschild geometry. Likewise, it is seen from equations (2.1.11) and (2.1.13) that $dl/dr = 0$ and $de/dr = 0$ at $r = 3r_g$, thus one concludes that $r_{ms} = 3r_g$, as an orbit can be stable only when $dl/dr \geqslant 0$ and $de/dr \geqslant 0$. The efficiency of

conversion of gravitational potential energy into radiation is given by $\eta = e/c^2$, so that at $r = r_{ms}$ equation (2.1.10) yields the result $\eta = 0.0625$, while the correct result for the Schwarzschild metric is 0.057. At smaller radii the relative agreement is even closer. It is therefore expected that errors introduced by using this model will not be more than 10%, while calculations will be greatly simplified.

The fact that the Newtonian model of a black hole very accurately describes the motion of free particles around the hole suggests strongly that accretion flows would also be accurately described by the model. Of course, in order to have confidence, a direct comparison between exact general relativistic calculations and those based on the Newtonian model is necessary. This will be done in the next chapter. Obviously, the Newtonian model can only describe a spherically symmetric gravitational field; it does not work for a rotating, especially a rapidly rotating, black hole. In that case the correct general relativistic equations must be applied. This will also be a task of the next chapter.

2.2 The full set of time-dependent equations

The basic equations describing the accretion flow are (cf. Landau and Lifshitz 1959 or Tassoul 1978):

i)Equation of continuity or mass conservation

$$\frac{\partial \rho}{\partial t} + \nabla_i(\rho v^i) = 0 \ . \qquad (2.2.1)$$

ii)Euler's equation or momentum conservation

$$\frac{\partial v^i}{\partial t} + v^j \nabla_j v^i = -g^{ij} \nabla_j \Phi - \frac{1}{\rho} g^{ij} \nabla_j P \ . \qquad (2.2.2)$$

iii)Equation of state

$$P = k \rho^{1 + 1/n} \ . \qquad (2.2.3)$$

Here ρ , P and $v^i \equiv dx^i/dt$ are, respectively, the density, pressure and velocity of the accreted gas, Φ is the gravitational potential which is given by (2.1.4). The indices i and j run through 1, 2, 3. The Einstein summation convention is used. The symbol v^i denotes a component of the coordinate velocity, not the physical velocity. For example, $v^\phi = d\phi/dt = \Omega$ = (angular velocity). The symbol ∇_i denotes the covariant derivative in the 3-dimensional space with the metric g_{ij}. Spherical coordinates are used, therefore $g_{rr} = 1$, $g_{\theta\theta} = r^2$, $g_{\phi\phi} = r^2 \mathrm{Sin}^2\theta$ and all the off-diagonal components of the metric are equal to zero. All physical quantities depend on the time t and the spatial coordinates r and θ but not on ϕ (axially symmetric flow).

An appropriate boundary condition must be imposed on the free surface of the flow. First, on the surface the pressure goes to zero; second, there is no motion of matter (e.g. in the form of a wind)

accross the surface, i.e. the flow lines must lie on the surface. Combining the two conditions gives

$$\left(\frac{\partial P}{\partial t} + v^i \nabla_i P\right)_{P=0} = 0 . \qquad (2.2.4)$$

Because the transonic part of the flow is likely to be geometrically thin, i.e. $|\mathrm{Cos}\,\theta| \leqslant |\mathrm{Cos}\,\theta_o| \ll 1$, where θ_o denotes the value of the θ-coordinate for the flow surface, all the physical quantities can be expanded with respect to $\mathrm{Cos}\,\theta$. The expansion form

$$X(r, \theta, t) = X_0(r,t) + X_2(r,t)\mathrm{Cos}^2\theta + X_4(r,t)\mathrm{Cos}^4\theta + \ldots$$

is used for the quantities which are not identically zero on the equatorial plane (ρ, P, v^r, v^ϕ), and the expansion form

$$Y(r, \theta, t) = Y_1(r,t)\mathrm{Cos}\,\theta + Y_3(r,t)\mathrm{Cos}^3\theta + \ldots$$

for v^θ, which obeys $v^\theta(r, \frac{\pi}{2}, t) = 0$. The expansions are terminated at the lowest possible order which can guarantee that the model of the flow is both self-consistent and reasonably accurate.

The zeroth-order expansions of the basic equations (2.2.1)-(2.2.3) do not form a closed set, as five unknown quantities (ρ_o, P_o, v_o^r, v_1^θ, v_o^ϕ) appear in four equations :

$$\frac{\partial \rho_o}{\partial t} + \rho_o \frac{\partial v_o^r}{r} + v_o^r \frac{\partial \rho_o}{\partial r} + \frac{2}{r} \rho_o v_o^r - \rho_o v_1^\theta = 0 , \qquad (2.2.5)$$

$$\frac{\partial v_o^r}{\partial t} + v_o^r \frac{\partial v_o^r}{\partial r} - r(v_o^\phi)^2 + \frac{GM}{(r - r_g)^2} + \frac{1}{\rho_o} \frac{\partial P_o}{\partial r} = 0 , \qquad (2.2.6)$$

$$\frac{\partial v_o^\phi}{\partial t} + v_o^r \frac{\partial v_o^\phi}{\partial r} + \frac{2}{r} v_o^r v_o^\phi = 0 , \qquad (2.2.7)$$

$$P_o = k \rho_o^{1+1/n} . \qquad (2.2.8)$$

Note that one cannot simply drop the term $\rho_o v_1^\theta$ in equation (2.2.5). Although the quantity (rv^θ) is much smaller than v^r, it does not mean that $(rv_1^\theta) \ll v_o^r$, as $v_1^\theta \approx v^\theta/\cos\theta$. This indicates that the horizontal and vertical structures of the accretion flow are always linked. In the classical models the flow equations were split into a horizontal and a vertical part by assuming that the flow is quasi-radial, i.e. v^θ vanishes everywhere in the flow, but this is rather crude. In order to determine the flow properties on the equatorial plane in the most general study of the problem, one must undertake the task of solving the off-equatorial plane equations, which are of higher order.

Fortunately, it is enough to consider the first and second order equations to close the system:

$$\frac{\partial v_2^r}{\partial t} + v_o^r \frac{\partial v_2^r}{\partial r} + v_2^r \frac{\partial v_o^r}{\partial r} - 2v_1^\theta v_2^r - r(v_1^\theta)^2 - 2rv_o^\phi v_2^\phi + r(v_o^\phi)^2 - \frac{\rho_2}{\rho_o} \frac{\partial P_o}{\partial r} + \frac{1}{\rho_o} \frac{\partial P_2}{\partial r} = 0 , \qquad (2.2.9)$$

$$\frac{\partial v_1^{\theta}}{\partial t} + v_o^r \frac{\partial v_1^{\theta}}{\partial r} + \frac{2}{r} v_o^r v_1^{\theta} - (v_1^{\theta})^2 - (v_o^{\phi})^2 - \frac{2P_2}{r^2 \rho_o} = 0 \ , \qquad (2.2.10)$$

$$\frac{\partial v_2^{\phi}}{\partial t} + v_o^r \frac{\partial v_2^{\phi}}{\partial r} + v_2^r \frac{\partial v_o^{\phi}}{\partial r} - 2 v_1^{\theta} v_2^{\phi} + \frac{2}{r} v_o^r v_2^{\phi}$$

$$+ \frac{2}{r} v_2^r v_o^{\phi} + 2 v_1^{\theta} v_o^{\phi} = 0 \ , \qquad (2.2.11)$$

$$P_2 = k(1 + 1/n) \rho_o^{1/n} \rho_2 \ , \qquad (2.2.12)$$

$$P_2 \frac{\partial P_o}{\partial t} - P_o \frac{\partial P_2}{\partial t} + P_2 v_o^r \frac{\partial P_o}{\partial r} - P_o \frac{\partial P_2}{\partial r} v_o^r$$

$$- P_o v_2^r \frac{\partial P_o}{\partial r} + 2 P_o P_2 v_1^{\theta} = 0 \ . \qquad (2.2.13)$$

The last equation is obtained by expanding (2.2.4) up to the second order and replacing $\mathrm{Cos}^2\theta_o$ in the expansion with $-P_o/P_2$ because on the surface

$$P_* = P_o + P_2 \mathrm{Cos}^2\theta_o = 0 \ . \qquad (2.2.14)$$

This equation determines the shape of the flow,

$$\theta_o = \theta_o(r,t) \ . \qquad (2.2.15)$$

Note that although (2.2.13) is obtained from the boundary conditions, it should hold everywhere in the flow, because all the quantities in it are functions of r and t only.

The nine equations (2.2.5)-(2.2.13) form a closed, self-consistent system for the nine unknown functions ρ_0, P_0, v_0^r, v_0^ϕ, v_1^θ, ρ_2, P_2, v_2^r, v_2^ϕ. They enable one to discuss the full time dependent behaviour of the accretion flow.

It should be pointed out that the second order expansion is the lowest possible level for having a closed system, and it is not very accurate close to the surface. For example, on the surface of the flow not only the pressure, but also the density must be zero. However, from (2.2.8),(2.2.12) and (2.2.14) it follows that the surface density is

$$\rho_* = \rho_0 \frac{1}{n+1} \,. \qquad (2.2.15)$$

The source of the inaccuracy lies in equation (2.2.14) which implies that P_0 and $P_2 \mathrm{Cos}^2\theta_0$ are of the same order, and this is in conflict with the basic assumption concerning the expansion scheme, $P_0 \gg P_2 \mathrm{Cos}^2\theta$. Thus one can improve the scheme by replacing (2.2.14) with the more accurate expression

$$0 = P_0 + P_2 \mathrm{Cos}^2\theta_0 + P_4 \mathrm{Cos}^4\theta_0 + \ldots \qquad (2.2.16)$$

and accordingly, going to the higher order expansion. Note that the system can always be closed at any even order. For example, one has 14 equations for 14 unknown functions at the fourth order. Generally, at the $2n^{th}$ order there are (5n+4) equations for the same amount of unknown functions.

2.3 Reduction of the basic equations in the stationary case

In the stationary case (i.e. $\frac{\partial}{\partial t} = 0$) all the functions depend on r only, so equations (2.2.5)-(2.2.13) reduce to

$$\rho_o \frac{dv_o^r}{dr} + v_o^r \frac{d\rho_o}{dr} + \frac{2}{r}\rho_o v_o^r - \rho_o v_1^\theta = 0 , \tag{2.3.1}$$

$$v_o^r \frac{dv_o^r}{dr} - r(v_o^\phi)^2 + \frac{GM}{(r - r_g)^2} + \frac{1}{\rho_o}\frac{dP_o}{dr} = 0 , \tag{2.3.2}$$

$$\frac{dv_o^\phi}{dr} + \frac{2}{r} v_o^\phi = 0 , \tag{2.3.3}$$

$$v_o^r \frac{dv_2^r}{dr} + v_2^r \frac{dv_o^r}{dr} - 2v_1^\theta v_2^r - r(v_1^\theta)^2 - 2rv_o^\phi v_2^\phi$$

$$+ r(v_o^\phi)^2 - \frac{\rho_2}{\rho_o^2}\frac{dP_o}{dr} + \frac{1}{\rho_o}\frac{dP_2}{dr} = 0 , \tag{2.3.4}$$

$$v_o^r \frac{dv_1^\theta}{dr} + \frac{2}{r}v_o^r v_1^\theta - (v_1^\theta)^2 - (v_o^\phi)^2 - \frac{2P_2}{r^2\rho_o} = 0 , \tag{2.3.5}$$

$$v_o^r \frac{dv_2^\phi}{dr} - 2v_1^\theta v_2^\phi + \frac{2}{r}v_o^r v_2^\phi + 2v_1^\theta v_o^\phi = 0 , \tag{2.3.6}$$

$$P_2 v_o^r \frac{dP_o}{dr} - P_o v_o^r \frac{dP_2}{dr} - P_o v_2^r \frac{dP_o}{dr} + 2P_o P_2 v_1^\theta = 0 , \tag{2.3.7}$$

$$P_o = k\rho_o^{1+1/n} , \tag{2.3.8}$$

$$P_2 = k(1 + 1/n)\rho_o^{1/n}\rho_2 . \tag{2.3.9}$$

The system consists of seven ordinary differential equations and two algebraic equations. Some of the differential equations, or their combinations, can be integrated directly. To present the results of these integrations and discuss the physical meaning of the integration constants it is convenient to define the following quantities:

$$\text{(sound velocity)} = a = (dP/d\rho)^{1/2} ,$$

$$\text{(specific angular momentum)} = l = r^2 v^{\phi} ,$$

(specific total energy) = e

$$= \frac{1}{2}\left[(v^r)^2 + (rv^{\theta})^2 + (rv^{\phi})^2\right] - \frac{GM}{r - r_g} + na^2 ,$$

$$\text{(mass accretion rate)} = \dot{m} = 4\pi r^2 \rho v^r \omega ,$$

where $\omega \equiv |\theta_o - \frac{\pi}{2}|$ is the half-opening angle of the flow, and expand them as follows:

$$a^2(r,\theta) = a_o^2(r) + a_2^2(r)\cos^2\theta + \ldots$$

$$l(r,\theta) = l_o(r) + l_2(r)\cos^2\theta + \ldots$$

$$e(r,\theta) = e_o(r) + e_2(r)\cos^2\theta + \ldots$$

$$\dot{m}(r) = \dot{m}_o(r)\omega(r) + \ldots$$

where

$$a_o^2 = k(1 + 1/n)\,\varrho_o^{1/n} , \tag{2.3.10}$$

$$a_2^2 = k(1 + 1/n)\,\frac{1}{n}\varrho_o^{1/n - 1}\varrho_2 , \tag{2.3.11}$$

$$l_o = r^2 v_o^{\phi} , \tag{2.3.12}$$

$$l_2 = r^2 v_2^{\phi} - r^2 v_o^{\phi} , \tag{2.3.13}$$

$$e_o = \frac{1}{2}(v_o^r)^2 + \frac{1}{2}\, l_o^2/r^2 - \frac{GM}{r - r_g} + na_o^2 , \tag{2.3.14}$$

$$e_2 = v_o^r v_2^r + \frac{1}{2}(rv_1^{\theta})^2 + l_o l_2/r^2 + \frac{1}{2}\, l_o^2/r^2 + 2na_o a_2 , \tag{2.3.15}$$

$$\dot{m}_o = 4\pi r^2 \varrho_o v_o^r = 4\pi r^2 \left(\frac{n}{k(1+n)}\right)^n a_o^{2n} v_o^r , \tag{2.3.16}$$

$$\omega = \left(-\frac{1}{2(n+1)}\,\frac{a_o}{a_2}\right)^{1/2} . \tag{2.3.17}$$

It is seen from (2.3.3) and (2.3.12) that l_o = const. and from (2.3.2) and (2.3.14) that e_o = const. The physical meaning of l_o and e_o is obvious: they are connected with conservation of angular momentum and energy along the fluid lines in the equatorial plane. In the stationary case the mass accretion rate $\dot{m}$ must be a constant, thus by using (2.3.1) and (2.3.16) one gets

$$\frac{d\omega}{dr} = -\omega \frac{v_1^{\theta}}{v_o^r} . \tag{2.3.18}$$

With the help of (2.3.17) and (2.3.18), it follows from (2.3.6) and (2.3.13) that

$$l_2 = C_l(a_2/a_o) \ , \tag{2.3.19}$$

and from (2.3.4) and (2.3.15) that

$$e_2 = C_e(a_2/a_o) \ , \tag{2.3.20}$$

where C_l and C_e are constants. To see the physical meaning of them, consider the vorticity tensor

$$\omega_{ij} = \frac{\partial v^i}{\partial x^j} - \frac{\partial v^j}{\partial x^i} \ . \tag{2.3.21}$$

The only non-zero components of this tensor are

$$\omega_{r\theta} = -\omega_{\theta r} = \frac{2}{v_o^r}(e_2 - v_o^{\phi} l_2) \ ,$$
$$\omega_{\theta\phi} = -\omega_{\phi\theta} = -2l_2 \ . \tag{2.3.22}$$

The choice $e_2 = l_2 = 0$, which is equivalent to $C_e = C_l = 0$, makes the vorticity tensor identically equal to zero. When $\omega_{ij} = 0$ the velocity can be, at least locally, expressed as a gradient of a scalar function, $v_i = \nabla_i \psi$. In this case the flow is called potential. For a potential flow, the energy and angular momentum are conserved not only along a

fluid line, but also throughout the flow. Thus one has (see also Carter 1979)

$$\left(\begin{array}{l}\text{The flow is}\\ \text{potential, i.e.}\\ \omega_{ij} = 0\end{array}\right) \Rightleftharpoons \left(\begin{array}{l}C_l = 0\\ C_e = 0\end{array}\right) \Rightleftharpoons \left(\begin{array}{l}\text{Energy and angular}\\ \text{momentum do not}\\ \text{depend on position}\end{array}\right)$$

It has been seen that there are seven first-order ordinary differential equations in the problem, and five independent integration constants (e_o, l_o, $\dot{m}$, C_e, C_l) are known, which means that the problem can be reduced to two first-order ordinary differential equations for two unknown functions. These two functions could be

$$v(r) \equiv v_o^r \ , \qquad v_\theta(r) \equiv r\, v_l^\theta \ . \tag{2.3.23}$$

After some tedious but straightforward algebra one obtains

$$\frac{dv}{dr} = v\,\frac{(B-2)a_o^2 r^2 - (l_o^2 - l_k^2)}{r^3(a_o^2 - v^2)} \ , \tag{2.3.24}$$

$$\frac{dv_\theta}{dr} = \frac{\left[Cr^4 a_o^{2(2n+1)} + B(B-1)\right] v^2 r^2 + l_o^2}{r^3 v} \ , \tag{2.3.25}$$

where

$$B \equiv v_\theta / v \ , \tag{2.3.26}$$

$$l_k^2(k) \equiv GMr^3/(r - r_g)^2 \tag{2.3.27}$$

is the Keplerian angular momentum distribution, and a_o can be algebraically expressed in terms of v:

$$a_o \equiv \frac{1}{\sqrt{n}}\left[e_o - \frac{1}{2}v^2 - \frac{1}{2}l_o^2/r^2 + \frac{GM}{r - r_g}\right]^{1/2} . \qquad (2.3.28)$$

The constant C depends on the accretion rate,

$$C = -32\pi^2 k^{-2n}\left(\frac{n}{n+1}\right)^{2n+1} \dot{m}^{-2} . \qquad (2.3.29)$$

By an examination of equations (2.3.24) and (2.3.25) one deduces the following important points:

a) They are horizontal structure equations, as the quantities appearing in them are all defined on the equatorial plane. Solving for v(r) and $v_\theta(r)$ from given boundary conditions and constants l_o, e_o and $\dot{m}$, the horizontal structure of the flow is completely determined as

$$v_o^\phi(r) = l_o/r^2 , \qquad (2.3.30)$$

$$\rho_o(r) = \left[\frac{n}{k(n+1)}\right]^n a_o^{2n} , \qquad (2.3.31)$$

$$P_o(r) = k^{-n}\left(\frac{n}{n+1}\right)^{n+1} a_o^{2(n+1)} . \qquad (2.3.32)$$

b) The two equations do not depend on the integration constants C_l and C_e. Therefore, without any loss of generality one can put

$C_e = C_1 = 0$, i.e. assume that the flow is potential. This may sometimes be convenient, since there are many important theorems concerning potential flows.

c) Once the horizontal structure is solved, the vertical structure is explicitly given by

$$a_2 = \frac{8\pi^2}{n+1}\left[\frac{n}{k(n+1)}\right]^{2n} \dot{m}^{-2} r^4 a_o^{4n+1} v^2 , \qquad (2.3.33)$$

$$\varrho_2 = 2n\left[\frac{n}{k(n+1)}\right]^{n} a_2 a_o^{2n-1} , \qquad (2.3.34)$$

$$P_2 = 2n\left[\frac{n}{k(n+1)}\right]^{n} a_2 a_o^{2n+1} , \qquad (2.3.35)$$

$$v_2^{\Phi} = \frac{C_1}{r^2}(a_2/a_o) + v_o^{\Phi} , \qquad (2.3.36)$$

$$v_2^{r} = \frac{1}{v}\left[C_e(a_2/a_o) - \frac{1}{2}(Bv)^2 - \frac{1}{2} l_o^2/r^2 - C_1(a_2/a_o) l_o/r^2 - 2na_o a_2\right] . \qquad (2.3.37)$$

Thus the whole problem of the stationary, geometrically thin, dissipation-free accretion flow onto a black hole has been reduced to only two first-order non-linear differential equations for the functions $v(r)$ and $v_\vartheta(r)$ by exact analytic integration of the remaining five differential equations. In the next three sections the critical points and global solutions of the two equations will be discussed.

2.4 The critical point of the radial motion equation

Equation (2.3.24) can be wtitten symbolically as

$$\frac{dv}{dr} = N/D \ . \qquad (2.4.1)$$

The denominator D vanishes at the sonic point ($v=a_o$), and the numerator N must vanish as well, in order to have a regular solution. The point where both D and N vanish is a 'critical point' of (2.4.1) in the usual mathematical sense of the term (cf. Birkhoff and Rota 1969). Note that (2.3.25) has no critical points and thus does not give any additional conditions. Therefore, if one chooses the values of v and B at the sonic point, v_s and B_s, as the two integration constants needed to solve equations (2.3.24) and (2.3.25), the two (and only two) sonic point conditions, D = 0 and N = 0, give two constraints on three quantities: v_s, B_s and the sonic radius r_s. One of them is therefore a free parameter and must be specified, in addition to the three constants already appearing in the two equations. It is concluded that in general one must specify four independent parameters to determine the adiabatic, regular accretion flow in the equatorial plane of a black hole. These parameters could be: l_o, e_o, $\dot{m}$ and B_s.

If the vertical structure of the flow is also considered, two additional integration constants (e_2, l_2) are needed. Thus the regularity condition of the transonic solution

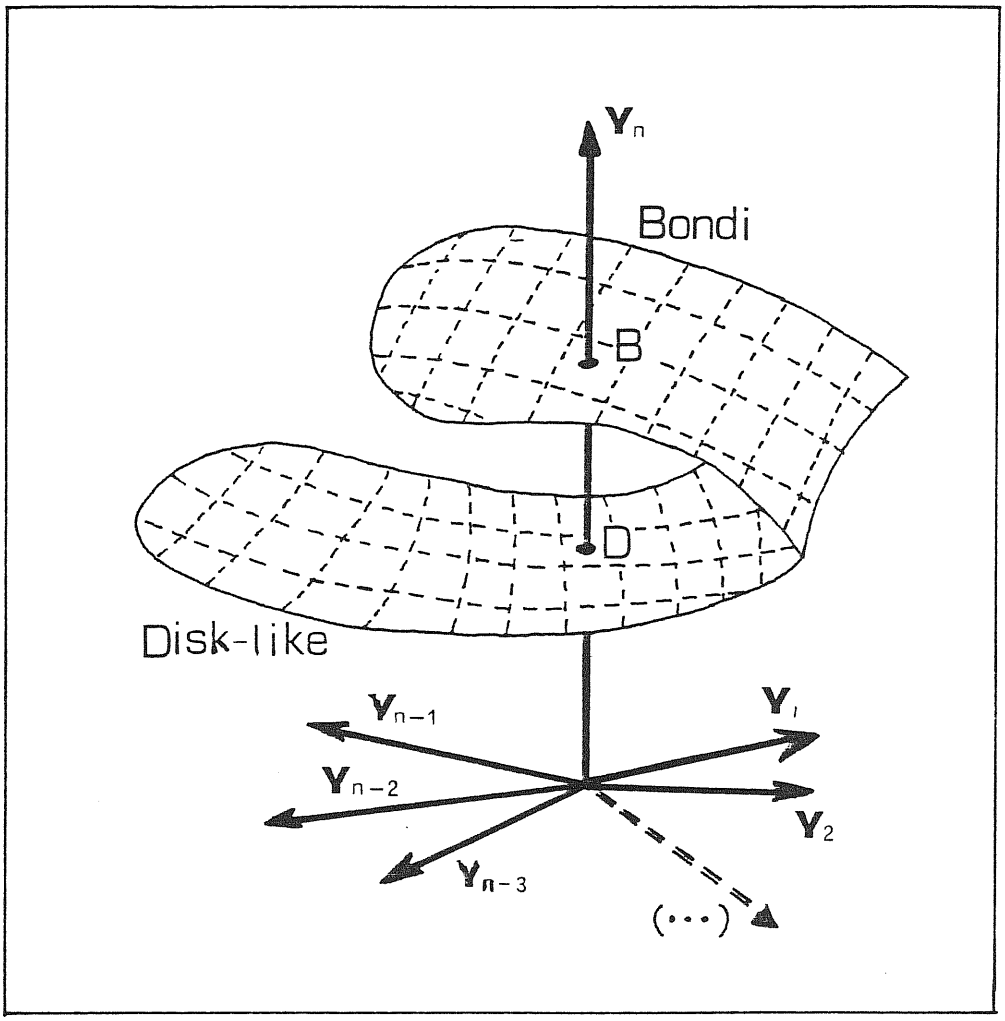

Fig. 4 In the general case the condition for the regular, stationary accretion reduces the number of free parameters (hypersurface shown here has less dimensions than the original parameter space). The bending defines two modes of accretion (see text).

$$F(l_o, C_l, e_o, C_e, \dot{m}, v_s, B_s) = 0 \qquad (2.4.2)$$

reduces the number of free parameters from seven to six. The six-dimensional (or multi-dimensional in the realistic case) hypersurface $F = 0$ is folded in the seven-dimensional (or higher dimensional) parameter space (Figure 4).

It should not be a surprise that six parameters are needed in the general case and only one for Bondi's spherical accretion. The reason for this can be seen more clearly by writing (2.4.2) in an equivalent way

$$F(l_o, C_l, e_o, C_e, \dot{m}, \omega_s, B_s) = 0 \ . \qquad (2.4.3)$$

In the Bondi case $l_o = C_l = C_e = B_s = 0$, and $\omega_s = 1$, so that (2.4.3) reduces to

$$F(e_o, \dot{m}) = 0 \ . \qquad (2.4.4)$$

The regularity condition also reduces the number of the free parameters by one.

The sonic point conditions $D = 0$ and $N = 0$ can be combined with the laws of angular momentum, energy and mass conservation, (2.3.12), (2.3.14) and (2.3.16), and then written in the dimensionless form as

$$V_s^2 (2 - B_s) = \frac{1}{R_s^2}\left[\frac{R_s^3}{2(R_s - 1)^2} - L^2\right] , \qquad (2.4.5)$$

$$E = (\frac{1}{2} + n)\, V_s^2 + \frac{1}{2} L^2/R_s^2 - \frac{1}{2(R_s - 1)} , \qquad (2.4.6)$$

$$\dot{M} = \dot{M}_o \omega_s = R_s^2\, V_s^{2n+1}\, \omega_s , \qquad (2.4.7)$$

by introducing the dimensionless variables

$$R = r/r_g,\ V = v/c,\ A = a/c,\ L = l_o/r_g c,\ E = e_o/c^2,$$

$$\dot{M} = \dot{m}\, k^n (1 + 1/n)^n / 4\pi r_g^2\, c^{2n+1} ,$$

where the subscript s denotes the values at the sonic point. From equations (2.4.5), (2.4.6) and (2.4.7) one can deduce how the location of the sonic point R_s, the radial velocity and the angular opening of the flow at the sonic point, V_s and ω_s, depend on the four parameters L, E, $\dot{M}$ and B_s which characterize the flow.

Before going on to the detailed calculations, however, it is worth stating some general constraints on the transonic accretion which can be obtained immediately. From equation (2.4.5) and the condition $B_s < 2$ one gets (cf (2.3.27))

$$L^2 < \frac{R_s^3}{2(R_s - 1)^2} = L_k^2(R_s) , \qquad (2.4.8)$$

which means that at the sonic point the angular momentum of a fluid element must be less than the corresponding Keplerian value. This was

noticed by Abramowicz and Zurek (1981) in the $B_s = 0$ case.

From equation (2.3.14) one gets (cf, also (2.4.6))

$$L^2 < 2R^2E + \frac{R^2}{R-1} \equiv f(E,R) \ . \qquad (2.4.9)$$

This inequality gives a necessary condition for the energy of the fluid element to be high enough to overcome the potential barrier connected with rotation. The function f(E,R) has a minimum

$$f_{min}(E) = \frac{\left[(1+16E)^{1/2} + 8E - 1\right]^2 \left[(1+16E)^{1/2} + 3\right]}{32E\left[(1+16E)^{1/2} - 1\right]} \ . \qquad (2.4.10)$$

Since L = const, inequality (2.4.9) implies that for the accretion to be possible, it is necessary that the condition

$$L^2 < f_{min}(E) \qquad (2.4.11)$$

be satisfied.

By combining equations (2.4.6) and (2.4.5) with the requirement $2n > 1 - B_s$ one gets

$$E > \frac{R_s}{4(R_s-1)^2} - \frac{1}{2(R_s-1)} = g(R_s) \ . \qquad (2.4.12)$$

Another necessary condition for the accretion to be possible is therefore

$$E > g_{min}(R_s) = -1/16 \ . \qquad (2.4.13)$$

The physical meaning of this condition will be seen below.

Note that $\dot{M}$ is not needed to determine R_s and V_s. These two quantities can be computed from given E, L and B_s through equations (2.4.5) and (2.4.6). By eliminating V_s between these two equations, one gets

$$\frac{4(2 - B_s)E}{2n + 1} R_s^2 (R_s - 1)^2 + \frac{2(2 - B_s)}{2n + 1} R_s^2 (R_s - 1) - R_s^3$$

$$+ \left[2 - \frac{2(2 - B_s)}{2n + 1}\right] L^2 (R_s - 1)^2 = 0 \ . \qquad (2.4.14)$$

For $B_s = 0$* and n = 3 the solution for $R_s = R_s(E,L)$ is shown in Figure 5. In the case of negative energy (Figure 5a), the transonic

---

* When $B_s \neq 0$ the location of the sonic point is shifted inwards or outwards, but the graphs have similar features as those for $B_s = 0$.

Fig. 5 The location of the sonic point as a function of the energy and angular momentum, for n = 3 and $B_s = 0$. Fig. 5a is for $E < 0$, and Fig. 5b $E \geq 0$. The heavy line corresponds to the Keplerian distribution of angular momentum. The dashed parts of the curves show unphysical critical points. Points in the dark region would correspond to a solution with $V_s^2 < 0$, which is impossible. Note that accretion can occur only for $E \geq -1/16$ and that for $0 < E < E_c \approx 0.02$ there are three different locations of the sonic point (e.g. points A,B,C). However, the points which are located on the parts of $L^2(R_s)$ curves with a positive slope do not represent a physical solution.

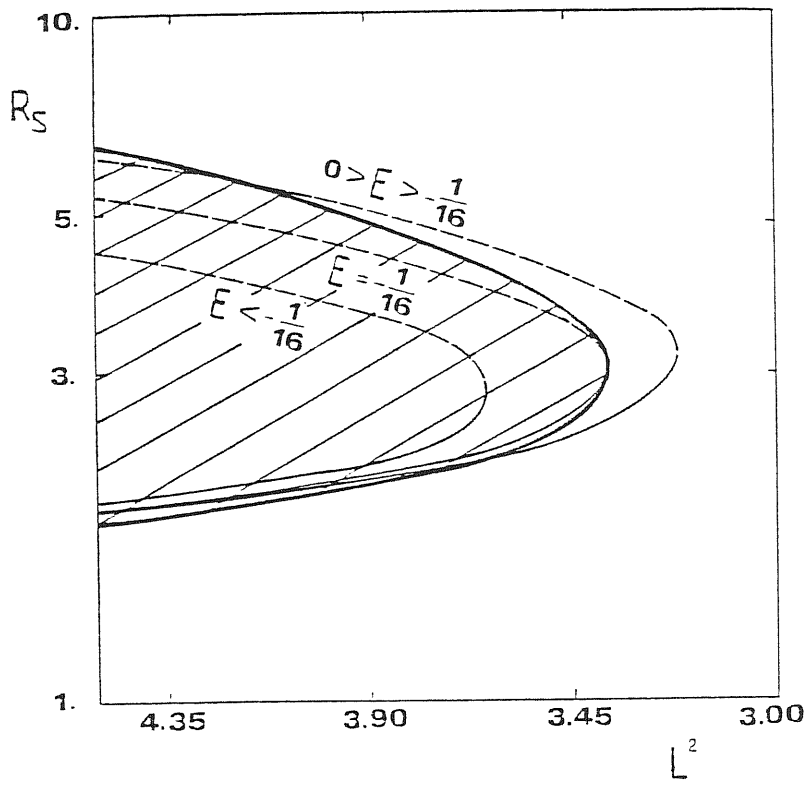
10.
R_S
5.
3.
1.
$0 > E > -\frac{1}{16}$
$E = -\frac{1}{16}$
$E < -\frac{1}{16}$
4.35
3.90
3.45
3.00
L^2

(a)

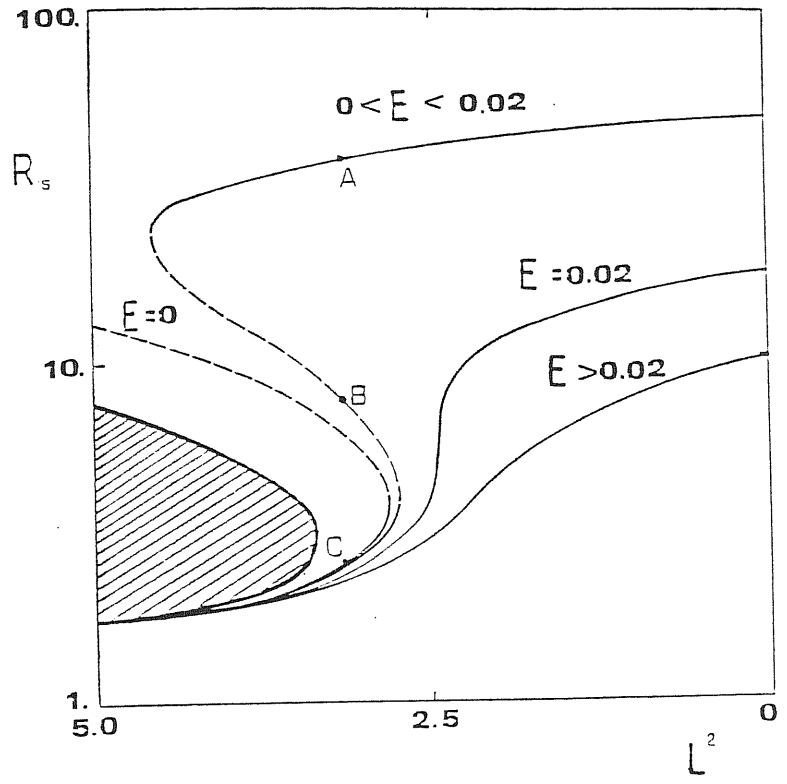
100.
R_s
10.
1.
$0 < E < 0.02$
A
$E = 0.02$
$E = 0$
$E > 0.02$
B
C
5.0
2.5
0
L^2

(b)

Figure 5

solution exists only for $E \geqslant -1/16$. For $E < -1/16$, the angular momentum is always larger than the corresponding Keplerian value, and this violates the condition (2.4.8). Muchotrzeb (1983a) examined the conditions for transonic accretion flows with dissipation using numerical models. She found that for thin flows, stationary transonic accretion does not exist if the α-viscosity is bigger than a critical value $\alpha_{crit} \approx 0.02$. Her critical solution has a sonic point at $R_s = R_{ms} = 3$, which is just the tangent point of the Keplerian angular momentum distribution curve and the curve of $L^2(R_s)$ when the energy $E = -1/16$, the critical value of the energy for the existence of a stationary transonic solution. Thus the condition (2.4.13) provides the physical explanation of her numerical result.

More interesting is the case of positive energy (Figure 5b, which is similar to a corresponding figure in Abramowicz and Zurek 1981). For a fixed pair of L and E there are three possibilities. The transonic solution does not exist at all when the energy is too low to overcome the potential barrier connected with the centrifugal force: $E < E_{Barr}(L)$ (cf. (2.4.9), (2.4.11) and Figure 3). When $E > E_c$ ($E_c \approx 0.02$ for $B_s = 0$), the location of the sonic point is always unique. In the most interesting case $E_{Barr} < E < E_c$ there are formally three locations of the sonic point (e.g. points A, B and C in Figure 5b). The first question is then: are all the three formal sonic points physically possible? Muchotrzeb (1983b) has pointed out that only two of them correspond to physically possible flows. Her conclusion can be examined and improved as follows.

Rewrite equation (2.4.1) in the dimensionless form

$$\frac{dV}{dR} = N/D \qquad (2.4.15)$$

where

$$N = \frac{1}{n}\left[E + \frac{1}{2(R-1)} - \frac{V^2}{2} - \frac{L^2}{2R^2}\right]\left(\frac{V_\theta}{R} - \frac{2V}{R}\right) - \frac{L^2 V}{R^3} + \frac{V}{2(R-1)^2} \quad ,$$

$$D = \frac{1}{n}\left[E + \frac{1}{2(R-1)} - \frac{L^2}{2R^2} - \frac{7V^2}{2}\right] . \qquad (2.4.16)$$

This is a non-linear differential equation. In the case where V_θ is nearly constant in the vicinity of the sonic point*, equation (2.4.15) can be linearized around the point as

$$\begin{bmatrix} d\,\delta V \\ d\,\delta R \end{bmatrix} = \begin{bmatrix} d & c \\ b & a \end{bmatrix} \begin{bmatrix} \delta V \\ \delta R \end{bmatrix} = A \begin{bmatrix} \delta V \\ \delta R \end{bmatrix} \quad , \qquad (2.4.17)$$

where

$$\delta V = V - V_s \quad , \qquad \delta R = R - R_s \quad ,$$

$$a = \left(\frac{\partial D}{\partial R}\right)_s \quad , \quad b = \left(\frac{\partial D}{\partial V}\right)_s \quad , \quad c = \left(\frac{\partial N}{\partial R}\right)_s \quad , \quad d = \left(\frac{\partial N}{\partial V}\right)_s \quad , \qquad (2.4.18)$$

---

* This assumption does not contradict the system (2.3.24), (2.3.25), and it makes the following analysis possible. Otherwise, the only way to examine the nature of a critical point of (2.4.15) is to use numerical methods.

the subscript in the partial derivatives, s, denotes their values at the sonic point. The nature of the critical point of the linearlized system (2.4.17) is completely determined by the set of two eigenvalues of the matrix A, and the critical point of (2.4.15) has essentially the same nature as that of (2.4.17) which is derived from it by taking the linear terms of the Taylor expansion for N and D (cf. e.g. Hurewicz 1958, Holzer 1977). The eigenvalues k_1 and k_2 of A can be obtained by solving the equation

$$\begin{vmatrix} d-k & c \\ b & a-k \end{vmatrix} = k^2 - (a + d)k + (ad - bc) = 0 \ . \qquad (2.4.19)$$

The classification of the critical point is given in Table 1.

Table 1. Classification of the critical point

$a + d$	sign $(ad - bc)$	k_1, k_2	critical point
$= 0$	+	purely imaginary	vortex
	−	real and of opposite sign	saddle
$\neq 0$	+	real and of the same sign, or complex	spiral or nodal
	−	real and of opposite sign	saddle

For the problem at hand, one can obtain, after some algebra:

$$a + d = -B_s V_s^2 / R_s \ , \qquad (2.4.20)$$

$$\text{sign}(ad - bc) = \text{sign}\left(\frac{dL^2}{dR_s}\right) \ . \qquad (2.4.21)$$

Here dL^2/dR_s denotes the slope of the curves $L^2(R_s)$ in Figure 5. When the slope is negative the corresponding critical point is always of the saddle type. When the slope is positive the critical point is of the vortex type for $B_s = 0$, and of the spiral or nodal type for $B_s \neq 0$. Numerical examples showing different types of critical point are given in Figure 6. Only a saddle type critical point corresponds to a physically possible sonic point, as only in this case there exists one characteristic passing regularly through the critical point (there is another characteristic having the same behaviour, but it represents the transition from subsonic to supersonic flow in the opposite direction, i.e. effluxion, rather than accretion). For the vortex type the critical point is located at the centre of a family of ellipses, so it can never be passed by any characteristic. For the spiral type, the critical point

---

Fig. 6 Types of the critical point (sonic point), for $n = 3$, $L^2 = 3.2$, $E = 0.006$. Fig. 6a is for the inner critical point. Fig. 6b and 6c the middle critical point, $B_s = 0$ and $B_s \neq 0$, respectively. Fig. 6d the outer critical point. The middle critical points, located on those parts of the $L^2(R_s)$ curves which have a positive slope, are unphysical. The physically possible solution is shown by a heavy line in Fig. 6a and 6d.

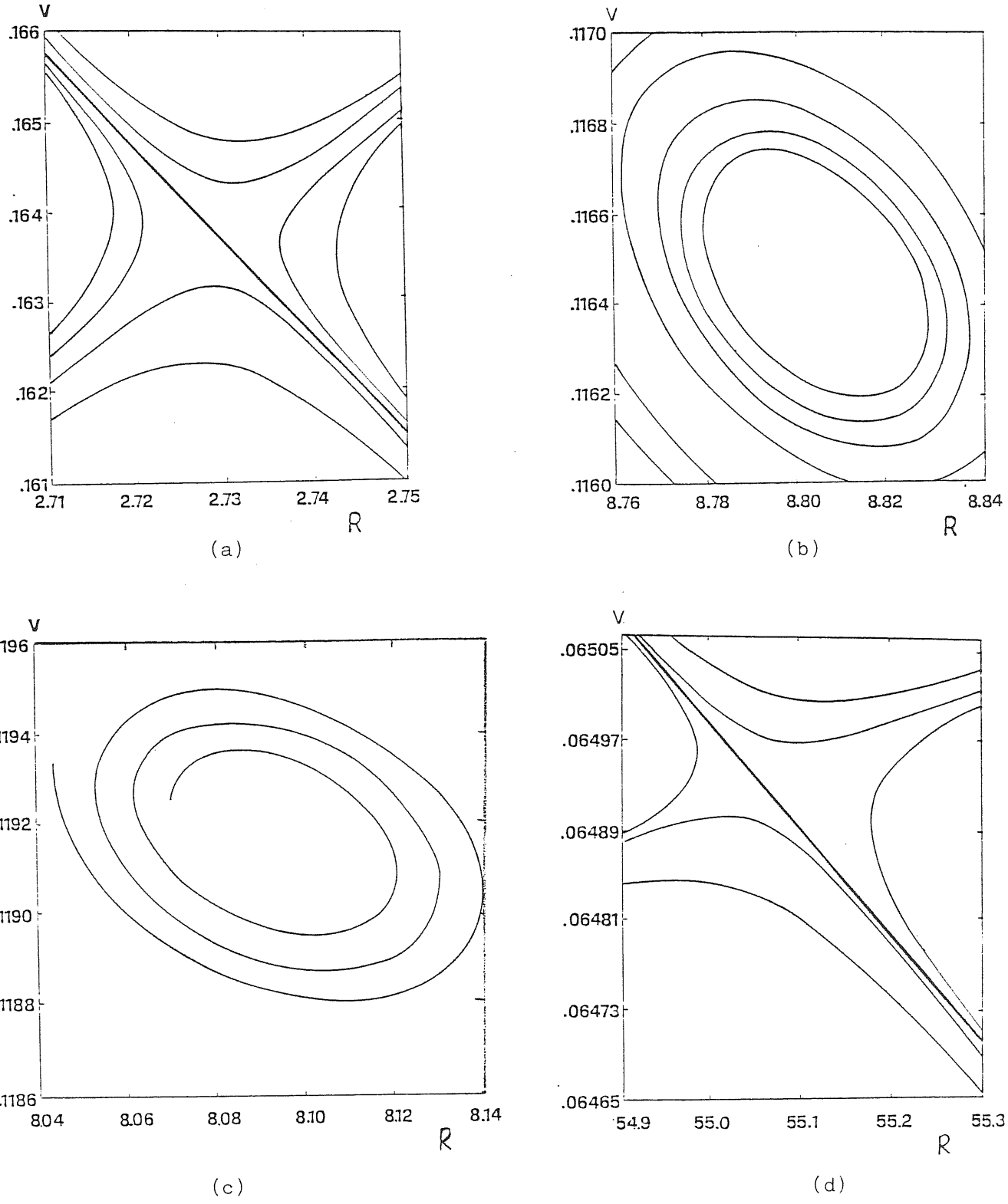
V
.166
.165
.164
.163
.162
.161
2.71
2.72
2.73
2.74
2.75
R
(a)
V
.1170
.1168
.1166
.1164
.1162
.1160
8.76
8.78
8.80
8.82
8.84
R
(b)
V
0.1196
0.1194
0.1192
0.1190
0.1188
0.1186
8.04
8.06
8.08
8.10
8.12
8.14
R
(c)
V
.06505
.06497
.06489
.06481
.06473
.06465
54.9
55.0
55.1
55.2
55.3
R
(d)

Figure 6

appears as tre terminus of all characteristics, it can be reached only after infinite spiraling. Thus these two types of critical point do not represent physical sonic points. It is concluded that, for negative energy, of the two formal sonic points corresponding to the same pair of E and L, only the inner one is physical (Fig. 5a) (this is consistent with the numerical results of Muchotrzeb 1983a and of Matsumoto et al. 1984 for transonic flows with dissipation). In the case of positive energy, there are two physically possible locations of the sonic point for a given pair of E and L (the outer one A and the inner one C, while the intermediate one B is always unphysical, see Fig. 5b).

It should, however, be noticed that the above examination is performed only locally, i.e. only in the vicinity of the critical point. There is yet another question which should be answered: does a locally physical sonic point represent a globally realizable transonic solution? In the case of a unique sonic point, it seems reasonable that there must be a (unique) transonic solution. When the location of the sonic point is non-unique, however, the question becomes more interesting and less transparent: is the global transonic solution also non-unique? The answer to this question is given in the next two sections.

2.5 Global solution: quasi-radial flow

In this section a simple case is studied. It is assumed that the

meridional velocity of the accreted gas vanishes everywhere in the flow, $V^{\theta} \equiv 0$. In this case the flow is termed quasi-radial. Then the system (2.4.5)-(2.4.7) reduces to

$$2 V_s^2 = \frac{1}{R_s^2}\left[\frac{R_s^3}{2(R_s - 1)^2} - L^2\right] , \qquad (2.5.1)$$

$$E = (\frac{1}{2} + n)V_s^2 + \frac{1}{2} L^2/R_s^2 - \frac{1}{2(R_s - 1)} , \qquad (2.5.2)$$

$$\dot{M}_o = \dot{M}/\omega_s = R_s^2 V_s^{2n+1} . \qquad (2.5.3)$$

Equations (2.5.1) and (2.5.2) enable one to obtain R_s and V_s from a given pair of E and L. When R_s and V_s are evaluated, the specific mass accretion rate, $\dot{M}_o$, is determined from equation (2.5.3). It is seen from (2.3.18) that for a quasi-radial flow, the opening angle of the flow, ω, is a constant, and thus $\dot{M}_o$ is also conserved in space. Note that (2.5.1) is the regularity condition which holds only at the sonic point, while (2.5.2) and (2.5.3) are versions of the laws of energy and mass conservation at the sonic point. They are in general (cf. (2.3.14) and (2.3.16)):

$$E = \frac{1}{2} V^2 + n A^2 + \frac{1}{2} L^2/R^2 - \frac{1}{2(R - 1)} , \qquad (2.5.4)$$

$$\dot{M}_o = R^2 A^{2n} V . \qquad (2.5.5)$$

Having E, L, and accordingly $\dot{M}_o$, these two equations can be used to

solve for V and A at any radial distance R, i.e. the global solution of the accretion is obtained by solving the two algebraic equations (2.5.4) and (2.5.5); there is no need to solve differential equation (2.3.24).

A global physically acceptable solution must satisfy the following conditions:

a) It passes through the critical point (sonic point) regularly.

b) After passing the sonic point, it remains supersonic until the black hole horizon.

c) Before reaching the sonic point, it is subsonic out to infinity.

d) It satisfies the boundary condition at infinity, i.e. $V \longrightarrow 0$ when $R \longrightarrow \infty$.

It is known from the last section that for $E_{Barr} < E < E_c$ there exist two physically possible locations of the sonic point, the inner one $R_s^{(1)}$ and the outer one $R_s^{(2)}$, $R_s^{(1)} < R_s^{(2)}$, and two different values of the radial velocity at the sonic point, $V_s^{(1)} > V_s^{(2)}$. In general they determine two different accretion rates. Figure 7 shows all the three

---

Fig. 7 Global solutions of stationary, quasi-radial, transonic accretion. The coordinates V/A and R are, respectively, the Mach number and the spherical radius scaled with the gravitational radius r_g. There exist two saddle type (X-shape) critical (sonic) points and one unphysical vortex (O-shape) critical point. The physically realized solution is shown by a heavy line. For $L < L_c$ the solution is of Bondi-type (Fig. 7a), while for $L > L_c$ it is of disk-type (Fig. 7c). In the case $L = L_c$ the physical solution is not unique (Fig. 7b).

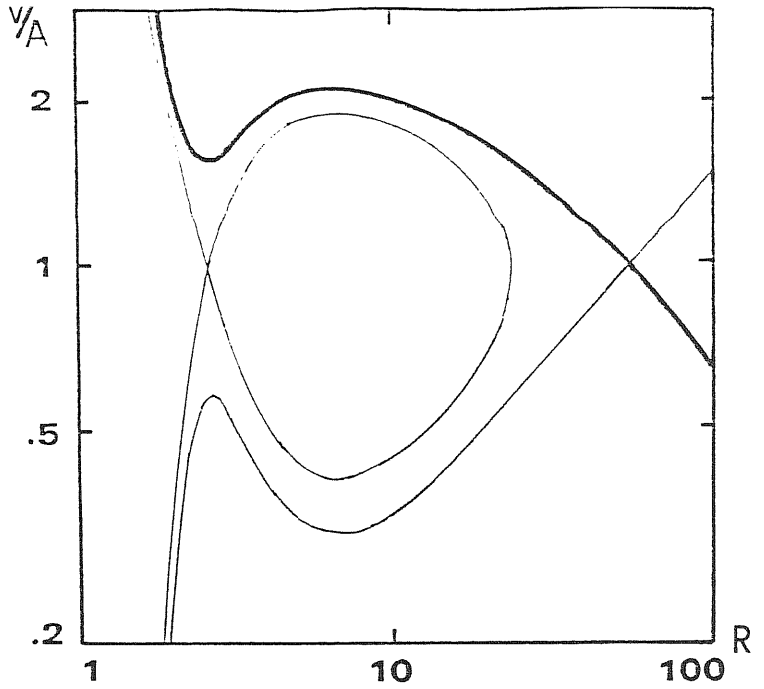

(a)

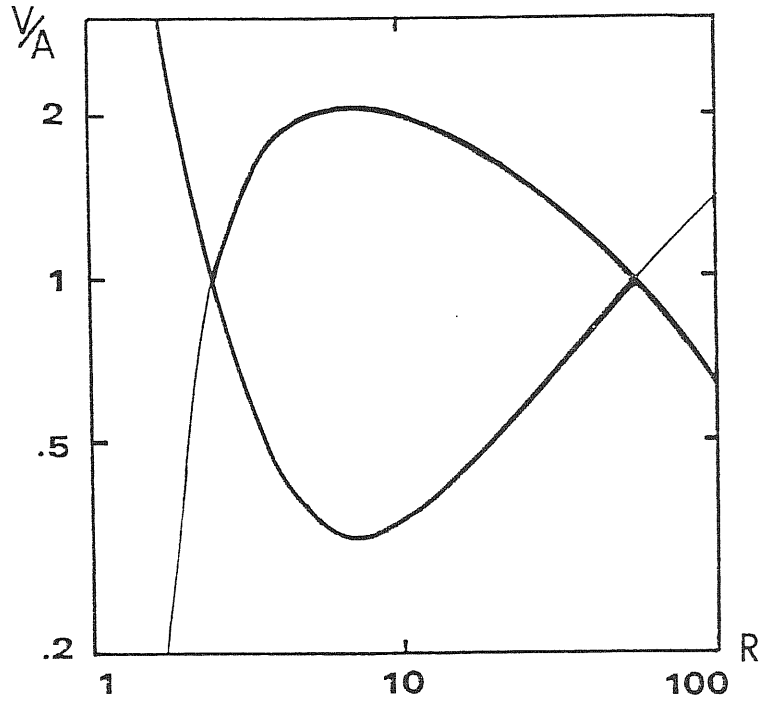

(b)

Figure 7

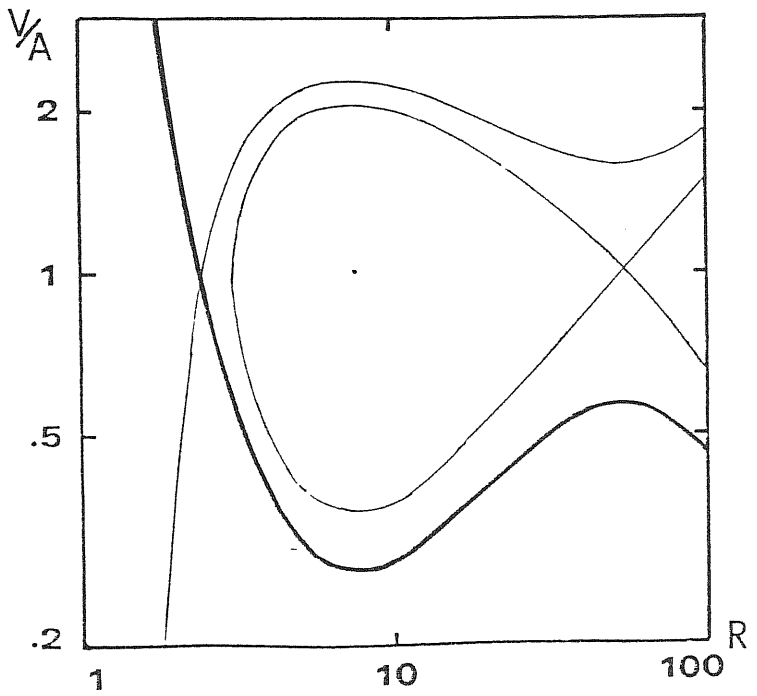

(c)

possible cases of the global solution. For a given E, there is a strictly defined value of angular momentum, $L_c = L_c(E)$. When $L \neq L_c$ the physical global solution is unique, and is always realized for the smaller of the two formal accretion rates, $\dot{M}_o^{(1)}$ and $\dot{M}_o^{(2)}$. For $L < L_c$ (Figure 7a) the global solution passes through the outer sonic point $R_s^{(2)}$, with accretion rate $\dot{M}_o^{(2)}$ smaller than the unrealizable one $\dot{M}_o^{(1)}$; $\dot{M}_o^{(2)} < \dot{M}_o^{(1)}$. For $L > L_c$ (Figure 7c) only the inner sonic point $R_s^{(1)}$ corresponds to a physical global solution, and the realizable accretion rate is again the smaller, $\dot{M}_o^{(1)} < \dot{M}_o^{(2)}$. When $\dot{M}_o^{(1)} = \dot{M}_o^{(2)}$, which happens only when $L = L_c$ (Figure 7b), the global solution is not unique: both $R_s^{(1)}$ and $R_s^{(2)}$ are possible as the sonic point. It is also seen from Figure 7 that both the inner and the outer critical points are of saddle type, while the intermediate one is of vortex type, consistent with the local analysis made in the last section.

The behaviour of the location of the sonic point as the angular momentum changes with a fixed value of the energy is shown in Figure 8 (cf. also Figure 5b). Starting with zero angular momentum, which is exactly the Bondi spherical accretion, the location of the sonic point is uniquely determined by the value of the energy (cf.(1.1.1); E is equivalently replaced by a_∞ there). With continuously increasing L, R_s moves inwards. It experiences a discontinuous jump when L reaches the critical value L_c. After jumping, it moves inwards, again continuously with continuously increasing L, until L is so large that the energy is insufficient to overcome the potential barrier.

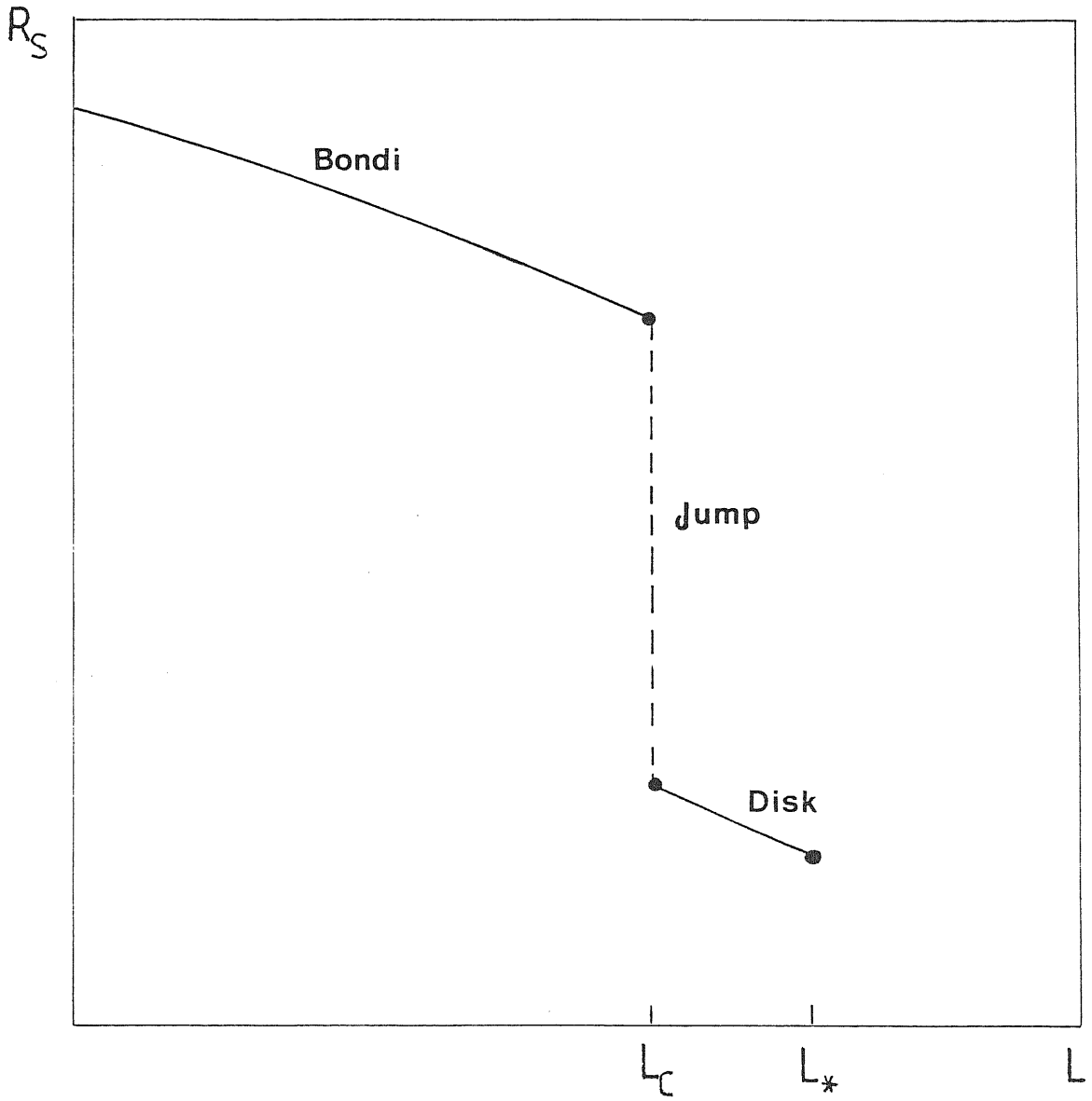

Fig. 8 There are two different regimes of accretion: Bondi-type and disklike. The location of the sonic point experiences a discontinuous jump when the continuously increasing angular momentum reaches the critical value L_c. For $L > L_* = L_*(E)$ accretion is impossible as the energy is too low to overcome the potential barrier.

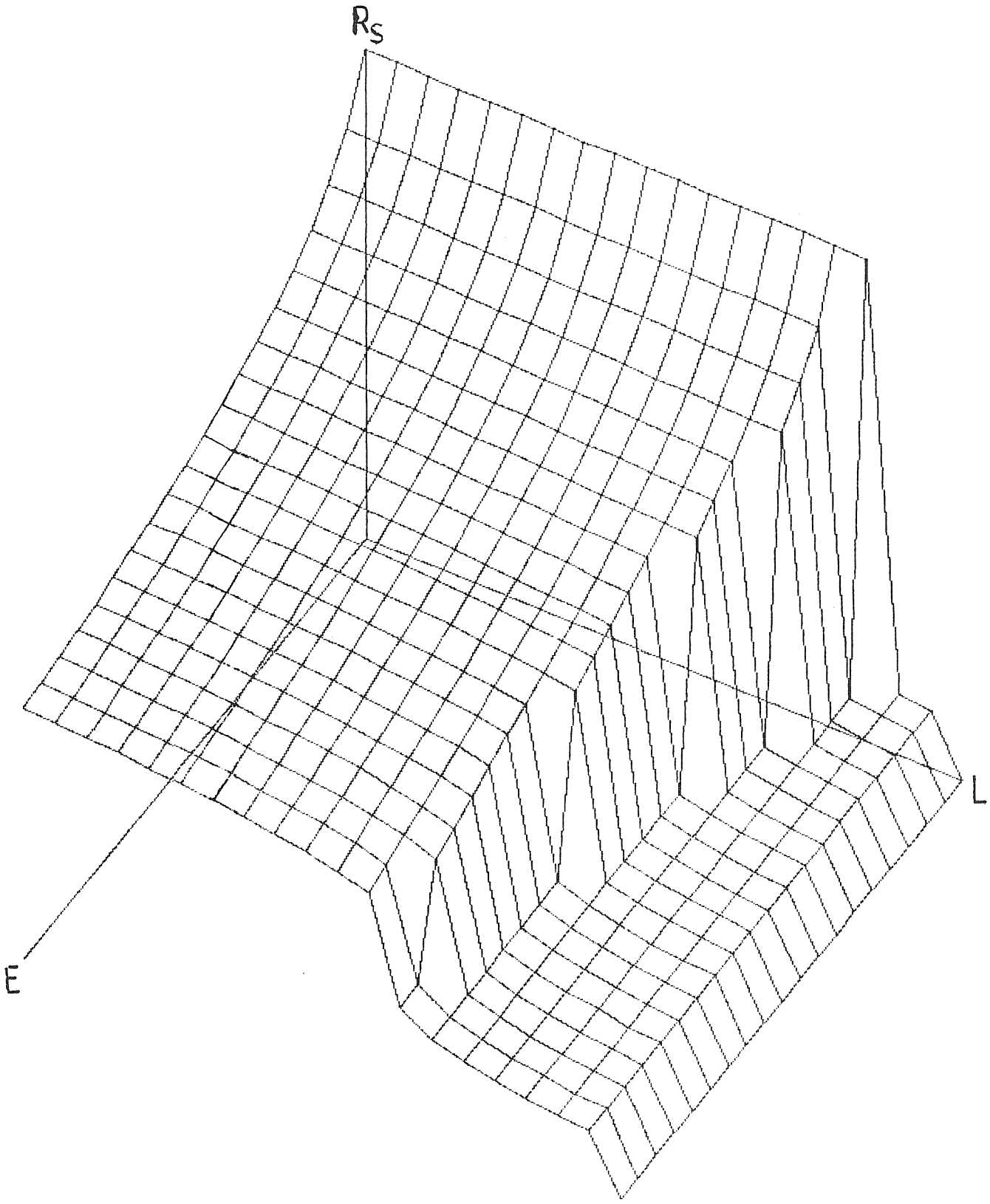

Fig. 9 The location of the realizable sonic point as a function of angular momentum and energy satisfying $E_{Barr} < E < E_c$.

The location of the realizable sonic point as a function of angular momentum and energy (satisfying $E_{Barr} < E < E_c$) is shown in the three dimensional graph Figure 9. The smaller the energy is, the larger the jump in the location of the sonic point, and the larger the value of the angular momentum at which the jump takes place, L_c. The location of the sonic point is always unique for a given pair of E and L.

The specific mass accretion rate is a continuous function of the independent parameters (Figure 10). It decreases monotonically with increasing angular momentum. There is, however, a turning point where the location of the sonic point jumps. Before the turning point the line has very small slope. This reflects the fact that the accretion rate depends only very weakly on the angular momentum. The nearly vertical line after the turning point shows that here rotational effects are dominant. In his classical paper, Bondi (1952) argued that for spherical (no rotation) accretion, the transonic solution always corresponds to the greatest possible mass accretion rate. Since it has been seen that the effect of rotation is always to decrease the accretion rate, Bondi's conclusion is reproved here, but under more general circumstances, i.e. rotation and general relativistic effects have been taken into account.

Another three-dimensional graph (Figure 11) shows the behaviour of $\dot{M}_o$ in L-E phase space. It is also a unique function of a given pair of L and E, and generally increases with increasing energy. The effect of the rotation is always to decrease the specific accretion rate.

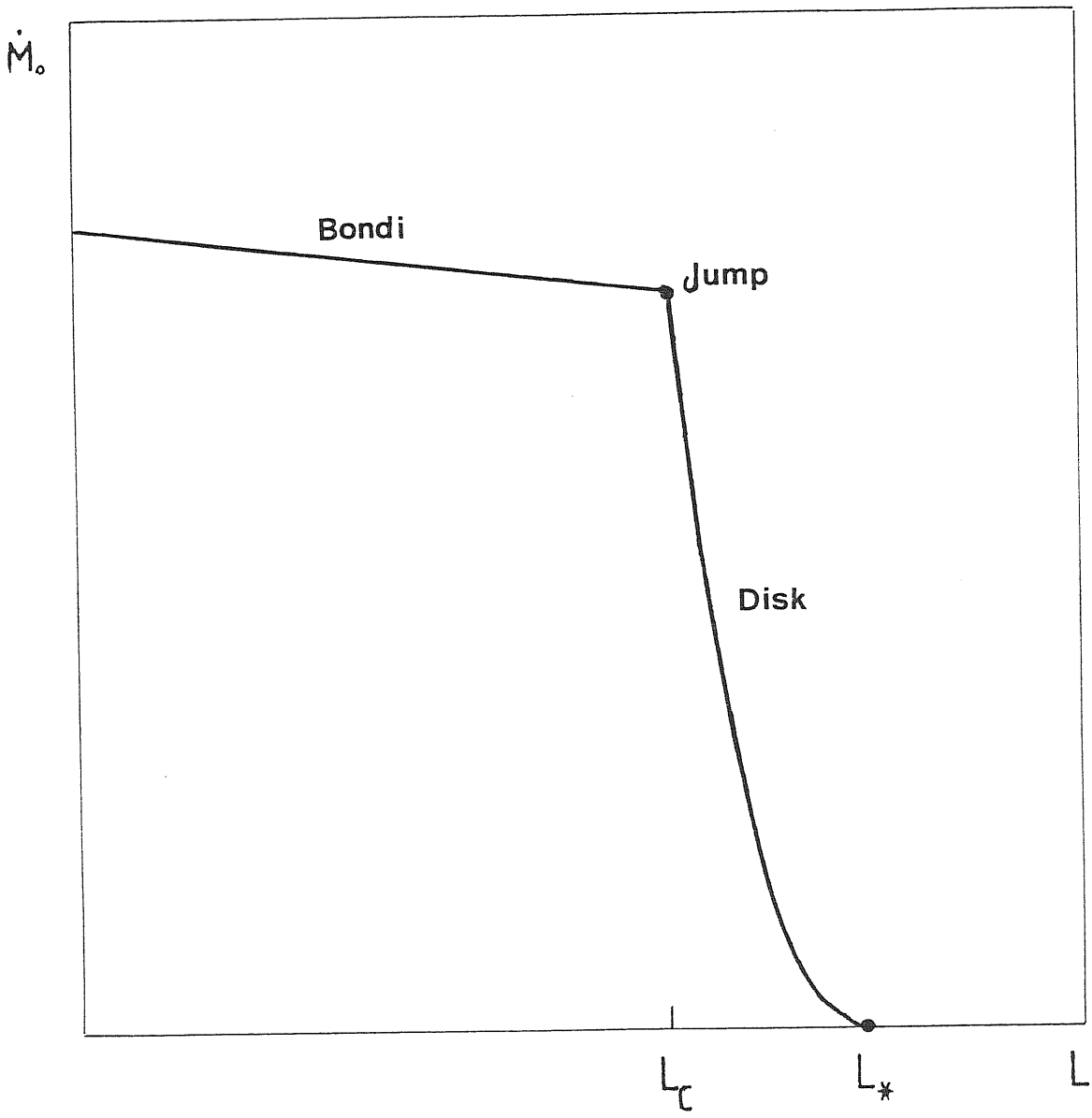

Fig. 10 The specific mass accretion rate is a continuous function of the angular momentum for a fixed value of the energy. The effect of rotation is negligible in the Bondi-type accretion regime, while in the disklike accretion regime it is dominant.

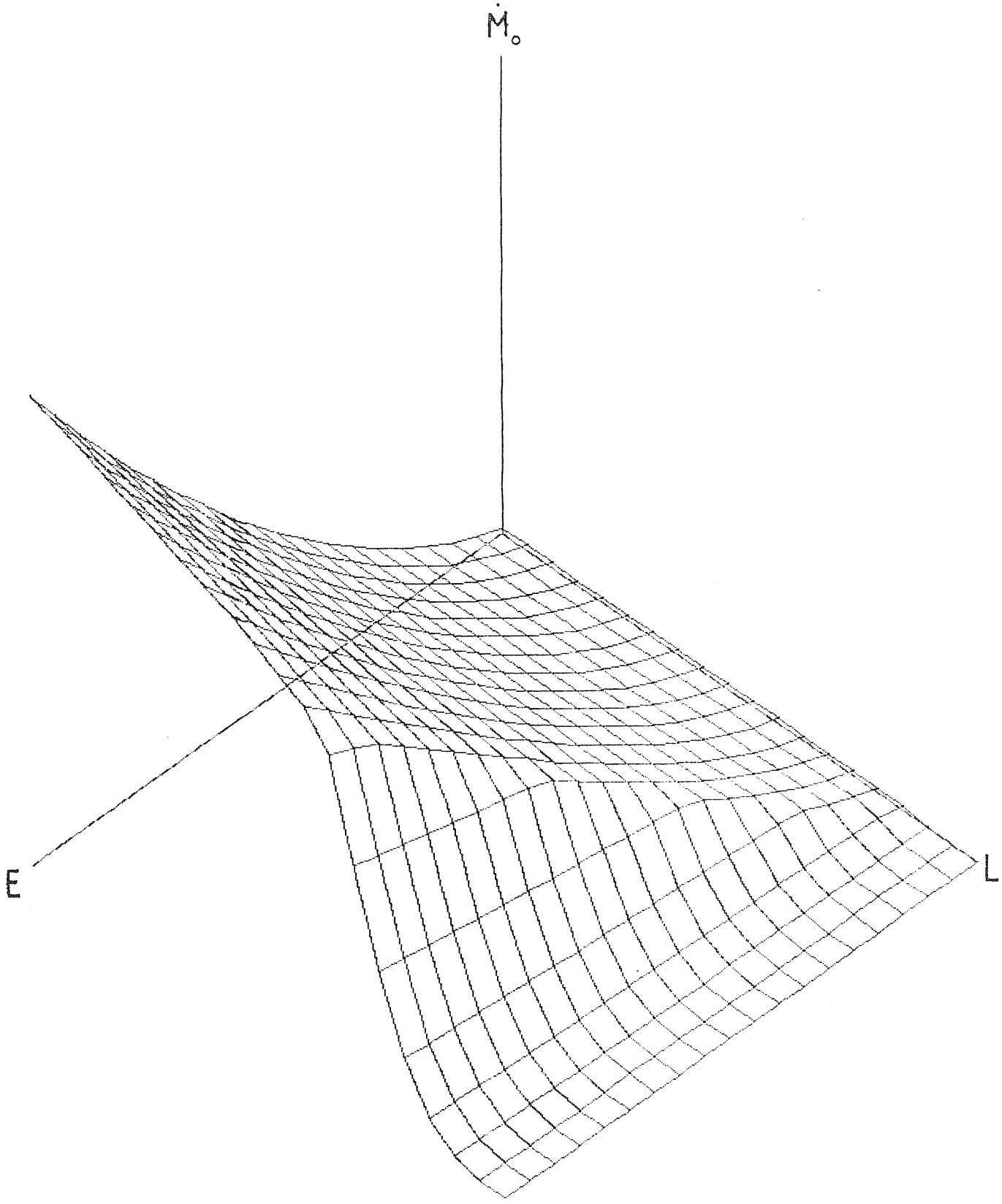

Fig. 11 The behaviour of $\dot{M}_o$ in the E-L phase space

Although it is the specific mass accretion rate $\dot{M}_o = \dot{M}/\omega$ which is depicted in Figures 10 and 11, it should be pointed out that the real mass accretion rate $\dot{M}$ should have the same behaviour, as the opening angle of the flow, ω, only depends strongly on ß, the ratio of the gas pressure to the total pressure, and very weakly on all the other parameters (cf. §1.3),

$$\omega_s \approx 10^{-2} X/\sqrt{ß} \ . \qquad (2.5.6)$$

The quantity $X \approx 1$ for central black holes with mass $M \sim 10M_\odot$, and $X \approx 0.1$ for those with $M \sim 10^8 M_\odot$. The quantity ß is an intrinsic property of the accreted matter. It is known that a mixture of ideal gas and black body radiation can be described by the polytropic equation of state with n = 3 and the polytropic constant

$$k = \left[\frac{48}{a}\frac{k_B}{m_p}\left(\frac{1-ß}{ß^4}\right)\right]^{1/3} = 6.6533X10^{15}\left(\frac{1-ß}{ß^4}\right)^{1/3} \ \frac{cm^3}{g^{1/3}\ sec^2} \ , \qquad (2.5.7)$$

where a is the radiation constant, k_B is the Boltzmann constant, and m_p is the proton mass. The unit for accretion rate used here depends on k:

$$\dot{M} = \dot{m}\ k^n(1 + 1/n)^n/4\pi r_g^2\ c^{2n+1} \ . \qquad (2.5.8)$$

The critical accretion rate $\dot{m}_{crit}$ is defined as the accretion rate

which would give the Eddington luminosity for a disk with its inner edge at the marginally stable orbit (see Paczyński 1981 for details):

$$\dot{m}_{crit} = \frac{32\pi m_p c}{\sigma_T} r_g = 2.24X10^{18}(\frac{r_g}{r_{g\odot}}) \quad \frac{g}{sec} \quad , \tag{2.5.9}$$

where σ_T is the Thompson cross section, and

$$r_{g\odot} = (\text{gravitational radius of the Sun}) = 2.96X10^5 \text{ cm} .$$

Combining (2.5.7)-(2.5.9) one gets, for $\beta \ll 1$:

$$\dot{M}_{crit} = \frac{6.5X10^{-20}}{\beta^4} (\frac{M_\odot}{M}) . \tag{2.5.10}$$

Thus the value of $\dot{M}_o$ which corresponds to the critical accretion rate is

$$\dot{M}_{o\,crit} = \frac{\dot{M}_{crit}}{\omega_s} \approx \frac{6.5X10^{-17}}{X\ \beta^{7/2}} (\frac{M_\odot}{M}) . \tag{2.5.11}$$

Formula (2.5.11) provides a physical scale for the accretion rate. For example, for a galactic black hole $M = 10M_\odot$, $\dot{M}_o = 1X10^{-5}$ in Figure 10 corresponds to $\dot{M} = \dot{M}_{crit}$ whne $\beta = 1.7X10^{-4}$.

It is concluded from the study in this section that, for $E_{Barr} < E < E_c$, although the regularity condition equation

$$F(L, E, \dot{M}_o) = 0 , \tag{2.5.12}$$

which is the reduction of the general regularity condition (2.4.2) in the case of a potential, quasi-radial flow, has two formal solutions, i.e. there are two formal values of $\dot{M}_0$ corresponding to the same pair of L and E, only one, the smaller $\dot{M}_0$, is realizable in the global physically acceptable transonic solution. Thus the accretion rate in the adiabatic, transonic accretion flow of rotating matter cannot be assumed but is an eigenvalue of the problem, it is always uniquely determined by two intrinsic parameters of the accreted matter, L and E:

$$\dot{M}_0 = \dot{M}_0(L, E) \ . \qquad (2.5.13)$$

This conclusion is similar to that reached by Bondi (1952) in the case of spherical, adiabatic, transonic accretion flows where the accretion rate is uniquely determined by only one intrinsic parameter (the energy):

$$\dot{M} = \dot{M}(E) \ . \qquad (2.5.14)$$

The difference is only that there is now one more dimension (L) in the phase space. One can therefore clearly define two different regimes of accretion: the first one bears a strong resemblance to the classical Bondi solution for accretion with no angular momentum. The sonic point lies very far from the black hole. Neither the rotation nor the relativistic effects are important in the transonic part of the flow. The second regime, on the other hand, is relativistic; it has no Newtonian analogy (and thus was missed by Henriksen and Heaton 1975 in

their earliest, but purely Newtonian, study of accretion with rotation). The sonic point lies very close to the hole and the rotation is one of the dominant features in the transonic part. Different names were given by Abramowicz and Zurek (1981) to these two accretion regimes: Bondi type to the former, and disklike to the latter.

Figure 12 shows the distribution of transonic solutions in the L-E phase space, where $L^2_{max}(E)$ and $L^2_{min}(E)$ denote the loci of maxima and minima of the curves $L^2(E, R_s)$ shown in Figure 5; $f_{min}(E)$ is the function given in (2.4.10). For $E < -1/16$, or $L^2 > f_{min}$, accretion is impossible (cf. (2.4.13) and (2.4.11)). For $-1/16 < E \leqslant 0$ or $E > E_c \approx 0.02$, the transonic solution is unique whenever it exists. For positive energy $E_{Barr} < E < E_c$ and $L^2_{min} < L^2 < L^2_{max}$, there are two possible locations of the sonic point, but the realizable transonic solution is unique. The regions of Bondi-type accretion and disklike accretion are divided by the curve $L^2_c(E)$.

2.6 Global solution: general flow

In general, accretion flows can not be exactly quasi-radial; there must be some motion of matter in the θ-direction. The equations discribing general flows are (2.3.24) and (2.3.25). They can be rewritten in dimensionless form with the help of the dimensionless variables given in §2.4 as

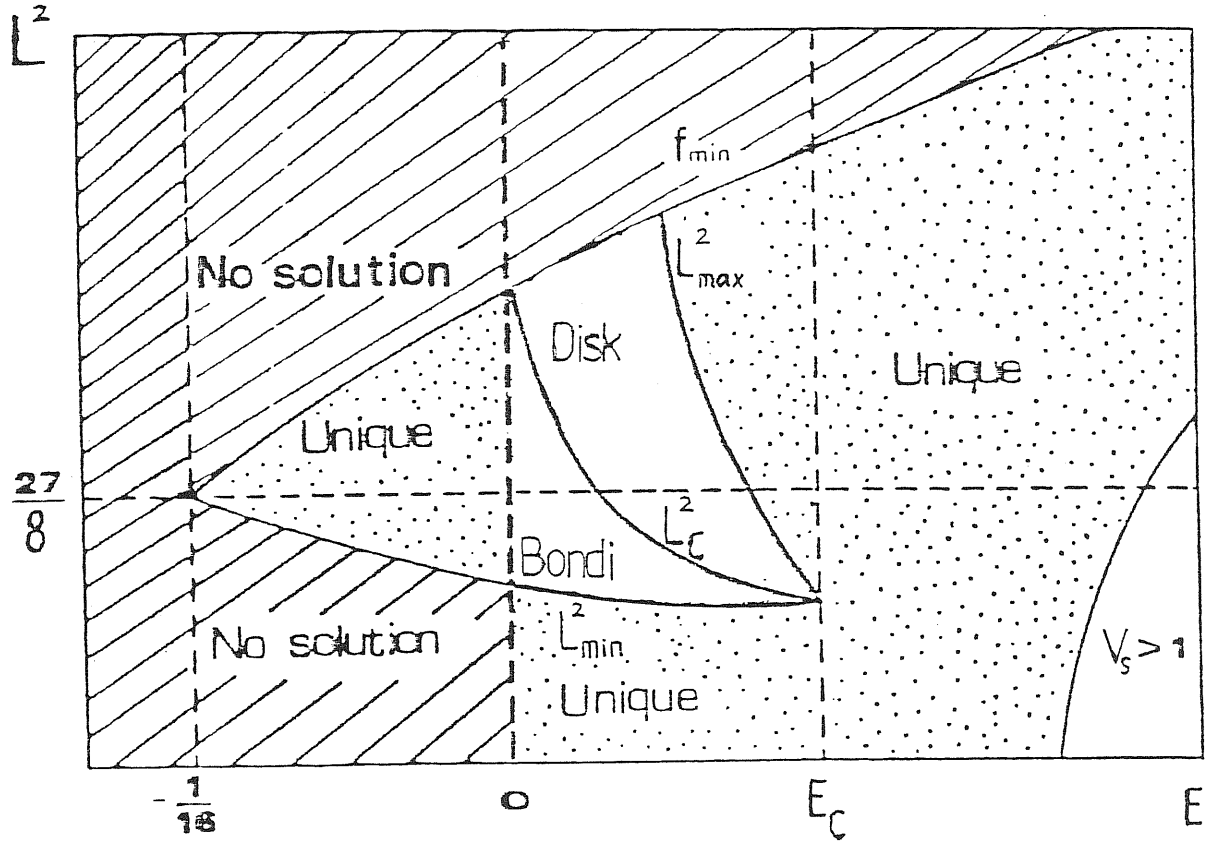

Fig. 12 The distribution of transonic solutions in L-E phase space. Three regions, no solution, unique solution and non-unique possible location of the sonic point but still unique physical solution, are shown. The region $V_s > 1$ means that the radial velocity at the sonic point would be larger than the light speed, which is impossible.

$$\frac{dV}{dR} = V \frac{(B-2)A^2R^2 - (L^2 - L_k^2)}{R^3(A^2 - V^2)} \quad , \tag{2.6.1}$$

$$\frac{dV_\theta}{dR} = \frac{\left[CR^4A^{2(2n+1)} + B(B-1)\right]V^2R^2 + L^2}{R^3V} \quad , \tag{2.6.2}$$

where

$$B = V_\theta/V,$$

$$A = \frac{1}{\sqrt{n}}\left[E - \frac{1}{2}V^2 - \frac{1}{2}L^2/R^2 + \frac{1}{2(R-1)}\right]^{1/2} ,$$

$$L_k^2 = R^3/2(R-1)^2 ,$$

$$C = -2\frac{n}{n+1}\dot{M}^{-2} .$$

Due to the appearence of V_θ , an analytic solution is no longer possible, and the only way to get a global solution from (2.6.1) and (2.6.2) is to use numerical methods.

Apart from the conditions stated in the last section, a physical global solution should satisfy one more boundary condition:

$$V_\theta \longrightarrow 0 \qquad \text{when } R \longrightarrow \infty .$$

It has been seen in §2.4 that the values of V and V_θ (or equivalently B) at the sonic point, V_s and $(V_\theta)_s$ (or B_s), are not independent of each other, provided three physical constants in (2.6.1) and (2.6.2), L, E and $\dot{M}$, are given. This is because the two sonic point conditions of (2.6.1), D = 0 and N = 0, give two constraints on three quantities: V_s, $(V_\theta)_s$ and R_s, and thus only one of them is free. This means that V_s and $(V_\theta)_s$ must obey the regularity condition

$$F(L,\ E,\ \dot{M},\ V_s,\ (V_\theta)_s) = 0\ . \qquad (2.6.3)$$

Starting the integration of (2.6.1) and (2.6.2) with V_s and $(V_\theta)_s$ at the sonic point R_s, one arrives at any other radial distance R* with V* and V_θ^* . The values of V* and V_θ^* will therefore be related to each other:

$$V_\theta^* = V_\theta^*\ (L,\ E,\ \dot{M},\ V^*). \qquad (2.6.4)$$

Proceeding further, one eventually arrives at infinity with V_∞ and $(V_\theta)_\infty$ and

$$(V_\theta)_\infty = (V_\theta)_\infty(L,\ E,\ \dot{M},\ V_\infty).$$

However, the boundary condition at infinity is

$$V_\infty = 0, \qquad (V_\theta)_\infty = 0\ . \qquad (2.6.5)$$

This means that not all the initial data $L = L_\infty$, $E = E_\infty$ and $\dot{M} = \dot{M}_\infty$ will give stationary, regular, transonic accretion but instead a condition

$$F(L,\ E,\ \dot{M}) = 0 \qquad (2.6.6)$$

must be fulfilled. If one chooses L and E as two independent parameters, the accretion rate $\dot{M}$ as well as the global solution, including the location of the sonic point, are determined accordingly. This general argument has

been confirmed in the last section for the special case of quasi-radial flows.

Confirmation of (2.6.6) for general flows is slightly more difficult. The reason for this is as follows. If one starts numerical integration of the system (2.6.1), (2.6.2) at infinity (at some large distance, in practice) using a given pair of E and L and boundary condition $V_\infty = (V_\theta)_\infty = 0$, it is very difficult (almost impossible in practice) to find a solution passing regularly through the sonic point. This is because both the denominator and the numerator of (2.6.1) vanish simultaneously at the sonic point, which is very hard to treat numerically. If the integration is satrted at the sonic point, and performed inwards toward the horizon and outward towards infinity, respectively, then the difficulty can be avoided. But in this case, in order to determine the location of the sonic point and the radial velocity at the sonic point, one has to specify a priori the value of $(V_\theta)_s$ (or B_s) in addition to L and E (cf. equations (2.4.5), (2.4.6)). This is not very nice of course because the values of all physical quantities at the sonic point should be determined by L, E and the boundary condition at infinity, through equations (2.6.1) and (2.6.2). Thus it seems that neither of these two integration methods works.

However, one can try a third way which is a combination of these two. Start the integration of (2.6.1) and (2.6.2) at infinity with given L, E and boundary condition. Although it is very hard to find the exact location of the sonic point, one still can, by choosing the value of $\dot{M}$ very carefully, go very close to it, and hence have at least some estimates of the values of V_s and $(V_\theta)_s$. Then, choose appropriate values of R_s, V_s and $(V_\theta)_s$ so

that the sonic point conditions N = D = 0 are fulfilled, and start the integration again at the sonic point (with the same L, E and $\dot{M}$, of course). If the solution obtained is always supersonic inside the sonic point, and subsonic outside it, and when R goes to infinity the asymptotic behaviour of the solution is consistent with that obtained by integration starting at infinity, then a global physical transonic solution has been found.

In practice, the first step of the integration (i.e. from infinity) can be started only at some sufficiently large distance (R = 500, say). It is reasonable to choose the boundary condition (i.e. the values of V and V_θ there) to be purely spherical Bondi accretion (with zero angular momentum) i.e. using the value of V which can be calculated from a given E (L = 0) and V_θ = 0 (this treatment was also adopted by Hawley and Smarr 1985 even at a much smaller distance R = 50).

A number of numerical integrations, using all the representative values of E and L, have been performed in this way. It is found that the global transonic solution whenever it exists is always unique, i.e. for a given pair of E and L, one can find one and only one value of $\dot{M}$ which makes the global transonic solution realizable. There are also two separate regimes of accretion: Bondi-type and disklike, depending on whether L is smaller or larger than the critical value which is defined by the value of E, $L_c = L_c(E)$. All these conclusions for general flows are consistent with the quasi-radial case. It is also found that the absolute value of the radio of V_θ to V at the sonic point, B_s, is usually less than 0.1 and the sign is negative. This means that the motion of the

matter in the θ-direction is to tend to leave the equatorial plane and go towards the surface of the flow.

Figure 13 gives two typical examples of global transonic solutions for general flows and compares them with quasi-radial flows and spherical accretion. It is seen that both the effect of rotation and that of motion in the θ-direction is to move the location of the sonic point inwards from that of spherical accretion. This can be understood as both rotation and motion in the θ-direction take some kinetic energy from the radial motion. Hence the accretion flow has to go further inwards to reach the sonic point, as the release of gravitational energy increases with decreasing distance. The following analytic analysis makes the numerical results in Figure 13 clearer.

Assuming $L \ll 1$ and $|B_s| \ll 1$, then the accretion flow is nearly spherical, and one can expand all the quantities of interest at the sonic point accotding to

$$Q(E, L, B_s) = Q_{sp}(E)\left[1 + L^2 Q_L(E) + B_s Q_B(E) + \ldots\right] \qquad (2.6.7)$$

The index sp refers to the Bondi(spherical) solution in the potential (2.1.4), the index L represents a correction to the Bondi solution due to a small rotation and the index B refers to a correction due to the small quantity B_s. All the functions Q depend only on one parameter (energy, say), as the Bondi solution is a one-parameter one. The results are:

Fig. 13 Examples of global transonic solutions for general flows (the curve c). For comparison, solutions for quasi-radial flows (the curve b) and spherical flows (the curve a) are also given. Fig. 13a is for $L < L_c(E)$ and Fig. 13b for $L > L_c(E)$.

(a)

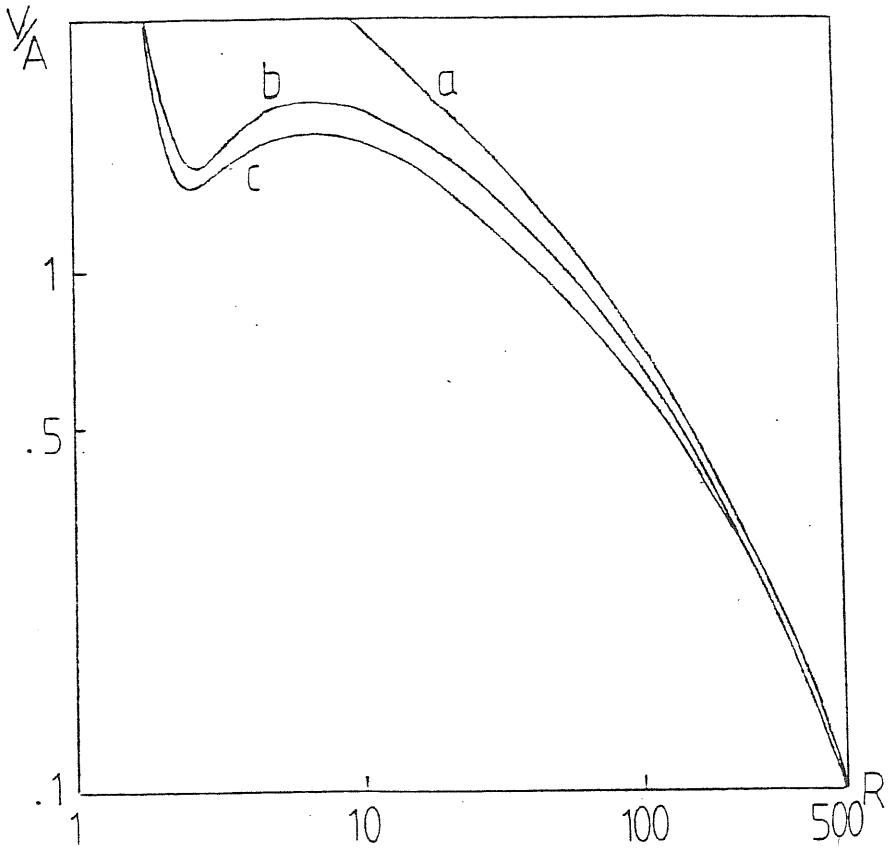

Figure 13

(b)

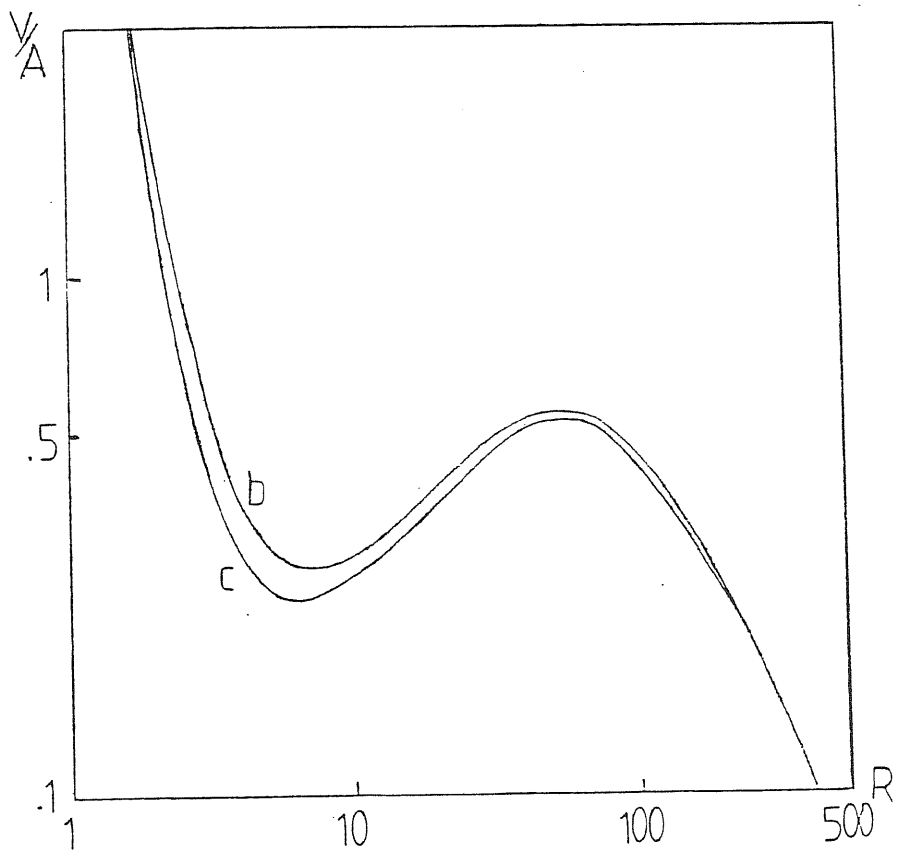

$$R_{sp}(E) = \frac{2n - 3 + \left[(2n - 3)^2 + 32(2n + 1)E\right]^{1/2}}{16E} + 1 \ , \qquad (2.6.8)$$

$$V^2_{sp}(E) = \frac{R_{sp}}{4(R_{sp} - 1)^2} \ , \qquad (2.6.9)$$

$$\dot{M}_{o_{sp}}(E) = R^2_{sp} \, V^{2n+1}_{sp} \ . \qquad (2.6.10)$$

The small corrections due to rotation and the θ-component of velocity, v^{θ}, are:

$$R_L(E) = \frac{2(1 - 2n)(R_{sp} - 1)^3}{R^3_{sp}\left[(2n - 3)R_{sp} + 2n + 5\right]} \ , \qquad (2.6.11)$$

$$V^2_L(E) = - \frac{4(R_{sp} - 1)^3}{(2n + 1)R^3_{sp}} \left[1 + \frac{2(1 - 2n)(R_{sp} - 1)}{(2n - 3)R_{sp} + 2n + 5}\right] , \qquad (2.6.12)$$

$$\dot{M}_{o_L}(E) = - 2(R_{sp} - 1)^2/R^3_{sp} \ , \qquad (2.6.13)$$

$$R_B(E) = \frac{(2n + 1)(R_{sp} - 1)}{2\left[(2n - 3)R_{sp} + 2n + 5\right]} \ , \qquad (2.6.14)$$

$$V^2_B(E) = - \frac{2(R_{sp} - 1)}{(2n - 3)R_{sp} + 2n + 5} \ , \qquad (2.6.15)$$

$$\dot{M}_{o_B}(E) = 0 \ . \qquad (2.6.16)$$

One sees from (2.6.11), (2.6.14) and (2.6.15) that a small rotation as well as a meridional circulation always makes the location of the sonic point move inwards if $n > 3/2$ (note that B_s is negative), and that a small meridional circulation increases the value of the radial velocity

at the sonic point. The corrections due to rotation are of the same order as those due to B_s as Figure 14 shows. One can also see something more interesting from (2.6.13) and (2.6.16): a small rotation always decreases the specific accretion rate independently of the equation of state, while a small meridional circulation does not change it at all.

Thus although the location of the sonic point and the radial velocity at the sonic point obtained from the quasi-radial accretion flow model in the last section are not quantitatively correct, the model can qualitatively describe the behaviour of the general flow. It gives the correct specific accretion rate, and the most important conclusion drawn from the model, i.e. that the regularity condition equation

$$\dot{M} = \dot{M}(L, E) \qquad (2.6.17)$$

has a unique solution, is confirmed in this section for the general flow.

One last remark should be made, however. The value of $\dot{M}$ satisfying (2.6.17) can only be obtained, unfortunately, after numerical integration of equations (2.6.1) and (2.6.2). It sometimes seems unphysical as it requires an opening angle of the flow, ω, larger than one. This is because one of the two basic equations, (2.6.2), is inaccurate as it is derived by terminating the expansions at the lowest possible (the second) order (cf. §2.2). This problem is not very serious if one is interested in qualitative conclusions rather than quantitative values. Anyway, if an unphysical value of $\dot{M}$ appears, one can always divide it by the corresponding value of the opening angle at the sonic point, ω_s, and then the resulting specific accretion rate, $\dot{M}_o$, is always consistent with that

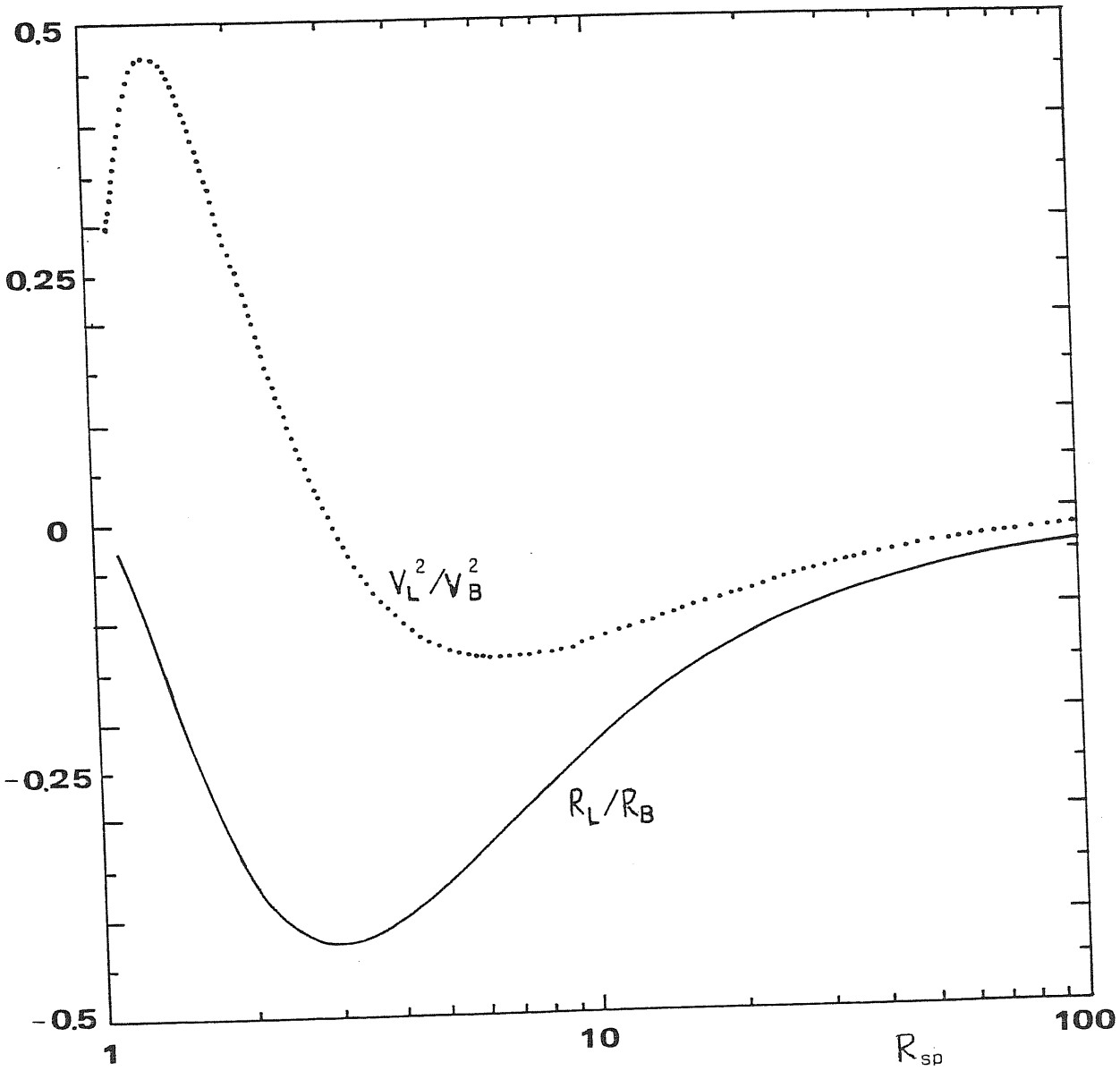

Fig. 14 Corrections to the location of the sonic point due to rotation, R_L, are of the same order as the corrections due to meridional circulation, R_B. The same is true for the corrections to the radial velocity at the sonic point.

obtained from the quasi-radial flow model. Of course, in order to get an exact value of $\dot{M}$, one can go to the higher order expansions and solve a larger set of differential equations instead of only two.

3. Stationary flow: relativistic theory

All the studies in the last chapter are based on a purely Newtonian model of a black hole. Although it is known from §2.1 that this model describes the motion of free particles very accurately, in order to see whether it has the same power for fluid motion, a correct general relativistic analysis of the problem and a comparison with the pseudo-Newtonian treatment are necessary. Furthermore, it is apparent that the pseudo-Newtonian model can only describe a spherically symmetric gravitational field. It does not work for a rotating black hole which produces an axially symmetric gravitational field and is described by the Kerr metric. In this chapter the correct relativistic equations are used to study transonic accretion onto a black hole, both in the Schwarzschild and the Kerr cases.

In addition to the assumptions stated in §§2.1, i.e. the accretion flow is geometrically thin, adiabatic, symmetric with respect to the axis and the equatorial plane, has negligible self-gravity, and obeys a polytropic equation of state; it is also assumed that the flow is quasi-radial (the θ-component of the four-velocity of the accreted gas, u^{θ}, vanishes) since, as seen in the last chapter, all conclusions drawn from the quasi-radial flow model are, qualitatively at least, correct for the general flow. For a quasi-radial flow, the expansion scheme given in §2.2 can make a closed system at the zeroth order (cf. (2.2.5)-(2.2.8)), i.e. the horizontal and vertical structure of the flow can be separated. It is therefore sufficient to study the

accretion flow on the equatorial plane, so that all quantities are reduced to functions of r only.

Geometric units, in which G = c = 1, are used.

3.1 Basic equations

The basic equations describing the accretion flow are:

i) Rest-mass conservation

$$(\rho_0 u^\alpha)_{;\alpha} = 0 \ , \tag{3.1.1}$$

ii) Euler's equation

$$h_{\alpha\beta} T^{\beta\gamma}{}_{;\gamma} = 0 \ , \tag{3.1.2}$$

iii)Local energy conservation

$$u_\alpha T^{\alpha\beta}{}_{;\beta} = 0 \ . \tag{3.1.3}$$

In these equations Greek indices α, β, and γ run from 0 to 3; the semicolon denotes the covariant derivative; ρ_0 is the rest-mass density; u^α is the four-velocity of the accreted gas, which obeys the normalization condition

$$u^\alpha u_\alpha = -1 \ ; \tag{3.1.4}$$

$T^{\alpha\beta}$ is the stress-energy tensor and $h_{\alpha\beta}$ is the orthogonal (to the flow) projection operator:

$$T^{\alpha\beta} = (\varrho + P)u^{\alpha}u^{\beta} + Pg^{\alpha\beta} , \qquad (3.1.5)$$

$$h_{\alpha\beta} = g_{\alpha\beta} + u_{\alpha}u_{\beta} . \qquad (3.1.6)$$

Here ϱ is the total mass-energy density and P is the pressure of the gas, as measured by a comoving (with a fluid element) observer (as well as ϱ_o), $g_{\alpha\beta}$ is the metric tensor and $g^{\alpha\beta}$ is its inverse,

$$g_{\alpha\gamma}g^{\gamma\beta} = \delta_{\alpha}^{\ \beta} , \qquad (3.1.7)$$

$\delta_{\alpha}^{\ \beta}$ is the Kronecker symbol,

$$\delta_{\alpha}^{\ \beta} = \begin{cases} 1 & \text{for } \alpha = \beta \\ 0 & \text{for } \alpha \neq \beta \end{cases} . \qquad (3.1.8)$$

In addition, an equation of state should be provided. The polytropic relations (Tooper 1965)

$$P = k\varrho_o^{1+1/n} , \quad \varrho = \varrho_o + nP , \qquad (3.1.9)$$

where k and n are constants, are adopted.

3.2 The Schwarzschild metric

The gravitational field of a non-rotating black hole is described by the Schwarzschild metric which, when the (-+++) signature is used, can be written in the spherical coordinate system as

$$g_{tt} = -(1 - 2M/r), \qquad g_{rr} = (1 - 2M/r)^{-1},$$
$$g_{\theta\theta} = r^2, \qquad g_{\phi\phi} = r^2 \mathrm{Sin}^2\theta ,$$

and (3.2.1)

$$g^{tt} = -(1 - 2M/r)^{-1}, \qquad g^{rr} = (1 - 2M/r),$$
$$g^{\theta\theta} = r^{-2}, \qquad g^{\phi\phi} = r^{-2}\mathrm{Sin}^{-2}\theta ,$$

and all the off-diagonal components of $g_{\alpha\beta}$ and of $g^{\alpha\beta}$ are equal to zero. The affine connection $\Gamma^{\gamma}_{\alpha\beta}$ is defined as

$$\Gamma^{\gamma}_{\alpha\beta} = \frac{1}{2} g^{\gamma\nu} \left(\frac{\partial g_{\alpha\nu}}{\partial x^{\beta}} + \frac{\partial g_{\beta\nu}}{\partial x^{\alpha}} - \frac{\partial g_{\alpha\beta}}{\partial x^{\nu}} \right). \qquad (3.2.2)$$

Its non-zero components in the Schwarzschild metric are (Weinberg 1972)

$$\Gamma^{t}_{tr} = \Gamma^{t}_{rt} = \frac{M}{r^2(1 - 2M/r)} ,$$

$$\Gamma^{r}_{rr} = -\frac{M}{r^2(1 - 2M/r)} , \qquad \Gamma^{r}_{\theta\theta} = -r(1 - 2M/r),$$

$$\Gamma^{r}_{\phi\phi} = -r(1 - 2M/r)\mathrm{Sin}^2\theta , \qquad \Gamma^{r}_{tt} = M(1 - 2M/r)/r^2,$$

$$\Gamma^{\theta}_{r\theta} = \Gamma^{\theta}_{\theta r} = 1/r \ , \qquad \Gamma^{\theta}_{\phi\phi} = -\mathrm{Sin}\theta\,\mathrm{Cos}\theta \ ,$$

$$\Gamma^{\phi}_{r\phi} = \Gamma^{\phi}_{\phi r} = 1/r \ , \qquad \Gamma^{\phi}_{\theta\phi} = \Gamma^{\phi}_{\phi\theta} = \mathrm{Cot}\theta \ . \qquad (3.2.3)$$

a) Spherical accretion

In the case of spherical accretion ($u^{\theta} = u^{\phi} = 0$), the basic equations (3.1.1)-(3.1.3) can be reduced to (by using (3.2.1) and (3.2.3) and writting on the equatorial plane)

$$\rho_o\left(\frac{du^r}{dr} + \frac{2}{r}u^r\right) + u^r\frac{d\rho_o}{dr} = 0 \ , \qquad (3.2.4)$$

$$(\rho + P)\frac{du_t}{dr} + u_t\frac{dP}{dr} = 0 \ , \qquad (3.2.5)$$

$$(\rho + P)\left(\frac{M}{r^2}u^t u^t + u_r\frac{du^r}{dr} - \frac{M}{r^2}u_r u_r\right) + (1 + u_r u^r)\frac{dP}{dr} = 0 \ , \qquad (3.2.6)$$

$$(\rho + P)\left(\frac{du^r}{dr} + \frac{2}{r}u^r\right) + u^r\frac{d\rho}{dr} = 0 \ . \qquad (3.2.7)$$

There are five unknown quantities in the equations, namely, ρ_o, ρ, P, u^t, u^r; but ρ_o, ρ, and P obey the two relations (3.1.9), u^t and u^r follow the normalization condition (3.1.4), and thus only two of the four equations are independent.

Equations (3.2.4) and (3.2.7) give the relation

$$\frac{d\rho}{dr} = H\frac{d\rho_o}{dr} \ , \qquad (3.2.8)$$

where H is the enthalpy per unit rest mass,

$$H = (\varrho + P)/\varrho_0 \ . \tag{3.2.9}$$

With the help of (3.2.8), the t-component of the Euler equation (3.2.5) can be integrated to give

$$Hu_t = -H_\infty = \text{const} \tag{3.2.10}$$

($u_t = -1$ at infinity if the gas is at rest there). The r-component of the Euler equation (3.2.6) and the equation of local energy conservation (3.2.7) can be combined to give the central equation for studying transonic accretion:

$$\frac{du^r}{dr} = N/D \ , \tag{3.2.11}$$

where

$$D = (1 - b^2)u_r u^r - b^2 \ , \tag{3.2.12}$$

$$N = (1 + u_r u^r)\frac{2}{r}u^r b^2 + \frac{M}{r^2}u_r u_r u^r - \frac{M}{r^2}u^t u^t u^r \ , \tag{3.2.13}$$

and b is the adiabatic sound speed,

$$b^2 = dP/d\varrho \ . \tag{3.2.14}$$

Critical points occur where both D and N vanish simultaneously. Replacing u^t with u^r by using (3.1.4), the two critical point conditions D = 0 and N = 0 yield

$$(u^r_c)^2 = \frac{1}{4R_c} , \tag{3.2.15}$$

$$b_c^2 = \frac{1}{4R_c - 3} = \frac{(u^r_c)^2}{1 - 3(u^r_c)^2} , \tag{3.2.16}$$

where R is the dimensionless form of r, $R = r/r_g = r/2M$, and the subscript c denotes the value at the critical point. The physical meaning of the critical point is not clear from (3.2.16), as what appears there is the four-velocity, not the physical three-velocity. Flammang (1982) has shown, however, that a critical point is a sonic point for a locally static observer.

In the case of the polytropic relations (3.1.9), the specific enthalpy can be expressed in terms of the sound speed as

$$H = (1 - nb^2)^{-1} . \tag{3.2.17}$$

Combining (3.1.4), (3.2.10), (3.2.15), (3.2.16) and (3.2.17), one obtains, after some algebra,

$$64(H_\infty^2 - 1)R_c^3 + \left[144 - 32(n + 3)H_\infty^2\right]R_c^2$$

$$+ \left[(2n + 6)^2 H_\infty^2 - 108\right] R_c + 27 = 0 . \tag{3.2.18}$$

Thus the location of the critical point is determined from a given constant H_∞ (the specific enthalpy at infinity) when the polytropic index n is fixed. All the above results are the same as those obtained by Michel (1972) and Begelman (1978), but are in a slightly different form.

Begelman (1978) made an approximate study of equation (3.2.18), and came to the following conclusions:

(i) There is no critical point for $0 < n < 1/2$;

(ii) There is one and only one critical point for $n > 3/2$, which is just the one found by Bondi (1952);

(iii) There is one and only one relativistic critical point for $1/2 < n < 3/2$, which was missed in Bondi's purely Newtonian analysis.

Ray (1980) studied (3.2.18) more rigorously. His results are as follows.

Case(i) $n < 1 - \frac{1}{2H_\infty}$, which approximately means $n < 1/2$ because, from physical considerations (cf. (3.2.17)), it should be true that

$$H_\infty > 1 , \tag{3.2.19}$$

and it is likely that

$$(H_\infty - 1) << 1 . \tag{3.2.20}$$

There is no critical point, consistent with Begelman's conclusion (i).

Case(ii) $1 - \frac{1}{2H_\infty} < n < 1 + \frac{1}{2H_\infty}$, which approximately means $1/2 < n < 3/2$. There is one and only one critical point, consistent with

Begelman's conclusion (iii).

Case(iii) $1 + \frac{1}{2H_\infty} < n$, which approximately means $n > 3/2$. There are two critical points lying outside the black hole horizon,

$$1 < R_c^{(1)} < \frac{n+3}{4} < R_c^{(2)} \quad . \tag{3.2.21}$$

(Note that R_c is in dimensionless form by regarding the Schwarzschild radius r_g as unity), contrary to Begelman's conclusion (ii).

An interesting question arrises from Ray's new result in case(iii). If both of the two critical points are physically possible, there would also be bistability for spherical accretion flows, as that for accretion flows with angular momentum, discussed in the last chapter. However, a very simple argument shows that, of Ray's two critical points, only one, $R_c^{(2)}$, is physical.

The key point is that the condition for a physical critical point, which was adopted by Begelman (1978) and Ray (1980),

$$R_c > 1 \tag{3.2.22}$$

is insufficient. From relations (3.1.9) it is easy to express the rest-mass density ρ_o as

$$\rho_o^{1/n} = \frac{nb^2}{k(n+1)(1-nb^2)} \quad . \tag{3.2.23}$$

ρ_o must be positive, and this requires that

$$b^2 < 1/n \ . \qquad (3.2.24)$$

Combining (3.2.24) and (3.2.16) gives

$$R_c > \frac{n+3}{4} \ . \qquad (3.2.25)$$

This condition is satisfied only by $R_c^{(2)}$ in (3.2.21).

Thus, condition (3.2.22) works only for $n < 1$, because in this case $(n + 3)/4 < 1$. It should be replaced by condition (3.2.25) when $n > 1$, then $(N + 3)/4 > 1$. Therefore, Ray's conclusion in his case(i) is correct, i.e. for $n < 1 - 1/2H_\infty$, no root of equation (3.2.18) satisfies (3.2.22). However, his case(ii) should be divided into two subcases:

Case(iia) $1 - \frac{1}{2H_\infty} < n < 1$, condition (3.2.22) is applicable. There are two positive roots of equation (3.2.18):

$$0 < R_c^{(1)} < 1 < R_c^{(2)} \ . \qquad (3.2.26)$$

Only $R_c^{(2)}$ represents a physical critical point.

Case(iib) $1 < n < 1 + \frac{1}{2H_\infty}$, condition (3.2.25) is applicable. One has now

$$0 < R_c^{(1)} < \frac{n+3}{4} < R_c^{(2)} \ . \qquad (3.2.27)$$

There is one and only one physical critical point.

Once the location of the critical point in a spherical accretion

flow is determined from given H_∞ and n, the rest-mass accretion rate can be obtained accordingly. Rewrite the equation of rest-mass conservation (3.2.4) in integrated form

$$\dot{m} = 4\pi r^2 \rho_0 u^r = \text{const} \tag{3.2.28}$$

By using (3.2.15), (3.2.16) and (3.2.23), the accretion rate can be expressed in dimensionless form as

$$\dot{M} = 2\pi R_c^{3/2} \left[\frac{1}{4R_c - 3 - n}\right]^n . \tag{3.2.29}$$

Thus, the accretion rate is a unique function of H_∞ when the polytropic index n and black hole mass M are fixed. The regularity condition

$$F(H_\infty, \dot{M}) = 0 \tag{3.2.30}$$

reduces the number of free parameters by one, so spherical accretion is a one-parameter problem.

The discussion has been complete. It has been shown that spherical accretion onto a black hole is characterized by a unique critical point (whenever it exists) in the flow, while bistability exists only for accretion of rotating matter, due to the non-uniqueness of the location of the critical point (a correct relativistic proof will be given later in this section). This gives an important distinction between the two types of accretion, with and without angular momentum.

b) Accretion of rotating matter

For accretion of rotating matter, the basic equations (3.1.1)-(3.1.3) read

$$\rho_0\left(\frac{du^r}{dr} + \frac{2}{r}u^r\right) + u^r\frac{d\rho_0}{dr} = 0 , \tag{3.2.31}$$

$$(\rho + P)\frac{du_t}{dr} + u_t\frac{dP}{dr} = 0 , \tag{3.2.32}$$

$$(\rho + P)\left(\frac{M}{r^2}u^t u^t + u_r\frac{du^r}{dr} - \frac{M}{r^2}u_r u_r - ru^\phi u^\phi\right)$$

$$+ (1 + u_r u^r)\frac{dP}{dr} = 0 , \tag{3.2.33}$$

$$(\rho + P)\frac{du_\phi}{dr} + u_\phi\frac{dP}{dr} = 0 , \tag{3.2.34}$$

$$(\rho + P)\left(\frac{du^r}{dr} + \frac{2}{r}u^r\right) + u^r\frac{d\rho}{dr} = 0 . \tag{3.2.35}$$

Only three of these five equations are independent, because the unknown functions ρ_0, ρ and P obey relations (3.1.9), and u^t, u^r and u^ϕ obey the condition (3.1.4). Equations (3.2.31) and (3.2.35) are exactly the same as (3.2.4) and (3.2.7), respectively. So the relation (3.2.8) still holds. Thus (3.2.32) can be integrated again to give (3.2.10). In addition, (3.2.34) can also be integrated to give

$$Hu_\phi = \text{const} \tag{3.2.36}$$

(3.2.36) and (3.2.10) are the relativistic Bernoulli equations.

The existence of two constants along the flow lines occurs because the flow is stationary and adiabatic, and the background spacetime is endowed with two Killing vector fields which satisfy the Killing equation

$$\xi_{\alpha;\beta} + \xi_{\beta;\alpha} = 0 \ . \qquad (3.2.37)$$

In this case the relativistic Bernoulli equation is implied

$$\frac{d(Hu_\alpha \xi^\alpha)}{d\tau} = 0 \ , \qquad (3.2.38)$$

here $d/d\tau$ is the derivative with respect to the proper time along the world lines of the fluid. In the spherical coordinate system, the Schwarzschild metric $g_{\alpha\beta}$ is symmetric with respect to the t- and the ϕ-coordinates,

$$\frac{\partial g_{\alpha\beta}}{\partial t} = \frac{\partial g_{\alpha\beta}}{\partial \phi} = 0 \ , \qquad (3.2.39)$$

thus the Killing vectors have components

$$\xi^\alpha_{(0)} = \delta^\alpha_0 \ ,$$

$$\xi^\alpha_{(3)} = \delta^\alpha_3 \ . \qquad (3.2.40)$$

The subscripts 0 and 3 represent t and ϕ, respectively. Equation (3.2.38)

gives (3.2.10) and (3.2.36). Note that the ratio of the two constants is

$$-\frac{u_\phi}{u_t} = L = (\text{the specific angular momentum as measured at infinity}) = \text{const} \qquad (3.2.41)$$

L is in the dimensionless form by regarding 2M as unity.

Now, combining (3.2.33) and (3.2.35) gives

$$\frac{du^r}{dr} = N/D \ , \qquad (3.2.42)$$

where

$$D = (1 - b^2)\, u_r u^r - b^2 \ , \qquad (3.2.43)$$

$$N = (1 + u_r u^r)\, \frac{2}{r}\, u^r\, b^2 + r\, u^r u^\phi u^\phi + \frac{M}{r^2}\, u_r u_r u^r - \frac{M}{r^2}\, u^t u^t u^r \ . \qquad (3.2.44)$$

Equation (3.2.42) has critical points where both D and N vanish. In contrast to the case of Newtonian theory, the physical meaning of the critical point is not apparent, since what appears here is the four-velocity, not the physical three-velocity. The measurement of the three-velocity depends on the observer, and in relativity there is no longer any uniform reference frame; all measurements can be made only locally. In the case of relativistic, adiabatic, spherical accretion (Flammang 1982), a critical point means a sonic point for a locally

static observer, i.e. the radial physical velocity measured by this observer is equal to the local sound velocity. It does not appear, however, that a static observer is also suitable for accretion flows with rotation. This can be checked as follows.

The four-velocity of the static observer in the Schwarzschild coordinate system is

$$w^{\alpha} = \left(\frac{1}{\sqrt{-g_{tt}}}, 0, 0, 0\right) , \qquad (3.2.44)$$

and the velocity of the accreted gas measured by him is

$$v^{\alpha} = - \frac{h^{\alpha}_{\beta}\, dx^{\beta}}{w_{\beta}\, dx^{\beta}} , \qquad (3.2.45)$$

where

$$h_{\alpha\beta} = g_{\alpha\beta} + w_{\alpha} w_{\beta}$$

is the observer's space-projection operator. Clearly,

$$v^{o} = 0 , \qquad v^{i} = \frac{u^{i}}{\sqrt{-g_{tt}}\, u^{t}} , \qquad (3.2.46)$$

the latin index i runs through only 1, 2 and 3. The physical velocity (ordinary three velocity) of the gas is defined as

$$v_{(i)} = (v_{i} v^{i})^{1/2} \qquad \text{for a fixed i .} \qquad (3.2.47)$$

By using (3.1.4), (3.2.41), (3.2.46) and (3.2.47), the relations

$$L = (1 - 1/R)^{-1/2} \, R \, v_{(\phi)} = \text{const} \tag{3.2.48}$$

and

$$u^t = (1 - 1/R)^{-1/2} \, (1 - v^2)^{-1/2} \, , \tag{3.2.49}$$

where

$$v^2 = v^2_{(r)} + v^2_{(\phi)} \, , \tag{3.2.50}$$

can be obtained.

Now, the conditions D = N = 0 at the critical point, together with (3.2.46)-(3.2.49), yield two relations

$$v^2_{(r)c} = b_c^2 \left[1 - L^2 (R_c - 1)/R_c^3 \right] \, , \tag{3.2.51}$$

$$\frac{1 - v^2_{(r)c}}{2(R_c - 1)} - \frac{L^2 (R_c - 1)}{R_c^3} = 2 b_c^2 \left[1 - L^2 (R_c - 1)/R_c^3 \right] . \tag{3.2.52}$$

The radial velocity of the gas measured by the static observer at a critical point is not equal to, but is less than, the local sound velocity. This is not a general-relativistic, but is a special-relativistic effect because the difference is caused by the "γ-factor" corresponding to the linear rotation velocity of the gas,

$$\gamma = (1 - v_{(\phi)}^2)^{-1/2} = \left[1 - L^2(R - 1)/R^3\right]^{-1/2} . \qquad (3.2.53)$$

Therefore it is expected that the sonic points and the critical points would coincide in the reference frame of the co-rotating observer.

The four-velocity of the co-rotating observer in the Schwarzschild coordinate system is

$$w^{\hat{\alpha}} = \left(\frac{\gamma}{\sqrt{-g_{tt}}}, 0, 0, \frac{\gamma\Omega}{\sqrt{-g_{tt}}}\right) , \qquad (3.2.54)$$

where Ω is the coordinate angular velocity of the gas, $\Omega = \frac{u^{\phi}}{u^t} = \frac{d\phi}{dt}$, and the velocity of the gas measured by him would be

$$v^{\hat{r}} = \frac{\gamma\, u^r}{\sqrt{-g_{tt}}\, u^t} = \gamma v^r . \qquad (3.2.56)$$

All other components of the measured velocity of the gas vanish. Thus equations (3.2.51) and (3.2.52) become, for this observer,

$$v_{(\hat{r})}^2 = b_c^2 , \qquad (3.2.57)$$

$$\frac{\gamma^2 - v_{(\hat{r})c}^2}{2(R_c - 1)} - (\gamma^2 - 1) = 2b_c^2 . \qquad (3.2.58)$$

This is just the expected result that a critical point is a sonic point and this fact can be realized only by the co-rotating observer.

By using (3.2.10), (3.2.17), (3.2.48), (3.2.49) and (3.2.53), the constant H_{∞} can be expressed as

$$H_\infty = (1 - 1/R)^{1/2} (1 - nb^2)^{-1} \left[1 - v_{(r)}^2 - L^2(R - 1)/R^3\right]^{-1/2}$$

$$= (1 - 1/R)^{1/2} (1 - nb^2)^{-1} (1 - v_{(\hat{r})}^2)^{-1/2} \gamma \quad . \qquad (3.2.59)$$

Equation (3.2.59) together with (3.2.51) and (3.2.52) (or (3.2.57) and (3.2.58)) can be used to obtain R_c, b_c and $v_{(r)c}$ (or $v_{(\hat{r})c} = b_c$) from the given constants L and H_∞. After considerable algebra, one can get

$$\left[- n^2\left(\frac{2R_c - 2}{4R_c - 3}\right)^3 + n(n + 2)\left(\frac{2R_c - 2}{4R_c - 3}\right)^2 - (2n + 1)\frac{2R_c - 2}{4R_c - 3} + 1\right]$$

$$\left[1 - \frac{L^2(R_c - 1)}{R_c^3}\right]^3 + \left[3n^2\left(\frac{2R_c - 2}{4R_c - 3}\right)^2 \frac{2R_c - 3}{4R_c - 3} - 4n(n + 2)\frac{(R_c - 1)(2R_c - 3)}{(4R_c - 3)^2}\right.$$

$$\left. + (2n + 1)\frac{2R_c - 3}{4R_c - 3} - (1 - 1/R_c)H_\infty^{-2}\right]\left[1 - \frac{L^2(R_c - 1)}{R_c^3}\right]^2$$

$$- \left[3n^2\left(\frac{2R_c - 2}{4R_c - 3}\right)\left(\frac{2R_c - 3}{4R_c - 3}\right)^2 - n(n + 2)\left(\frac{2R_c - 3}{4R_c - 3}\right)^2\right]\left[1 - \frac{L^2(R_c - 1)}{R_c^3}\right]$$

$$+ n^2\left(\frac{2R_c - 3}{4R_c - 3}\right)^3 = 0 \quad , \qquad (3.2.60)$$

which is much more complicated than the corresponding formula (3.2.18) for spherical accretion, and also than that for accretion with rotation in the pseudo-Newtonian theory.

The solution of equation (3.2.60) for the location of the critical point R_c as a function of the specific angular momentum L and the specific enthalpy H_∞ is shown in Figure 15. The graph is very similar to the corresponding one in the pseudo-Newtonian theory, Figure 5b. Note from (3.2.17) that

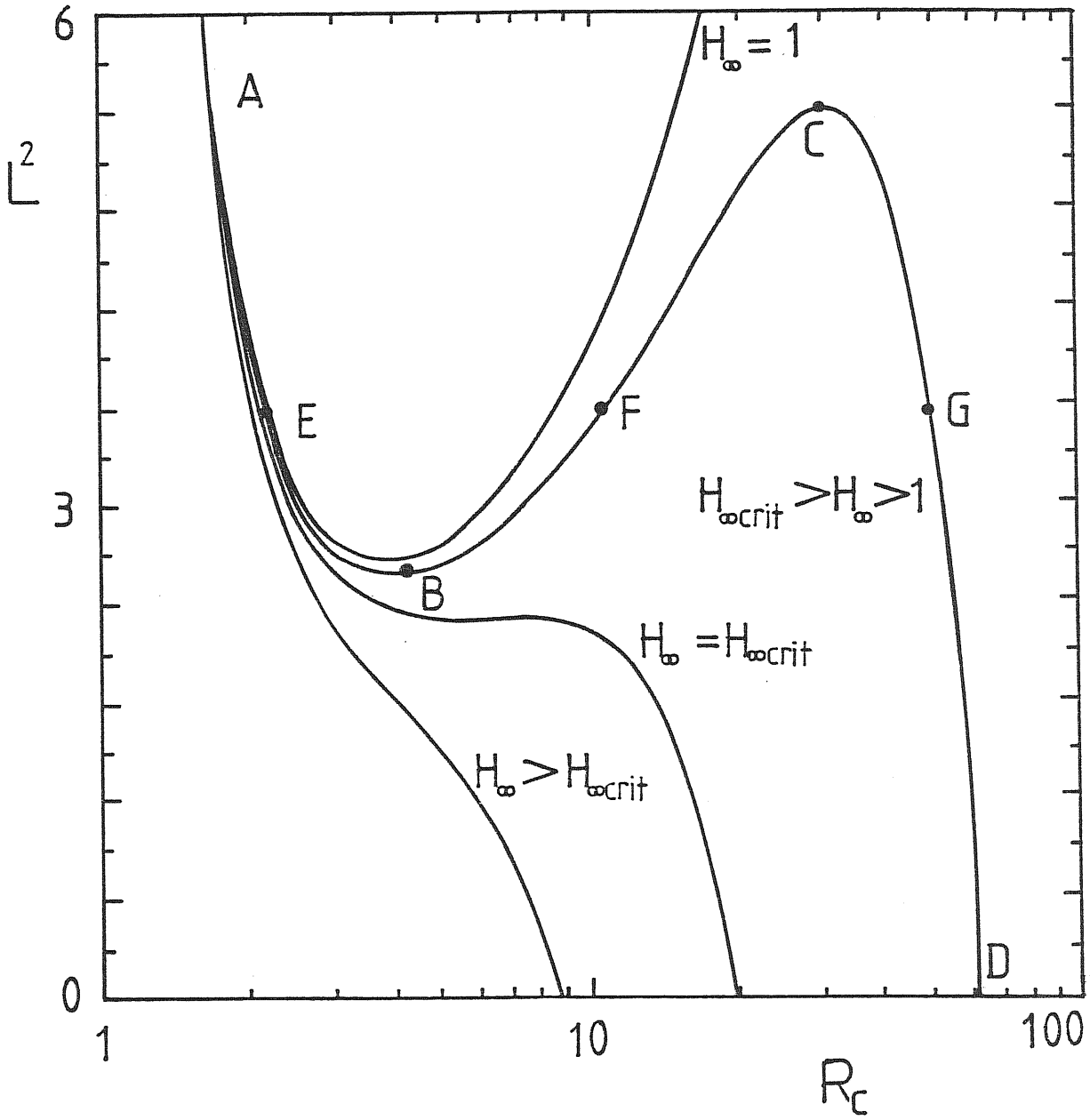

Fig. 15 The location of the critical point R_c as a function of the specific enthalpy at infinity H_∞ and the specific angular momentum L

$$H_\infty \approx 1 + E \ , \qquad \text{for } E \ll 1 \qquad (3.2.61)$$

because

$$E = nb^2_\infty \ . \qquad (3.2.62)$$

It is seen from Figure 15 that for $1 < H_\infty < H_{\infty crit} \approx 1.02$, there exist three formal critical points (e.g. points E, F and G) for a given pair of L and H_∞. According to the analysis in §2.4 and §2.5, only two of them, the inner one (E) and the outer one (G), are physically possible because they are saddle type critical points, while the intermediate one (F) is a vortex type critical point. Only one of E and G, depending on the value of L when H_∞ is fixed, corresponds to a realizable global transonic solution.

The specific rest-mass accretion rate can be obtained once the location of the critical point, the sound velocity and the radial velocity of the gas at the critical point are evaluated. Integrating (3.2.31) gives

$$r^2 \rho_o u^r = \frac{\dot{m}}{4\pi\omega} = \text{const} \qquad (3.2.63)$$

where $\dot{m}$ is the rest-mass accretion rate and ω is the opening angle of the flow. Using (3.2.23) and (3.2.46)-(3.2.49), the specific rest-mass accretion rate can be expressed in the dimensionless form as

$$\dot{M}_o = \frac{\dot{M}}{\omega} = R^2(1 - 1/R)^{1/2}\left(\frac{b^2}{1 - nb^2}\right)^n v_{(r)}\left[1 - v^2_{(r)} - \frac{L^2(R - 1)}{R^3}\right]^{-1/2}$$

$$= R^2(1 - 1/R)^{1/2}\left(\frac{b^2}{1 - nb^2}\right)^n v_{(\hat{r})}(1 - v^2_{(\hat{r})})^{-1/2}$$

$$= \text{const} \qquad (3.2.64)$$

Figure 16 gives $\dot{M}_0$ as a fuction of L for a fixed H_∞. For comparison, the relevant result in the pseudo-Newtonian theory is also given. This is calculated using the Newtonian formula (cf. Figure 10)

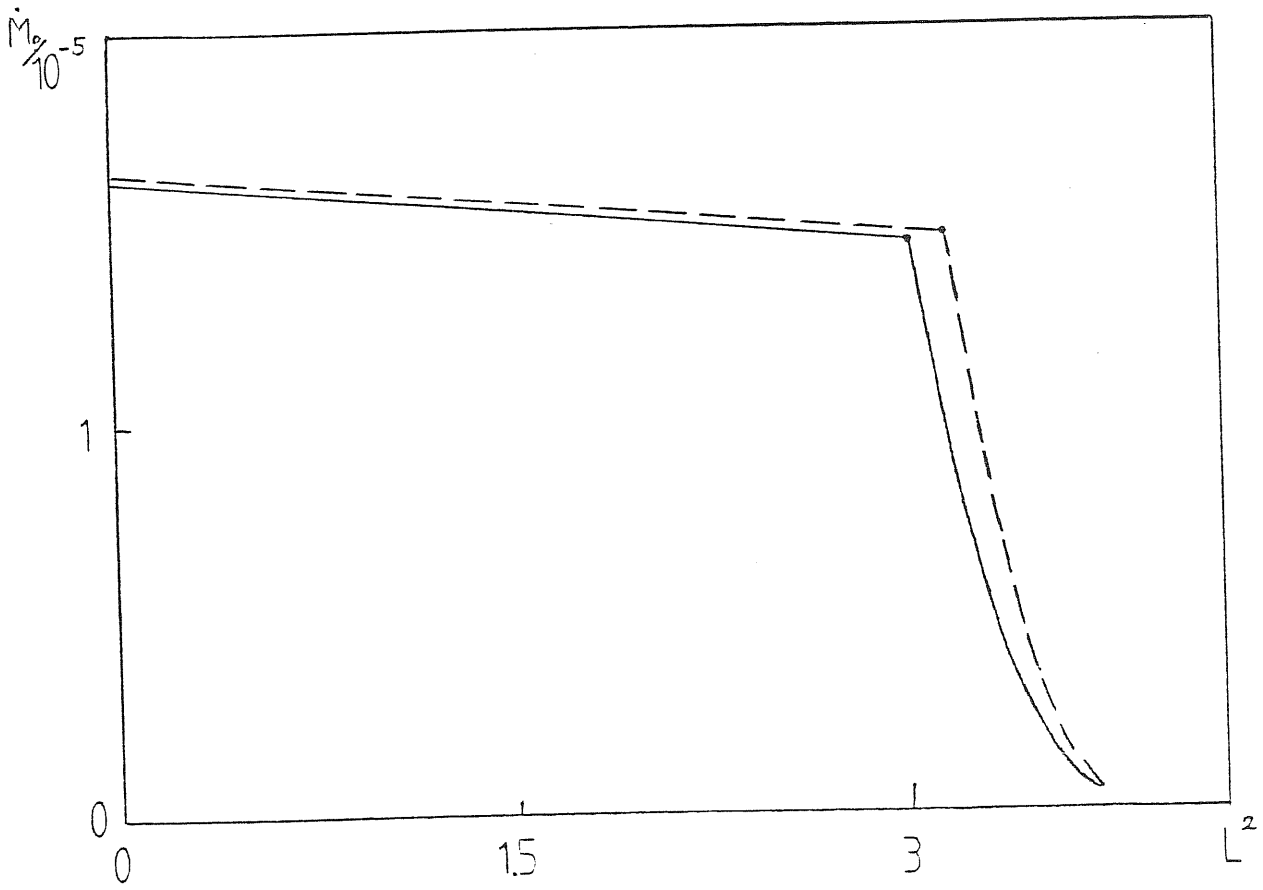

Fig. 16 The specific rest-mass accretion rate $\dot{M}_0$ as a function of the specific angular momentum L for a given value of the specific enthalpy at infinity, $H_\infty = 1.006$ (solid line). The relevant result in the pseudo-Newtonian theory is also presented (dashed line).

$$\dot{M}_0 = R^2 \, b^{2n} \, v_{(r)} \, . \qquad (3.2.65)$$

Two accretion regimes (Bondi-type and disklike), defined in the last

chapter, are clearly seen in the relativistic theory.

Quantitatively, the specific rest-mass accretion rate is systematically overestimated by the pseudo-Newtonian theory. However, as reflected in the exterme similarity of the shape of the two curves, and in the very small quantitative difference between them, Paczyńnski's purely Newtonian model of a black hole provides a very good description of accretion flows onto black holes, and greatly simplifies the calculations.

3.3 The Kerr metric

In the standard Boyer-Lindquist coordinate system, the Kerr metric is

$$g_{\alpha\beta} = \begin{pmatrix} -(1 - 2Mr/\Sigma) & 0 & 0 & -2MarSin^2\theta/\Sigma \\ 0 & \Sigma/\Delta & 0 & 0 \\ 0 & 0 & \Sigma & 0 \\ -2MarSin^2\theta/\Sigma) & 0 & 0 & ASin^2\theta/\Sigma \end{pmatrix} \tag{3.3.1}$$

$$g^{\alpha\beta} = \begin{pmatrix} -A/\Sigma\Delta & 0 & 0 & -2Mar/\Sigma\Delta \\ 0 & \Delta/\Sigma & 0 & 0 \\ 0 & 0 & 1/\Sigma & 0 \\ -2Mar/\Sigma\Delta & 0 & 0 & \dfrac{\Delta - a^2Sin^2\theta}{\Sigma\Delta Sin^2\theta} \end{pmatrix}$$

where

$$\Delta = r^2 - 2Mr + a^2 ,$$

$$\Sigma = r^2 + a^2\cos^2\theta ,$$

$$A = (r^2 + a^2)^2 - a^2\Delta\sin^2\theta ,$$

and a is the specific angular momentum (angular momentum per unit mass) of the black hole.

The non-zero components of the affine connection, calculated from (3.2.2) and (3.3.1), are:

$$\Gamma^t_{tr} = \Gamma^t_{rt} = (2Ma^2r\sin^2\theta - A)\frac{M}{\Sigma^2\Delta}(1 - 2r^2/\Sigma),$$

$$\Gamma^t_{t\theta} = \Gamma^t_{\theta t} = \frac{2Ma^2r\sin\theta\cos\theta}{\Sigma^3\Delta}\left[2Mr(r^2 + a^2) - A\right],$$

$$\Gamma^t_{r\phi} = \Gamma^t_{\phi r} = \frac{Ma\sin^2\theta}{\Sigma^2\Delta}\left[A - 4(r^2 + a^2)r^2 + 2a^2r(r - M)\sin^2\theta\right],$$

$$\Gamma^t_{\theta\phi} = \Gamma^t_{\phi\theta} = \frac{Mar}{\Sigma^2\Delta}\left[\frac{2A(r^2 + a^2)\sin\theta\cos\theta}{\Sigma} - 2\sin\theta\cos\theta(A - a^2\Delta\sin^2\theta)\right],$$

$$\Gamma^r_{tt} = -\frac{M\Delta}{\Sigma^2}\left(1 - \frac{2r^2}{\Sigma}\right) ,$$

$$\Gamma^r_{t\phi} = \Gamma^r_{\phi t} = \frac{Ma\Delta\sin^2\theta}{\Sigma^2}(1 - 2r^2/\Sigma),$$

$$\Gamma^r_{r\theta} = \Gamma^r_{\theta r} = -a^2\sin\theta\cos\theta/\Sigma ,$$

$$\Gamma^r_{rr} = \frac{1}{\Sigma}\left[r - \frac{\Sigma(r - M)}{\Delta}\right],$$

$$\Gamma^r_{\theta\theta} = -\Delta r/\Sigma ,$$

$$\Gamma^{r}_{\phi\phi} = \frac{\Delta \sin^2\theta}{\Sigma^2}\left[\frac{Ar}{\Sigma} - 2r(r^2 + a^2) + a^2\sin^2\theta\,(r - M)\right],$$

$$\Gamma^{\theta}_{tt} = -2Ma^2 r \sin\theta\cos\theta/\Sigma^3,$$

$$\Gamma^{\theta}_{rr} = a^2\sin\theta\cos\theta/\Sigma\Delta,$$

$$\Gamma^{\theta}_{\theta\theta} = -a^2\sin\theta\cos\theta/\Sigma,$$

$$\Gamma^{\theta}_{\phi\phi} = -\frac{\sin\theta\cos\theta}{\Sigma^2}(A - a^2\Delta\sin^2\theta),$$

$$\Gamma^{\theta}_{r\theta} = \Gamma^{\theta}_{\theta r} = r/\Sigma,$$

$$\Gamma^{\phi}_{tr} = \Gamma^{\phi}_{rt} = -\frac{1}{\Sigma^2\Delta}\left[2M^2 ar + Ma(\Delta - a^2\sin^2\theta)\right](1 - 2r^2/\Sigma),$$

$$\Gamma^{\phi}_{t\theta} = \Gamma^{\phi}_{\theta t} = -\frac{2\sin\theta\cos\theta}{\Sigma^3\Delta}\left[2M^2a^3r^2 + \frac{Mar(\Delta - a^2\sin^2\theta)(r^2 + a^2)}{\sin^2\theta}\right],$$

$$\Gamma^{\phi}_{r\phi} = \Gamma^{\phi}_{\phi r} = \frac{1}{\Sigma^2\Delta}\left\{2M^2a^2 r\sin^2\theta\,(1 - \frac{2r^2}{\Sigma}) + \frac{1}{2}(\Delta - a^2\sin^2\theta)\right.$$

$$\left.\left[4r(r^2 + a^2) - 2a^2\sin^2\theta\,(r - M) - \frac{2Ar}{\Sigma}\right]\right\},$$

$$\Gamma^{\phi}_{\theta\phi} = \Gamma^{\phi}_{\phi\theta} = \frac{2\sin\theta\cos\theta}{\Sigma^2\Delta}\left\{\frac{2M^2a^2r^2(r^2 + a^2)}{\Sigma} + \frac{1}{2}\left[\frac{\Delta - a^2\sin^2\theta}{\sin^2\theta}(A - a^2\Delta\sin^2\theta)\right]\right\}. \tag{3.3.2}$$

By using (3.3.1) and (3.3.2), the basic equations (3.1.1)-(3.1.3)

keep their explicit form (on the equatorial plane). The equation of rest-mass conservation, the t- and the ϕ-components of the Euler equation, and the equation of local energy conservation are, respectively, exactly the same as (3.2.31), (3.2.32), (3.2.34) and (3.2.35). Thus (3.2.10) and (3.2.36) also hold here, i.e. there exist two constants of motion along the flow lines. This is because the Kerr metric in the Boyer-Lindquist coordinate system is also symmetric with respect to the t- and ϕ-coordinates, i.e. the spacetime is also endowed with two Killing vector fields.

However, in contrast to (3.2.33), the r-component of the Euler equation is now

$$(\rho + P)\left[\frac{\Sigma}{\Delta} u^r \frac{du^r}{dr} + \frac{a^2 r - Mr^2}{\Delta^2} u^r u^r - \frac{M(r^2 + a^2)}{\Sigma\Delta} u^t u_t - \frac{Ma}{\Sigma\Delta} u^t u_\phi \right.$$

$$\left. + \frac{3Mar^2 + Ma^3}{\Sigma\Delta} u_t u^\phi - \frac{r^3 - Ma^2 - 2Mr^2}{\Sigma\Delta} u^\phi u_\phi \right]$$

$$+ (1 + u_r u^r) \frac{dP}{dr} = 0 , \qquad (3.3.3)$$

which can be combined with the equation of local energy conservation (3.2.35) to give

$$\frac{du^r}{dr} = N/D , \qquad (3.3.4)$$

where

$$D = u_r u^r - b^2(1 + u_r u^r), \tag{3.3.5}$$

$$N = \frac{2b^2 u^r}{r}(1 + u_r u^r) + \frac{1}{r^2\Delta}\Big[(Mr^2 - a^2 r)u^r u^r u_r + (Mr^2 + Ma^2)u^t u_t u^r$$

$$+ Mau^t u^r u_\phi - (3Mar^2 + Ma^3)u_t u^r u^\phi + (r^3 - Ma^2 - 2Mr^2)u^r u^\phi u_\phi\Big]. \tag{3.3.6}$$

From the discussion in the last section, it is apparent that a co-rotating observer is a suitable one for understanding the physical meaning of the critical point of (3.3.4). The only non-vanishing component of the physical three-velocity of the accreted gas measured by this observer can be obtained by the Lorentz transformation

$$v_{(\hat{r})} = \frac{v_{(r)}}{(1 - v^2_{(\phi)})^{1/2}} , \tag{3.3.7}$$

where

$$v_{(r)} = -(-g_{tt}g^{rr})^{1/2}\ \frac{u_r}{u_t} , \tag{3.3.8}$$

$$v_{(\phi)} = -(g^{\phi\phi})^{1/2}\left[(-g_{tt})^{1/2}\ \frac{u_\phi}{u_t} + \frac{g_{\phi t}}{(-g_{tt})^{1/2}}\right] , \tag{3.3.9}$$

are, respectively, the physical radial and azimuthal velocities measured by a locally static observer.

By using (3.3.7)-(3.3.9) and the normalization condition (3.1.4), one can obtain the expression

$$u_t = -(-g_{tt})^{1/2}(1 - v_{(\hat{r})}^2)^{-1/2}(1 - v_{(\phi)}^2)^{-1/2}$$

$$= -(-g_{tt})^{1/2}(1 - v_{(\hat{r})}^2)^{-1/2}\left\{1 - g^{\phi\phi}\left[(-g_{tt})^{1/2}L - \frac{g_{\phi t}}{(-g_{tt})^{1/2}}\right]^2\right\}^{-1/2} , \tag{3.3.10}$$

where L is the specific angular momentum of the gas defined in (3.2.41), and the critical point condition D = 0 reads

$$v_{(\hat{r})}^2 = b_c^2 . \tag{3.3.11}$$

Thus, for adiabatic accretion onto a rotating black hole, the sonic point is located at the critical point of (3.3.4), and this fact can be realized only by the co-rotating observer. The other critical point condition N = 0 yields another useful relation:

$$\frac{(2r_c^2 - 3Mr_c - a^2)\left\{r_c^2(r_c^2 - 2Mr_c + a^2) - \left[(r_c - 2M)L + 2Ma\right]^2\right\}}{r_c - 2M} v_{(\hat{r})c}^2$$

$$+ (r_c^3 - 4Mr_c^2 + 4M^2r_c - Ma^2)L^2 - (8M^2ar_c - 6Mar_c^2 - 2Ma^3)L$$

$$+ (4M^2a^2r_c - 2Ma^2r_c^2 - Ma^4 - Mr_c^4) = 0 . \tag{3.3.12}$$

By substituting (3.2.17) and (3.3.10) into (3.2.10), the constant H_∞ can be expressed as

$$H_\infty = (1 - 2M/r)^{1/2}(1 - nb^2)^{-1}(1 - v_{(\hat{r})}^2)^{-1/2}\left\{1 - \frac{\left[(r - 2M)L + 2Ma\right]^2}{r^2(r^2 - 2Mr + a^2)}\right\}^{-1/2} \tag{3.3.13}$$

Equation (3.3.13) together with (3.3.12) can be used to obtain r_c and $v_{(\hat{r})c}$ $(= b_c)$ from the given constants L and H_∞. By eliminating $v_{(\hat{r})c}$ between these two equations one obtains, after quite hard algebra,

$$\left[n^2D^3/A^3 - E^3 - (n^2 + 2n)D^2E/A^2 + (2n + 1)E^2D/A\right]L^6$$

$$- \left[3n^2CD^2/A^3 - 3E^2F - (n^2 + 2n)D^2F/A^2 - 2(n^2 + 2n)CDE/A^2\right.$$

$$\left. + (2n + 1)E^2C/A + 2(2n + 1)EFD/A\right]L^5$$

$$+ \left\{3n^2C^2D/A^3 + 3n^2BD^2/A^3 - 3E^2G - 3EF^2 + \left[3 - (1 - 2M/r_c)H_\infty^{-2}\right]E^2\right.$$

$$+ (n^2 + 2n)D^2/A^2 - (n^2 + 2n)C^2E/A^2 - (n^2 + 2n)D^2G/A^2 - 2(n^2 + 2n)BDE/A^2$$

$$- 2(n^2 + 2n)CDF/A^2 - 2(2n + 1)ED/A + (2n + 1)E^2B/A + (2n + 1)F^2D/A$$

$$\left. + 2(2n + 1)EFC/A + 2(2n + 1)EGD/A\right\}L^4$$

$$- \left\{2\left[3 - (1 - 2M/r_c)H_\infty^{-2}\right]EF - F^3 - 6EFG + n^2C^3/A^3 + 6n^2BCD/A^3\right.$$

$$+ 2(n^2 + 2n)CD/A^2 - (n^2 + 2n)C^2F/A^2 - 2(n^2 + 2n)BCE/A^2$$

$$- 2(n^2 + 2n)BDF/A^2 - 2(n^2 + 2n)CDG/A^2 - 2(2n + 1)EC/A - 2(2n + 1)FD/A$$

$$\left. + (2n + 1)F^2C/A + 2(2n + 1)EFB/A + 2(2n + 1)EGC/A + 2(2n + 1)FGD/A\right\}L^3$$

$$+\left\{\left[3-(1-2M/r_c)H_\infty^{-2}\right](F^2+2EG)-3EG^2-3F^2G+3n^2B^2D/A^3\right.$$

$$+3n^2BC^2/A^3+(n^2+2n)C^2/A^2+2(n^2+2n)BD/A^2-(n^2+2n)B^2E/A^2$$

$$-(n^2+2n)C^2G/A^2-2(n^2+2n)BCF/A^2-2(n^2+2n)BDG/A^2+(2n+1)D/A$$

$$-2(2n+1)EB/A-2(2n+1)FC/A-2(2n+1)GD/A+(2n+1)F^2B/A$$

$$+(2n+1)G^2D/A+2(2n+1)EGB/A+2(2n+1)FGC/A$$

$$\left.+\left[2(1-2M/r_c)H_\infty^{-2}-3\right]E\right\}L^2$$

$$-\left\{2\left[3-(1-2M/r_c)H_\infty^{-2}\right]FG-3FG^2+3n^2B^2C/A^3+2(n^2+2n)BC/A^2\right.$$

$$-(n^2+2n)B^2F/A^2-2(n^2+2n)BCG/A^2+(2n+1)C/A-2(2n+1)FB/A$$

$$-2(2n+1)GC/A+(2n+1)G^2C/A+2(2n+1)FGB/A$$

$$\left.+\left[2(1-2M/r_c)H_\infty^{-2}-3\right]F\right\}L$$

$$+(n^2+2n)B^2/A^2-(n^2+2n)B^2G/A^2+(2n+1)B/A-2(2n+1)GB/A$$

$$+(2n+1)G^2B/A-(1-2M/r_c)H_\infty^{-2}+\left[2(1-2M/r_c)H_\infty^{-2}-3\right]G$$

$$+\left[3-(1-2M/r_c)H_\infty^{-2}\right]G^2-G^3+n^2B^3/A^3+1=0\ , \qquad (3.3.14)$$

where

$$A = (2r_c^6 - 7Mr_c^5 + 6M^2r_c^4 + 3a^2r_c^4 - 5Ma^2r_c^3 + a^4r_c^2)/(r_c - 2M) ,$$

$$B = 4M^2a^2r_c - 2Ma^2r_c^2 - Ma^4 - Mr_c^4 ,$$

$$C = 8M^2ar_c - 6Mar_c^2 - 2Ma^3 ,$$

$$D = r_c^3 - 4Mr_c^2 + 4M^2r_c - Ma^2 ,$$

$$E = (r_c - 2M)^2/r_c^2(r_c^2 - 2Mr_c + a^2) ,$$

$$F = -4Ma(r_c - 2M)/r_c^2(r_c^2 - 2Mr_c + a^2) ,$$

$$G = 4M^2a^2/r_c^2(r_c^2 - 2Mr_c + a^2) .$$

The solution of equation (3.3.14) for the locations of the critical point r_c as functions of the specific angular momentum and the specific enthalpy at infinity, L and H_∞, are shown in Figure 17 for different values of a. When a = 0 (Schwarzschild black hole), the graph is perfectly symmetric with respect to the axis L = 0 (Figure 17a), as it should be.

Fig. 17 The location of the critical point r_c as functions of the specific angular momentum and the specific enthalpy measured at infinity, L and H_∞, for four different values of the specific angular momentum of the black hole a. Fig. (a), (b), (c) and (d) are for a = 0, 0.1, 0.9 and 1, respectively. In all the figures curves a, b, c and d are for H_∞ = 1, 1.004, 1.02 and 1.085, respectively.

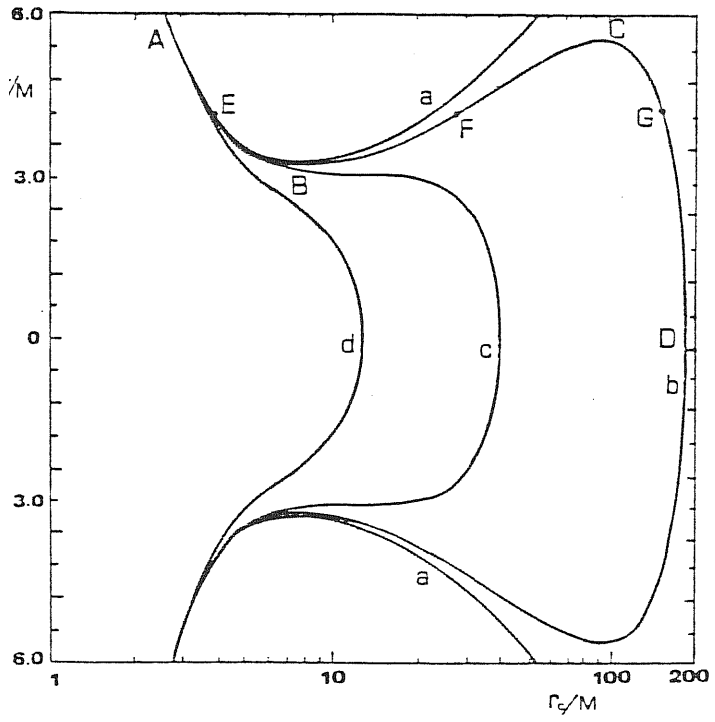

(a)

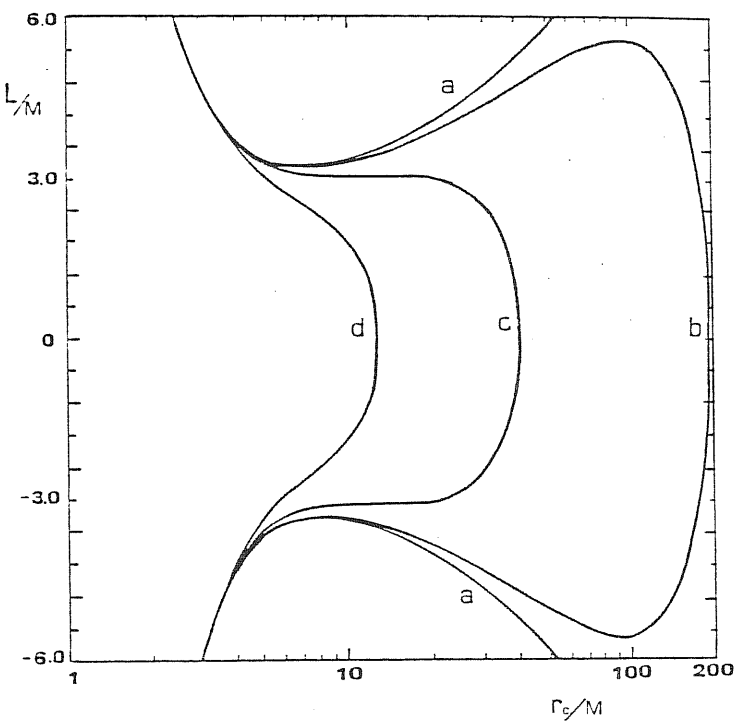

(b)

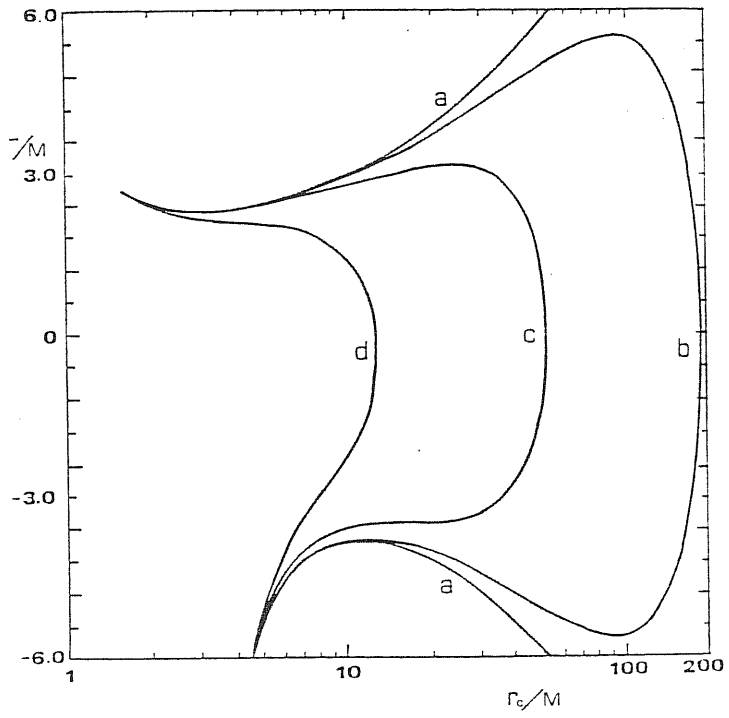

(c)

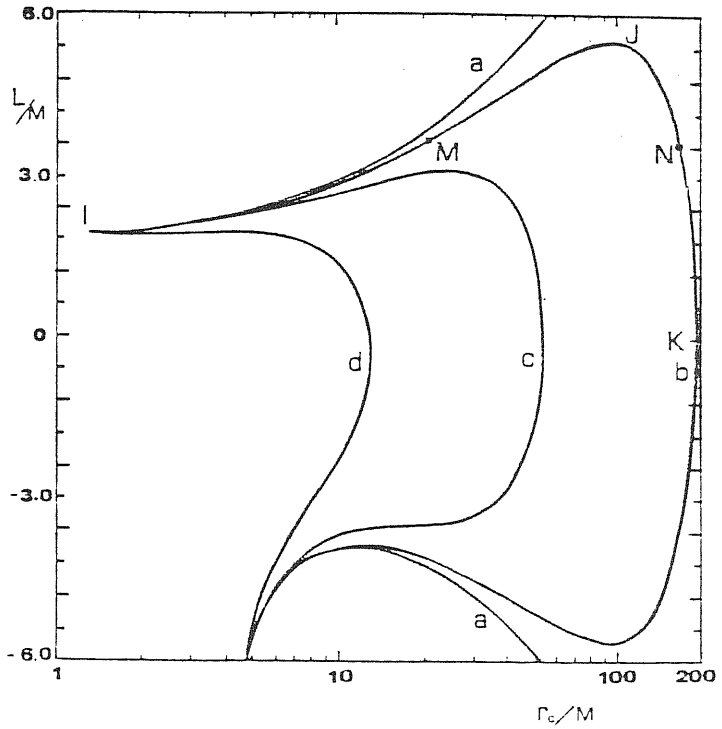

(d)

Figure 17

It is exactly the same as Figure 15 and needs no discussion. For non-zero, but small, values of a, the asymmetry in the graph caused by a is very small (Figure 17b), and all the properties for accretion onto a Schwarzschild black hole still hold. For $1 < H_\infty < H_{\infty crit}$, there may exist three formal locations of the sonic point corresponding to the same L and H_∞, but only two of them are physically possible, and only one corresponds to a globally realizable transonic accretion flow; there exist two separate regimes of accretion: Bondi-type and disklike.

More interesting is the case of a sufficiently large value of a. When $a \gtrsim 0.9$ (Figure 17c,d), the effect of the interaction between the spin of the black hole and the rotation of the accreted gas (spin-rotation interaction) plays an important role in determining the location of the sonic point. According to the criterion given in §2.4,

$$\text{sign}\left(\frac{dL^2}{dr_c}\right) = \text{sign}\left(2L\,\frac{dL}{dr_c}\right)\begin{cases} + \longrightarrow \text{vortex type critical point} \longrightarrow \text{unphysical} \\ - \longrightarrow \text{saddle type critical point} \longrightarrow \text{physical} \end{cases}$$

it is seen from the lower part of the curve b in Figure 17d that there exist two physically possible locations of the sonic point, thus two accretion regimes, only for accretion flows with negative angular momentum. Note that

$$L = -u_\phi/u_t = \frac{g_{\phi\phi}(\omega - \Omega)}{g_{t\phi}(\Omega + g_{tt}/g_{t\phi})}$$

$$= -\frac{(r^3 + ra^2 + 2Ma^2)}{2Ma}\,\frac{(\omega - \Omega)}{(\Omega + \frac{r - 2M}{2Ma})}\,, \qquad (3.3.15)$$

where Ω is the coordinate angular velocity of the gas, and

$$\omega = - g_{\phi t}/g_{\phi\phi} = \frac{2Ma}{r^3 + ra^2 + 2Ma^2} \qquad (3.3.16)$$

is the angular velocity of the locally nonrotating observer (cf. Bardeen et al. 1973). Thus $L<0$ means $\Omega<\omega$, i.e. the flow is rotating in retrograde orbits. For co-rotating flows (direct orbits, $L>0$, $\Omega>\omega$), of the two formal locations of the critical point corresponding to the same L and H_∞ (e.g. points M and N), only the outer one (N) represents a physical sonic point. The two-regime-character of the accertion is now destroyed by the spin-rotation interaction, and only the Bondi-type accretion is possible (the piece JK), i.e. the flow becomes supersonic when it is far from the black hole. The properties of a co-rotating accretion flow onto a very rapidly rotating black hole are similar to those of a spherical (no rotation) accretion flow onto a non-rotating hole. The case that both a black hole and an accretion flow are rotating in the same direction seems to be equivalent to both of them being non-rotating.

Astrophysically realistic accretion flows are likely to be co-rotating (e.g. in the case where the accreted matter is from a normal star which together with a rotating black hole form a binary system). On the theoretical side, it has been pointed out that for the inner regions of an accretion disk, the angular momenta of the disk and the black hole are aligned. This is because the rotation of inertial frames close to the hole causes precession of the disk and eventual alignment (Bardeen and Petterson 1975). Thus, a clear distinction appears between the accretion of rotating matter onto a very rapidly rotating black hole and that onto a non-rotating, or slowing rotating, one. The astrophysical implications of this distinction need to be studied.

4. Time-dependent flow: a simple model

The discussion of stationary, adiabatic, regular, transonic accretion of rotating matter onto a black hole has been completed in the last two chapters. The results can be summarized in one sentence: the accretion rate is an eigenvalue of the problem and is uniquely determined by the given physical situation (fixed specific energy and specific angular momentum); it cannot be assumed.

However, the accretion rate could be fixed by outside physical processes (e.g. by the mass-losing star in a binary system), or in numerical calculations by outside boundary conditions. In this case the regularity condition (2.6.6) is in general not fulfilled, and then the regular, stationary, transonic solution is impossible. What will happen for such a flow? Abramowicz and Zurek (1981) argued that the flow would oscillate between the Bondi-type and the relativistic solutions. It will be confirmed in this chapter that this oscillatory behaviour is indeed possible, by discussing a time-dependent model of the flow. It will also be shown that a large variety of temporal behaviour can be expected from black hole accretion.

4.1 Formalism

Two simplifications are still adopted here: the relative general-relativistic effects can be simulated by the Newtonian model of a non-rotating black hole, and the flow is quasi-radial. As seen in the last two chapters, these two assumptions are not essential as the qualitative

conclusions are not changed by them.

For the quasi-radial flow, the basic equations (2.2.1)-(2.2.3) can form a closed system at the zeroth order of expansion (withdrawing the subscript 0 and using $v = v^r$, $L = r^2 v^\phi$):

$$\frac{\partial \rho}{\partial t} + \rho \frac{\partial v}{\partial r} + v \frac{\partial \rho}{\partial r} + \frac{2}{r} \rho v = 0 , \tag{4.1.1}$$

$$\frac{\partial v}{\partial t} + v \frac{\partial v}{\partial r} - L^2/r^3 + \frac{GM}{(r - r_g)^2} + \frac{1}{\rho} \frac{\partial P}{\partial r} = 0 , \tag{4.1.2}$$

$$\frac{\partial L}{\partial t} + v \frac{\partial L}{\partial r} = 0 , \tag{4.1.3}$$

$$P = k \rho^{1+1/n} . \tag{4.1.4}$$

If it is further assumed for simplicity that the angular momentum L is constant in time (and thus in space), then the above equations can be reduced by using the polytropic relation

$$\rho = \left[\frac{n}{k(n+1)}\right]^n a^{2n} , \tag{4.1.5}$$

where a is the adiabatic sound speed, to

$$2n \frac{\partial a}{\partial t} + a \frac{\partial v}{\partial r} + 2nv \frac{\partial a}{\partial r} + \frac{2}{r} va = 0 , \tag{4.1.6}$$

$$\frac{\partial v}{\partial t} + v \frac{\partial v}{\partial r} + 2na \frac{\partial a}{\partial r} + \frac{\partial W}{\partial r} = 0 , \tag{4.1.7}$$

where

$$W = - \frac{GM}{r - r_g} + \frac{1}{2} L^2/r^2 \qquad (4.1.8)$$

is the effective potential for radial motion.

Regular accretion onto a black hole must be transonic, even if it is non-stationary, because two boundary conditions still hold: the radial velocity of the flow is highly subsonic at large distances from the hole and reaches the velocity of light at the horizon. If one denotes by $r_s(t)$ the location of the sonic point on the equatorial plane, and by $X_s(t)$ the value of every physical quantity X at the sonic point, then

$$X_s(t) \equiv X(t, r_s(t)), \qquad (4.1.9)$$

and

$$\frac{dX_s}{dt} = \left(\frac{\partial X}{\partial r}\right)_s \frac{dr_s}{dt} + \left(\frac{\partial X}{\partial t}\right)_s . \qquad (4.1.10)$$

Note from the definition (4.1.9) that

$$v_s(t) = -a_s(t) , \qquad (4.1.11)$$

and

$$\frac{dv_s}{dt} = - \frac{da_s}{dt} . \qquad (4.1.12)$$

(v is regarded as negative because for accretion flows $v = \frac{dr}{dt} < 0$).

From (4.1.10)-(4.1.12) one gets

$$\frac{dr_s}{dt} = - \frac{(\frac{\partial a}{\partial t})_s + (\frac{\partial v}{\partial t})_s}{(\frac{\partial a}{\partial r})_s + (\frac{\partial v}{\partial r})_s} \quad , \tag{4.1.13}$$

$$\frac{da_s}{dt} = \frac{(\frac{\partial a}{\partial t})_s(\frac{\partial v}{\partial r})_s - (\frac{\partial v}{\partial t})_s(\frac{\partial a}{\partial r})_s}{(\frac{\partial a}{\partial r})_s + (\frac{\partial v}{\partial r})_s} \quad . \tag{4.1.14}$$

Replacing the time derivatives in (4.1.13) and (4.1.14) with spatial ones by using equations (4.1.6) and (4.1.7), and after some straightforward algebra, one can derive the following two basic equations:

$$\frac{dr_s}{dt} = - \frac{(2n - 1)a_s\left[\frac{1}{2n}(\frac{\partial v}{\partial r})_s - (\frac{\partial a}{\partial r})_s\right] + \frac{1}{n} a_s^2/r_s - (\frac{\partial W}{\partial r})_s}{(\frac{\partial a}{\partial r})_s + (\frac{\partial v}{\partial r})_s} \quad , \tag{4.1.15}$$

$$\frac{da_s}{dt} = \frac{2na_s\left[(\frac{\partial a}{\partial r})_s^2 - (\frac{\partial v}{\partial r})_s^2/4n^2\right] + \frac{1}{n} a_s^2(\frac{\partial v}{\partial r})_s/r_s + (\frac{\partial a}{\partial r})_s(\frac{\partial W}{\partial r})_s}{(\frac{\partial a}{\partial r})_s + (\frac{\partial v}{\partial r})_s} \quad . \tag{4.1.16}$$

4.2 Limit cycles

It is still not easy to fully solve the system of equations (4.1.15) and (4.1.16). However, the purpose now is to demonstrate that the system is capable, in principle at least, of producing a periodic variability

under certain circumstances. It is assumed for the moment that $(\frac{\partial v}{\partial r})_s$ and $(\frac{\partial a}{\partial r})_s$ are known functions of r_s and a_s (their actual knowledge does of course require a full solution). The system then has the form (for a given constant angular momentum and polytropic index)

$$\frac{dr_s}{dt} = F_1(r_s, a_s) \ , \tag{4.1.17}$$

$$\frac{da_s}{dt} = F_2(r_s, a_s) \ , \tag{4.1.18}$$

where F_1 and F_2 are two nonlinear functions. For the sake of definiteness it is now assumed as an example that $(\frac{\partial a}{\partial r})_s \approx 0$ (which actually means $|(\frac{\partial a}{\partial r})_s| \ll |(\frac{\partial v}{\partial r})_s|$). In the stationary case at least, this approximation is not entirely bad. In this case it can be shown that for consistency with the stationary flow one needs $(\frac{\partial v}{\partial r})_s = \zeta\, r_s^{-9/7}$ where ζ is determined by the accretion rate.

The equilibrium curves (EC) $F_1 = 0$ and $F_2 = 0$ in this case ($\zeta = 0.394$, $L^2 = 3.15$) are shown in Figure 18 in the (r_s, a_s) phase space. It can be shown that F_1 is negative above its EC while F_2 is positive above its respective EC. Under these conditions, points A and B are points of stability exchange, namely, the intermediate branch of the EC of F_1, AB, is unstable while the inner and outer branches are stable. A small perturbation from the inner or outer branch cannot grow in time, while it does grow if it is from the intermediate branch. The intersection (equilibrium) point O therefore becomes a doubly unstable nodal point.

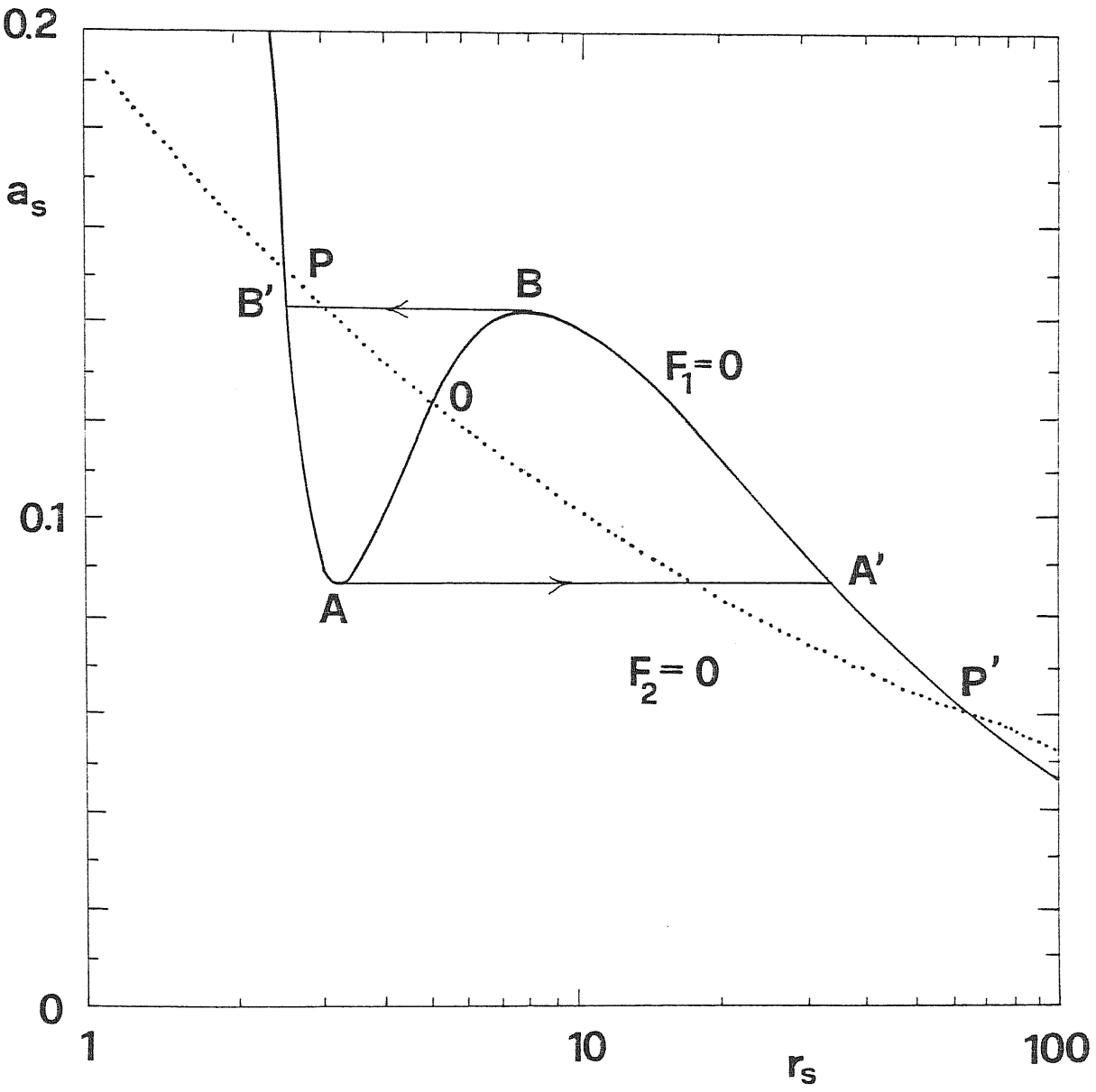

Fig. 18 The equilibrium curves of equations (4.1.17)-(4.1.18). The limit cycle is represented by the curve AA'BB' (see text).

As a consequence, this system can exhibit a limit cycle AA'BB', namely, if an accretion flow is in its equilibrium state and is described by a point on the A'B branch, then the only possible direction of evolution is that towards B. This is because A'B is above the EC of F_2, and in this region F_2 is positive, i.e. a_s can only increase in time evolution. When the point B is reached, the gradual evolution cannot continue as AB is unstable. But it is possible that a jump from B to B' happens. After jumping, the flow can evolve only towards A, as AB' is below the curve $F_2 = 0$, and in this region a_s should decrease in evolution. When A is reached, another jump to A' happens. The limit cycle here is similar to the one obtained, for example, in the case of Liénard's equation (e.g. Minorsky 1962). If the functions F_1 and F_2 satisfy in addition $|F_2| \ll |F_1|$, then the limit cycle is a relaxation oscillation, the system evolving from A to A' (as well as from B to B') on a timescale that is short compared to the period. If $|F_2|$ is not small compared to $|F_1|$, the existence of the limit cycle is not ensured but is still possible, provided that the other equilibrium points P and P' are sufficiently far from B' and A' (in the particular case considered here $|F_2|/|F_1| \sim |(\frac{\partial v}{\partial r})_s| < 1$).

It is extremely important to note that the S shape of the EC of F_1, which is the essential ingredient for producing the limit cycle, is a direct consequence of the general relativistic potential near the black hole (represented by a pseudo-Newtonian form here). An S shape is not obtained using a purely Newtonian potential. It should also be emphasized that only the possibility of obtaining a limit cycle has been demonstrated, as $|F_2|$ may not be sufficiently small compared to

$|F_1|$ in the present approximation scheme. To determine whether such a limit cycle is actually obtained and what timescales emerge will require a full solution of the time-dependent problem with realistic parameters. Another point that has to be made is that while it is true that a limit cycle produces a "perfect clock", it suffices that some of the parameters assumed constant (such as angular momentum) do change a little, to change the exact periodicity into a quasi-periodic variability.

4.3 Conclusion and discussion

The model presented here is very simple and crude. However, some quite definite conclusions can be drawn even now:

An isolated cloud with angular momentum could tune itself to a state in which the regularity condition (2.6.6) is fulfilled, but a non-isolated one may not. This suggests that there are two different types of accretion flows. One in which the accretion rate is not determined by outside conditions can be stationary and regular, as condition (2.6.6) is fulfilled. In the second type of accretion flow the accretion rate is determined by the outside conditions and (2.6.6) is not fulfilled. In this case the accretion cannot be stationary, but is either:

(a) Not stationary and not regular. This means that shock fronts are developed. This possibility was numerically examined by Hawley and Smarr (1983).

(b) Not stationary, but regular, i.e. shock free as suggested in this chapter. The accretion flow undergoes a limit cycle behaviour: it

oscillates between Bondi-type and disklike solutions. Since the Bondi-type solution always corresponds to a higher accretion rate, it can be called high state while the disklike solution is low state.

5. Astrophysical implications

Many of the objects believed to be black holes accreting rotating matter show violent variability. Very short term (in the range of hours or minutes), irregular or quasi-periodic variations in luminosity of active galactic nuclei have been monitored in many observational programs (e.g. O'Dell et al. 1978, Abramowicz and Nobili 1982, Carrasco et al. 1985, Valtaoja et al. 1985, and the recent review of Wiita 1985). They provide the best upper limit for the size of active regions in these objects. The evidence for long-term (months or years) periodicities has also been found in, for example, the light curves of the quasars 3C273 (Smith 1965) and 3C345 (Barbieri et al. 1977, Kidger and Beckman 1985), the intensity of the broad emission lines H_α and H_β in the Seyfert galaxy NGC1566 (Alloin et al. 1985) and soft X-ray outbursts in some other active galactic nuclei (e.g. Marshall et al. 1981, or Lawrence 1980). In addition, it is well known that the X-ray luminosity of the galactic black hole candidate Cyg X-1 oscillates between high and low states, with irregular durations of weeks to years (e.g. Margon et al. 1971, Sadeh et al. 1979, Ogawara et al. 1982, Ling et al. 1983, and the recent review of Liang and Nolan 1984).

The mechanism for this variability is not clear. Of course, it could be a consequence of extremely complex conditions which are, in addition, different for each object. If this is indeed the case, no general explanation would be possible. A much more appealing hypothesis would be, however, that there exists a simple and universal mechanism producing all these complex phenomena. A theoretical proof that such a mechanism

operates due to some black hole properties would give strong observational support for the existence of black holes.

Such a universal mechanism may indeed exist due to the non-unique location of the sonic point in the transonic accretion of rotating matter onto a black hole. This was noticed a few years ago by Abramowicz and Zurek (1981) and confirmed more rigorously in this thesis. Non-stationary accretion flows would most likely oscillate between the Bondi-type and the disklike solutions. Since the Bondi-type solution always corresponds to a state of higher accretion rate, and the disklike solution to a lower accretion rate, the oscillation may lead to a quasi-periodic or chaotic behaviour in luminosity. This model has two attractive advantages: it is characteristic only of accretion onto a black hole, because the inner sonic point is located at a few gravitational radii and therefore cannot be realized for accretion onto a Newtonian object; it depends weakly on the inherent uncertainties in the microphysics which plague the models of black hole environments.

The amplitude of the variations observed in some parameter can be roughly estimated as (cf. Figure 10)

$$A = \frac{\dot{M}_{Bondi} - \dot{M}_{Disk}}{\dot{M}_{Bondi}} \lesssim 1 \ . \qquad (5.1.1)$$

This agrees with the relative luminosity variations in quasars (~ 0.4, see,e.g. Wiita 1985) and Cyg X-1 (~ 1, see, e.g. Liang and Nolan 1984).

Much more difficult would be to estimate the timescale for variation. The observational data suggest that in the case of Cyg X-1 the mass is

$\sim 10M_{\odot}$ and the typical timescale of variation ~ 0.1 yr, while in the case of quasars the mass is $\sim 10^{8}M_{\odot}$ and the timescale ~ 1yr. Thus, if the timescale depends mainly on the mass, there should be a scaling $t \sim M^{1/3}$. This would not be possible when the timescale $t = bt_{dyn}$ with b having the same value for Cyg X-1 and quasars. If however the quantity b depends on some other properties of the model (e.g. radiation pressure) one could in principle explain the variations of both Cyg X-1 and quasars by the same mechanism. An accurate estimation of the timescales must be achieved by solving (numerically) the relativistic, time-dependent equations, in order to confidently compare theory with already existing observational data.

References

Abramowicz M.A., 1985, Publ. Astron. Soc. Japan (in press).

Abramowicz M.A., Blaes O.M. and Lu J.F., 1985, Proceedings of the Trieste meeting on "Structure and Evolution of Active galactic nuclei"(in press).

Abramowicz M.A., Calvani M. and Nobili L., 1980, Ap. J., 242, 772.

Abramowicz M.A., Jaroszynski, M. and Sikora M., 1978, Astr. Astrophys., 63, 221.

Abramowicz M.A. and Lasota J.P., 1980, Acta Astron., 30, 35.

Abramowicz M.A. and Nobili L., 1982, Nature, 300, 506.

Abramowicz M.A. and Zurek W.H., 1981, Ap. J., 246, 314.

Alcock C. and Illarionov A., 1980, Ap. J., 235, 541.

Alloin D., Pelat D., Philips M. and Whittle M., 1985, Ap. J., 288, 205.

Barbieri C., Romanov G., di Serego S. and Zambon M., 1977, Astr. Astrophys., 59, 419.

Bardeen J.M. and Petterson J.A., 1975, Ap. J. Lett., 195, L65.

Bardeen J.M., Press W.H. and Teukolsky S.A., 1973, Ap. J., 178, 347.

Begelman M.C., 1978, Astr. Astrophys., 70, 583.

Birkhoff G. and Rota G.C., 1969, Ordinary Differential Equations, Chapter 5, Section 1, Blaisdell Publishing Co.

Bisnovatyi-Kogan G.S. and Blinnikov S.I., 1980, Mon. Not. R. Astr. Soc., 191, 711.

Bisnovatyi-Kogan G.S. and Ruzmaikin A.A., 1974, Astrophys. Sp. Sci., 28, 45.

Blumenthal G.R. and Mathews W.G., 1976, Ap. J., 203, 714.

Bondi H., 1952, Mon. Not. R. Astr. Soc., 112, 195.

Brinkmann W., 1980, Astr. Astrophys., 85, 146.

Burbidge G.R., 1972, Comm. Astrophys. Sp. Phys.

Cameron A.G.W. and Mock M., 1967, Nature, 215, 464.

Carrasco L., Dultzin-Hacyan D. and Cruz-Gonzalez I., 1985, Nature, 314, 146.

Carter B., 1979, in Active Galactic Nuclei, Eds. C.Hazadr and S.Mitton (Cambridge Univ. Press), P. 273.

Carter B., Gibbons G.W., Lin D.N.C. and Perry M.J., 1976, Astr. Astrophys., 52, 427.

Cunningham C.T., 1973, Ph.D. thesis.

Fang L.Z., 1981, Mon. Not. R. Astr. Soc.,194, 177.

Flammang R.A., 1982, Mon. Not. R. Astr. Soc., 199, 833.

Hawley J.F. and Smarr L.L., in Numerical Astrophysics, a Festschrift in honour of James R. Wilson, eds. J. Centerella, J.Le Blanc and R.Bowers, Jones & Bartlett, Boston, 1983.

Hawley J.F. and Smarr L.L., 1985, preprint of University of Illinois.

Hayakawa S. and Matsuoko M., 1964, Prog. Theor. Phys. Suppl., 30, 204.

Henriksen R.N. and Heaton K.C., 1975, Mon. Not. R. Astr. Soc., 171, 27.

Holzer T.E., 1977, J. Geophys. Res., 82, 23.

Hurewicz W., 1958, Lectures on Ordinary Differential Equations, Chapter 4, Massachusetts Institute of Technology.

Isper J.R. and Price R.H., 1977, Ap. J., 216, 578.

Isper J.R. and Price R.H., 1982, Ap. J., 255, 654.

Isper J.R. and Price R.H., 1983, Ap. J., 267, 371.

Jaroszynski M., Abramowicz M.A. and Paczyński B., 1980, Acta Astr., 30, 1.

Jeffreys H., 1924, The Earth, Cambridge Univ. Press.

Kato S., Fukue J., Inagaki S. and Okazaki A.T., 1982, Publ. Astron. Soc. Japan, 34, 51.

Kidger M. and Beckman J., 1985, preprint of Instituto de Astrofisica de Canarias.

Kozlowski M., Jaroszynski M. and Abramowicz M.A., 1978, Astr. Astrophys., 63, 209.

Lamb F.K. and Petrick C.J., 1974, Proc. 16th Solvay Conf. (Brussels).

Landau L.D. and Lifshitz E.M., 1959, Fluid Mechanics, London, Pergaman Press.

Lawrence A., 1980, Mon. Not. R. Astr. Soc., 192, 83.

Liang E.P. and Nolan P.L., 1984, Space Science Reviews, 38, 353.

Liang E.P.T. and Thompson K.A., 1980, Ap. J., 240, 271.

Lightman A.P., 1974, Ap. J., 194, 419.

Lightman A.P., 1974, Ap. J., 194, 429.

Ling J.C., Mahoney W.A., Wheaton W.A., Jacobson A.S., Kaluzienski L. and Holt S.S., 1983, Ap. J., 275, 307.

Loska Z., 1982, Acta Astro. 32, 13.

Lüst R., 1952, Z. Naturforsch., 7a, 87.

Lynden-Bell D., 1960, Ph.D. thesis.

Lynden-Bell D., 1969, Nature, 223, 690.

Lynden-Bell D. and Pringle J.E., 1974, Mon. Not. R. Astr. Soc., 168, 603.

Lynden-Bell D. and Rees M.J., 1971, Mon. Not. R. Astr. Soc., 152, 461.

Maraschi L., Perola G.C., Reina C. and Treves A., 1979, Ap. J., 230, 243.

Maraschi L., Reina C. and Treves A., 1976, Ap. J., 206, 295.

Maraschi L., Roasio R. and Treves A., 1982, Ap. J., 253, 312.

Margon B., Lampton M., Bowyer S. and Cruddace R., 1971, Ap. J. Lett., 169, L23.

Marshall N., Warwick R.S. and Pounds K.A., 1981, Mon. Not. R. Astr. Soc., 194, 987.

Matsumoto R., Kato S., Fukue J. and Okazaki A.T., 1984, Publ. Astron. Soc. Japan, 36, 71.

Mészàros P. 1975a, Astr. Astrophys., 44, 59.

Mészàros P. 1975b, Nature, 258, 583.

Michel K., 1972, Astrophys. Space Sci., 15, 153.

Minorsky N., 1962, Nonlinear Oscillations, van Nostrand, Princeton.

Misner C.W., Thorne K.S. and Wheeler J.A., 1973, Gravitation, W.H. Freeman and Company, San Francisco.

Moncrief V., 1980, Ap. J., 235, 1038.

Muchotrzeb B., 1983a, Acta Astron., 33, 79.

Muchotrzeb B., 1983b, Ph.D. thesis.

Muchotrzeb B. and Paczyński B., 1982, Acta Astron., 32, 1.

Novikov I.D. and Thorne K.S., 1973, in Black Holes, Les Houches, eds. B.DeWitt and C.DeWitt, New York, Gordon & Breach.

Novikov I.D. and Zel'dovich Y.B., 1966, Nuovo Cim. Suppl., 4, 810.

O'Dell S.L., Poschell J.J., Stein W.A. and Warner J.W., 1978, Ap. J. Suppl., 38, 267.

Ogawara Y., Mitsuda K., Masai K., Vallerga J.V., Cominsky L.R., Grunsfeld J.M., Kroper J.S. and Ricker G.R., 1982, Nature, 295, 675.

Paczyński B., 1977, unpublished.

Paczyński B., 1978, private communication.

Paczyński B., 1981, Mitt. Astron. Ges., 57, 27.

Paczyński B. and Abramowicz M.A., 1982, Ap. J., 253, 897.

Paczyński B. and Bisnovatyi-Kogan G., 1981, Acta Astron., 31, 283.

Paczyński B. and Wiita P.J., 1980, Astr. Astrophys., 88, 23.

Page D.N. and Thorne K.S., 1974, Ap. J., 191, 499.

Papaloizou J.C.B. and Pringle J.E., 1984, Mon. Not. R. Astr. Soc., 208, 721.

Peek B.M., 1942, J. Brit. Astron. Assoc., 53, 23.

Prendergast K.H. and Burbidge G.R., 1968, Ap. J. Lett., 151, L83.

Pringle J.E. and Rees M.J., 1972, Astr. Astrophys., 21, 1.

Ray D., 1980, Astr. Astrophys., 82, 368.

Sadeh D., Meidav M., Wood K., Yentis D., Smathers H., Meekins J., Evans W., Byram E.T., Chubb T.A. and Friedman H., 1979, Nature, 278, 436.

Salpeter E.E., 1964, Ap. J., 140, 796.

Schmidt-Burgk J., 1978, Astrophys. Space Sci., 56, 191.

Shakura N.I., 1972a,Soviet Astron. - A. J., 49, 495.

Shakura N.I., 1972b,Soviet Astron. - A. J., 49, 642.

Shakura N.I. and Sunyaev R.A., 1973, Astr. Astrophys., 24, 337.

Shapiro S.L., 1973a, Ap. J., 180, 531.

Shapiro S.L., 1973b, Ap. J., 185, 69.

Shklowsky I.S., 1967, Ap. J. Lett., 148, L1.

Shvartzman V.F., 1971, Soviet Astron. - A. J., 15, 377.

Smith H.J., 1965, Quasi Stellar Objects and Gravitational Collapse, eds. Robinson I., Schild A. and Schücking E.L., university of Chicago.

Stoeger W.R., 1976, Astr. Astrophys., 53, 267.

Stoeger W.R., 1980, Ap. J., 235, 216.

Tassoul J.L., 1978, Theory of Rotating Stars, Princeton Univ. Press.

Thorne K.S., 1974, Ap. J., 191, 507.

Thorne K.S., Flammang R.A. and Zytkow A.N., 1981, Mon. Not. R. Astr. Soc., 194, 475.

Tooper R.F., 1965, Ap. J., 142, 1541.

Urpin V.A., 1983, Astronphys. Space Sci., 90, 79.

Valtaoja E., Letho H., Teerikorpi P., Korhouen T., Valtonen M., Terasranta H., Salonen E., Urpo S., Tiuri M., Piirola V. and Saslaw W.C., 1985, Nature, 314, 148.

Vitello P., 1984, Ap. J., 284, 394.

von Weizsäcker C.F., 1943, Z. Astrophys., 22, 319.

von Weizsäcker C.F., 1948, Z. Naturforsch., 3a, 524.

Weinberg S., 1972, Gravitation and Cosmology, John Wiley & Sons, Inc.

Wiita P. J., 1982, Ap. J., 256, 666.

Wiita P.J., 1985, Physics Reports, 123, No.3, 117.

Yahel R.Z. and Brinkmann W., 1981, Ap. J. Lett., 244, L7.

Yahel R.Z., 1982, Ap. J., 252, 356.

Zel'dovich Y.B., 1964, Sov. Phys. Doklady, 9, 195.

Zel'dovich Y.B. and Guseynov O.H., 1966, Ap. J., 144, 840.

Zel'dovich Y.B. and Novikov I.D., 1971, Relativistic Astrophysics,
Vol.1: Stars and Relativity, Chicago Univ. Press.

Zhang J.L. and Jiang S.D., 1983, Astrophys. Space Sci., 91, 9.

Zhu C.S., 1981, Mon. Not. R. Astr. Soc., 195, 697.